2020-04-09

Novel Strategies for Organosulfur Analysis in Gas Chromatography with Flame Photometric Detection

McKelvie, Kaylan Halcyon

UNIVERSITY OF CALGARY

Novel Strategies for Organosulfur Analysis in Gas Chromatography with Flame Photometric Detection

by

Kaylan Halcyon McKelvie

A THESIS

SUBMITTED TO THE FACULTY OF GRADUATE STUDIES

IN PARTIAL FULFILMENT OF THE REQUIREMENTS FOR THE

DEGREE OF DOCTOR OF PHILOSOPHY

GRADUATE PROGRAM IN CHEMISTRY

CALGARY, ALBERTA

APRIL, 2020

Abstract

This thesis describes the development of novel methods to analyze organosulfur compounds using gas chromatography (GC) with flame photometric detection (FPD). The first area of exploration utilizes a water stationary phase for sulfur separations. Several organosulfur compounds are retained to varying degrees on this phase, while non-polar hydrocarbons are unretained. This prevents the co-elution of sulfur analytes with hydrocarbons and the response quenching that is often observed in GC-FPD. Overall, the water stationary phase is shown to be a useful alternative for the analysis of organosulfur compounds in complex matrices.

Next, a sample preparation method using lead oxide particles or plumbite solution is demonstrated to complex thiols into a solid lead thiolate moiety that can be physically separated from complex sample matrices and then reconstituted as the original thiol in a simple replacement solvent for analysis. The method allows thiols to be selectively isolated from co-eluting peaks, which can simplify their determination and greatly reduce interference from signal quenching when using an FPD. As an extension of this technique, a selective chromatographic system is also demonstrated. This uses PbO or plumbite as a pre-column trap for thiols, which allows non-thiols to separate as normal while thiols are not eluted until in situ reconstitution. This illustrates the potential for their controlled GC analysis. Accordingly, results indicate that these methods could be useful alternative approaches for the selective analysis of such thiol-containing samples.

Lastly, a novel miniaturized GC-FPD device built within a titanium platform (Ti μGC-FPD) is presented. The monolithic Ti device contains both a separation column and a

shielded cavity to house the detector flame. The FPD employs a micro counter-current flame that is stabilized by opposing relatively low flows of oxygen and hydrogen, with minimum detectable limits of about 70 pg S/s for sulfur and 8 pg P/s for phosphorous. Overall, good separations with stable and sensitive detector performance are obtained with the device, and its sturdy Ti structure supports robust operation. Results indicate that this Ti μGC-FPD device may be a useful alternative approach for incorporating selective FPD sensing in μGC analyses.

Preface

Portions of Chapter Two and Chapter Three have been published as K.H. McKelvie, K.B. Thurbide, Analysis of sulfur compounds using a water stationary phase in gas chromatography with flame photometric detection, Anal. Methods. 9 (2017) 1097–1104. doi:10.1039/C6AY03017C. Reproduced with permission from Royal Society of Chemistry.

Portions of Chapter Two and Chapter Four have been published as K.H. McKelvie, K.B. Thurbide, A Rapid Analytical Method for the Selective Quenching-Free Determination of Thiols by GC-FPD, Chromatographia. 81 (2018) 1559–1567. doi:10.1007/s10337-018-3619-9. Reproduced with permission from Springer Nature.

Portions of Chapter Two and Chapter Six have been published as K.H. McKelvie, K.B. Thurbide, Micro-Flame Photometric Detection in Miniature Gas Chromatography on a Titanium Tile, Chromatographia. 82 (2019) 935–942. doi:10.1007/s10337-019-03723-y. Reproduced with permission from Springer Nature.

Acknowledgements

First and foremost, I would like to acknowledge my amazing supervisor, Dr. Kevin Thurbide, for his ongoing support, encouragement, and kindness throughout my degree. Working with him will always be one of the highlights of my career. I would also like to thank my supervisory committee members, Dr. Gailer, Dr. Marriott, and the late Dr. Hinman. I have appreciated the suggestions made for this work and have learned so much from all of them.

A special thank you to members of the Thurbide group, past and present, for helping to make this an enjoyable experience. In particular, I am grateful for the kind leadership and guidance from Fadi Alkhateeb and Jill Murakami. I would further like to thank the core research group at Waters Corporation, particularly Mike Fogwill, for the opportunity to participate in an unforgettable four-week research program.

I am thankful for the invaluable chemistry department staff, such as Janice Crawford, Mark Toonen, and Ed Cairns for their expertise and help throughout my degree.

Finally, I am grateful for the unwavering support and love from my parents, siblings, and husband throughout my educational pursuits.

To my mom and dad,

who taught me that I can be whatever I want to be.

And to Stuart,

for his endless support and love.

Table of Contents

List of Tables

List of Figures and Illustrations

List of Symbols, Abbreviations, and Nomenclature

t_r'	adjusted retention time
x	by
cm	centimeter
°C	degree Celsius
°C/min	degrees Celsius per minute
dFPD	dual flame photometric detector
e.g.	exempli gratia (for example)
FID	flame ionization detector
FPD	flame photometric detector
g	gram
g/mL	grams per milliliter
GC	gas chromatography
h	hour
i.d.	internal diameter
i.e.	id est (in other words)
k'	capacity factor (retention factor)
K	Kelvin
LC	liquid chromatography
m	meter
µg	micrograms
µGC	micro (or miniaturized)-gas chromatography

mC/gC	millicoulomb per gram of carbon
MDL	minimum detectable limit
mFPD	multiple flame photometric detector
min	minute
mL	milliliter
n	number of trials
N	number of theoretical plates
ng	nanogram
ng/µL	nanogram per microliter
$N_{p\text{-}p}$	noise – peak-to-peak
N_{rms}	noise – root-mean-square
o.d.	outer diameter
pg	picogram
pg X/s	picogram of element X per second
PMT	photomultiplier tube
ppm	parts per million
RSD	relative standard deviation
R	resolution
α	selectivity factor
s	seconds
SS	stainless steel
SCD	sulfur chemiluminescence detector
Ti	titanium

t_m	time spent in the mobile phase (void time)
t_s	time spent in the stationary phase
VSC	volatile organosulfur compound
$w_{b,avg}$	width of peak at base (average)

CHAPTER ONE: INTRODUCTION

1.1 Importance of Organosulfur Compounds

Volatile organosulfur compounds (VSCs) are important to a wide range of industries. For example, organosulfur compounds present in the air can contribute to environmental pollution. In fact, when sulfur-compounds exist in refined petroleum products such as gasoline, the combustion products that contain sulfur can pollute the air as SO_x which can lead to acid rain and result in detrimental effects on buildings, trees, and other surfaces [1]. In areas surrounding factories that make rubber, organosulfur pollution is also observed in air and/or water, due to the sulfur used to strengthen rubber products (such as car tires) in a process called vulcanization [2–4]. Similarly, natural VSCs from soils and vegetation can also get into water streams and contaminate them [5], affecting animal life and endangering human consumption. Another area where VSCs are important is the food and beverage industry. Of note, the flavoring and odor of numerous foodstuffs is often reliant on the concentration and class of different sulfur-compounds present in them. For instance, foods such as garlic, mustard, and coffee each contain VSCs that are essential to their aroma or taste [6]. Notably, many sulfur compounds display a potent odor, even at very low concentrations. In foods, often the low concentration sulfur component has a subtle impact on flavor and smell. However, if a food product has a high concentration (i.e. too much) of an organosulfur compound, both the flavor and smell can be adversely affected [6]. Organosulfur compounds are also frequently present in other diverse applications such as chemical warfare agents [7,8] and pesticides [9,10].

Due to their importance and prevalence, VSCs must be regularly monitored to ensure quality control and avoid negative effects to the environment. Thus, analytical methods that can rapidly and accurately determine the sulfur compounds of interest in these different settings are desirable. Unfortunately, a large barrier often encountered with VSC analysis is the complexity of the matrix from which it comes. For example, there are hundreds of different hydrocarbons present amongst the sulfur compounds in gasoline, and foodstuffs similarly contain many other flavor and odor components in addition to sulfur-bearing analytes. This myriad of compounds present in a sample can make it difficult to effectively select for and analyze the sulfur-containing analyte(s), due to the significant background interference that can be generated by non-sulfur analyte signals. In an attempt to minimize this matrix interference, gas chromatography with selective detection is often employed as a sulfur-selective analysis technique. This method both increases the separation between interfering compounds and the sulfur component(s) of interest and enhances the signals of the latter. The focus of this thesis will be on the development of novel sulfur-selective methods of gas chromatography analysis that can be applied in various complex mixtures.

1.2 Gas Chromatography

As a whole, gas chromatography (GC) is one of the most commonly used analytical techniques for the determination of volatile organic compounds, including organosulfur compounds. This technique generally relies upon gas-phase analyte interactions between a mobile phase and a stationary liquid or solid phase for retention and separation of mixtures on a column, and was first demonstrated in 1952 by James and Martin [11]. Over half a century later, GC has greatly evolved and has been commercialized into a technique that is

commonly used by laboratories throughout the world. For example, GC is now readily employed in various industries such as pharmaceuticals, oil and gas, food sciences, air quality, forensics, and others [9,12,13–20,21]. Its prevalence can be partially attributed to the success GC has had with increasing the analytical selectivity for numerous organic compounds. Since its inception, advances in GC column chemistries have been able to demonstrate improvement for separation and resolution between analytes in complex mixtures. Thus, there is continual development of columns for the intent of optimizing analysis for many different types of compounds [22,23]. Further, various detection methods can be used to discriminate between classes of compounds in a mixture that elute off the GC column. This discrimination increases the selectivity that can be invoked in the system. As such, GC is an effective tool for deriving qualitative and quantitative information from both known and unknown samples. Due to its widespread applicability, other advances in GC technology are also on-going. For example, recent innovations have led to the miniaturization of this technique [14], where micro-columns and micro-detectors have been the subject of much exploration [24–32]. Therefore, overall further development of GC methods remains of great interest.

1.2.1 GC Instrumentation & Parts

In GC, the sample is introduced into the system through a hot injector to allow for analyte (and solvent) volatilization. This vaporized sample is then carried onto a separation column by an inert carrier gas (i.e. mobile phase) where partition interactions occur between the analyte and the stationary phase inside of a GC column. As different analytes have varying degrees of phase interactions, each spends a unique portion of time interacting with

the stationary phase. Thus, analytes naturally begin to separate from one another as they are carried to the outlet of the column. As each analyte elutes off the column, they enter a detector. The detector is a sensor that signals when the analyte elutes from the column and can often provide other information about the analyte, such as concentration and compound identification. A schematic of a GC set up is shown in Figure 1-1.

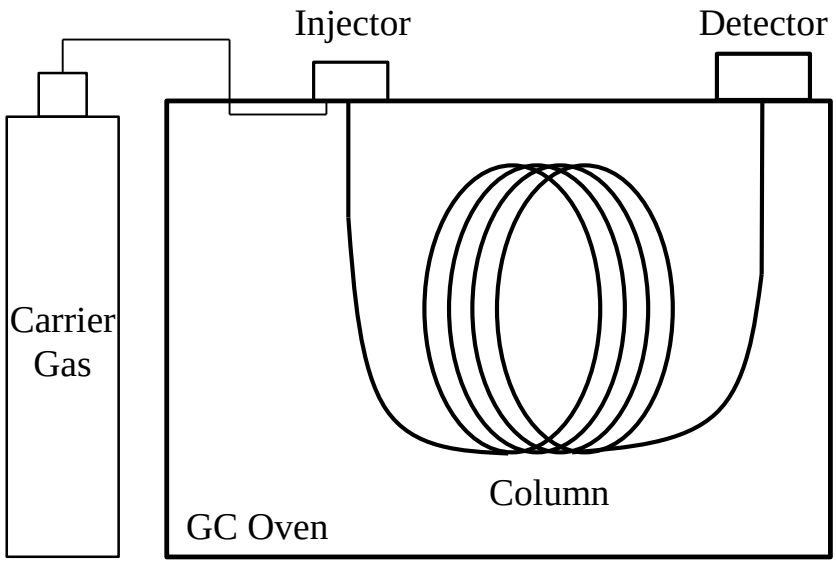

Figure 1-1: A general schematic of GC instrumentation.

1.3 The Separation Column

The purpose of a GC column is to allow separation of a mixture into its individual components. Although factors such as column internal diameter, stationary phase particle size or coating thickness, and column length can have influence on the efficiency of a separation [33], the chemical composition of the stationary phase is a primary feature that impacts the resulting chromatography obtained on a column. This is often described by the

selectivity ($\propto$) of the column for two separated analytes, which is greatly influenced by the stationary phase used (Equation 1).

$$\alpha = t'_{r,b}/t'_{r,a} \qquad \text{Equation 1}$$

As shown in Equation 1, the theoretical selectivity can be expressed by the adjusted retention time (t'_r) of two analytes *a* and *b*. The more retained analyte value is given in the numerator and α gives a representation of how much more one component is retained relative to another. Retention can be represented in different ways. The adjusted retention time only considers the time an analyte spends partitioned to the stationary phase (t_s), and not the time spent in the mobile phase (t_m), which is constant for each analyte. Alternatively, the retention factor, k', indicates the fraction of time each analyte spends in the stationary phase relative to time spent in the mobile phase (t_s/t_m). As such, it too can also be used to calculate α. Overall then, due to individual analyte interactions with the stationary phase, varying selectivities can be achieved for separations by using different stationary phases with different affinities for particular types of analytes. This phase chemistry is therefore an important characteristic to consider when choosing a column for specific analyte separations.

Related to the selectivity of a column is the separation efficiency. Since the goal of chromatography is often to obtain well-resolved, narrow analyte peaks, the efficiency of this process is commonly measured through determining the resolution (R; Equation 2) between two peaks.

$$R = \Delta t_r / w_{b,avg} \qquad \text{Equation 2}$$

As seen, resolution measures how well separated two analytes are by the difference in their chromatographic retention times (Δt_r) relative to their average peak widths at base (w_b). To ensure good separation, a resolution value ≥ 1.5 is required, which corresponds to very little overlap of the two analyte peaks. Resolution can also be measured through the Purnell equation (Equation 3).

$$R = \frac{\sqrt{N}}{4}\left(\frac{\alpha - 1}{\alpha}\right)\left(\frac{k'_b}{1+k'_b}\right) \qquad \text{Equation 3}$$

Although both resolution equations present the same result, Equation 3 outlines some important variables that affect a separation in a chromatogram. For instance, Equation 3 relies on N, α, and k'. It should be noted that N indicates the number of theoretical plates in a column, in which each theoretical plate represents an equilibration event between the stationary and mobile phases where analyte interaction occurs. N is calculated in Equation 4.

$$N = \frac{16\, t_r^2}{w_b^2} \qquad \text{Equation 4}$$

If there is a high number of plates (N) then there are more opportunities for analytes to separate from one another, which is desirable. One way to increase N is to increase the length of a GC separation column. In the context of Equation 3, however, it can be seen that changing N has much less of an effect on resolution (due to the square root relationship) than changing the selectivity, α, or retention factor k'. However, since increasing resolution through increasing k' requires much larger retention times, this route is also often

impractical. Thus, selectivity, and therefore the stationary phase, has the greatest direct influence on resolution for a separation.

GC columns are generally categorized as either packed or capillary (Figure 1-2). A packed column is filled with solid particles that can be coated with stationary liquid phase, while a capillary column is open tubular and is often coated with stationary phase along the inner walls of the tube. Packed columns usually have more stationary phase per unit length than a capillary column due to the increased surface area available from the particles. This results in an increase in theoretical plates per unit length and can be very useful.

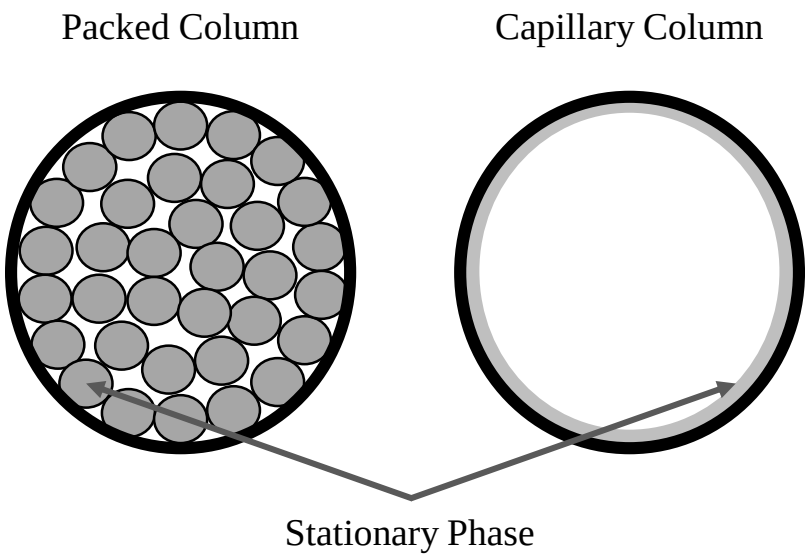

Figure 1-2: Schematic representation of the cross section from packed (left) and wall-coated open tubular capillary (right) columns.

However, packed columns are limited by their length, as longer columns require higher pressures to ensure carrier flow through the column. In contrast, capillary open tubular columns are less restrictive to flow, so much longer lengths can be achieved without

undergoing the same pressure drop over the column that packed columns suffer from. This means that longer lengths of capillary and more frequent partition interactions can occur overall, and so generally capillary columns have more theoretical plates and a better ability to resolve analytes than packed columns. For this reason, capillary columns are most commonly used in modern GC and will be used extensively throughout this thesis.

1.3.1 Fused Silica Columns

The most common columns in GC are made of a fused silica capillary support [22]. These columns are coated with a liquid stationary phase that can be bonded and cross-linked onto the inside wall of the tube/support. This bonded nature enhances the durability of the stationary phase [34], allowing the column to endure high temperatures (~350 °C) with very little 'bleed' (where bleed refers to the stationary phase decomposing and coming off of the column support and into the detector). A typical GC stationary phase is often comprised of polysiloxanes. The simplest form of this coating is a non-polar polydimethylsiloxane, where the polymer is 100% methyl-substituted, as seen in Figure 1-3. This is used in commercial GC columns such as the well-known DB-1 column. Other functional groups may be added to the polymer for additional column selectivity and/or polarity, such as phenyl and cyanopropyl groups. Normally, larger analytes with higher boiling points are more retained on these typical GC columns than smaller compounds with lower boiling points. However, any means of increasing the selectivity between components with similar properties and boiling points can still work to improve separations and analysis speed.

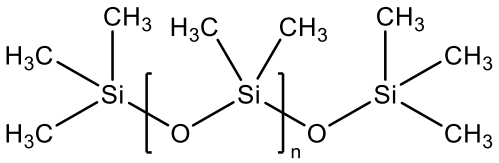

Figure 1-3: Chemical structure of polydimethylsiloxane.

To this end, developments to increase selectivity, separation and resolution in GC columns have been ongoing since the inception of GC [22]. Accordingly, many stationary phases are commercially available for the purpose of optimizing methodologies for specific applications. However, purchasing a catalog of several different column chemistries for specific analyses can be extremely costly and perhaps impractical since they have a finite lifespan. Additionally, from an environmental standpoint, the polymers and other materials used to develop columns are not always green and can produce hazardous waste from both column development and their eventual disposal. Thus, there is a need for simpler and more cost effective ways to develop columns with unique selectivity.

1.3.2 Water Phase Columns

In this manner, water is an interesting component to investigate. Water has unique physical and chemical properties in addition to being non-toxic, non-flammable and widely available. In chromatography, water has been utilized for various applications. It is most commonly used as a mobile phase or modifier in liquid chromatography (LC). For example, this provides a highly polar mobile phase for reverse-phase LC. Another technique, subcritical-water chromatography (SWC), exploits the chemical properties of water at elevated (sub-critical point) temperatures for use as a mobile phase to accomplish separations [35]. Notably, as the temperature of water increases toward its critical point (374 °C), its

polarity decreases [36]. This indicates that SWC has the potential to separate analytes with little-to-no harmful organic solvent [35]. Thus, the use of water in other chromatographic separations could be beneficial as a useful alternative green approach.

In recent years, water as a stationary phase for use in capillary GC and supercritical fluid chromatography has been developed [37–45]. In GC, both Gallant et al. and Darko et al. found that applying water to the interior walls of a stainless steel capillary resulted in a stable stationary water phase that could be used reliably up to temperatures around 140-160 °C [39,43–45]. The water stationary phase showed very unique separations with high selectivity for polar compounds. Correspondingly, this phase also demonstrated little retention and selectivity for non-polar hydrocarbons. For example, a gasoline matrix composed of hundreds of hydrocarbons eluted completely within the void volume region in the water phase system [39,44], presenting the opportunity to better separate out any moderately polar compounds of interest that would have otherwise eluted with and been obscured by the bulk matrix components in the detector. Conversely, very highly polar compounds were found to partition into the phase and not elute at all [43,44]. Similarly, due to the aqueous nature of the phase, direct aqueous samples could also be easily analyzed without the need for any sample preparation prior to analysis. These retention characteristics lend themselves well to further applications for selective GC with compounds containing polar moieties in a complex matrix. While several oxygen and nitrogen-bearing hydrocarbons have been investigated with this phase [39,43–45], organosulfur compounds have been very little explored using it. Thus, analysis of organosulfur compounds using a water stationary phase would be interesting to examine.

1.4 Detection

After the analyte elutes off of the column, it enters a detector that produces a signal proportional to the amount present. In GC, there are many different detectors available for use. In order to recognize and utilize the ideal detector for analysis, an understanding of how a detector responds to a class of compounds is important. Therefore, how the analyte signal is generated and what type of compounds they respond to dictates the classification of such detectors.

1.4.1 Concentration and Mass-Flow Detectors

The primary means by which a detector generates an analyte signal can be broadly categorized as either concentration or mass-flow sensitive. In a concentration sensitive detector, a signal is produced that is proportional to the analyte concentration inside of a detection cell. Therefore, the volume of the cell can drastically impact the signal, as it affects the concentration being monitored. An example of a concentration sensitive GC detector is the thermal conductivity detector. In contrast to this, the signal in mass-flow detectors is generated based on the rate at which an analyte flows through the detection cell. Thus, a signal is produced based on the mass of analyte flowing per unit time through the detector. Some common mass-flow GC detectors are the flame ionization detector (FID) and the flame photometric detector (FPD). The latter are used extensively in this thesis and will be expanded upon later in the text.

An important feature to recognize between the above two detector types is their dependency on column flow rate for chromatographic peak heights and areas. A concentration sensitive detector only senses the observed concentration, and thus flow rate

through the cell theoretically has little effect on peak height (signal) in a chromatogram. However, since flow rate impacts the time the analyte spends in the detection cell, the peak area can be greatly affected. On the other hand, mass-flow sensitive detectors observe the absolute mass of the analyte flowing through the detector per unit time, rather than its concentration. Thus, if the flow rate were to change in a mass-flow detector, the same mass would pass through the detector at a different rate and the peak height would change accordingly while peak area theoretically remains the same at either flow. This characteristic can sometimes make comparisons between these detector types difficult, such as when reporting limits of detection where a concentration (e.g. g/mL) or a mass-flow rate (e.g. g X/s, where X is an element that the detector responds to) can be quoted depending on the type of detector. Either way, it is useful to know how a detector responds in this regard and how the measurement of peak height or area may be affected in this regard.

1.4.2 Universal and Selective Detectors

Another important classification for GC detectors is their response to compounds with different properties. The most common classes encountered are universal and selective detectors. A universal detector is a sensor that theoretically responds uniformly to all analytes that elute from the column. The FID is an example of a universal detector, as it responds uniformly with the same response factor to (nearly all) carbon compounds [46]. These detectors are particularly useful for analyzing and characterizing unknown samples. For instance, qualitative and quantitative information can be obtained from using a universal detector in GC, to indicate how many compounds are present and how much of each exists in the sample.

Alternatively, a selective detector typically only responds to a particular sample type, such as compounds with a specific atom or functional group. This kind of detector therefore provides a specific chromatogram, where only the compounds the detector can sense are observed. This is useful in the analysis of complex matrices, where the target compound may not be distinguishable from numerous others when using a universal detector. Additionally, selective detectors can often enhance detection limits of the target compound since background interference is usually low. Notably, the FPD is a selective GC detector most commonly utilized for sulfur and phosphorous detection [46,47].

1.5 Detector Performance Characteristics

1.5.1 Sensitivity and Detection Limits

Due to the wide range of applications for GC analysis, there is need for sensitive detectors with low detection limits. From a detector's output, information is gathered about both the analyte (signal) and the background response (noise). These are both important features that can help determine the sensitivity and the minimum detectable limit (MDL) of a detector. Sensitivity refers to the capability of a detector to respond reliably to small changes in analyte concentration [33]. It is calculated as the response per mass of analyte introduced and is often determined as the slope from a typical calibration curve. High sensitivity is an important characteristic as it determines how effective (i.e. 'sensitive') the detector is at responding to the eluting analyte.

Another important aspect that determines a detection limit is the background noise. Noise constitutes the random variations and fluctuations of the detector output in the absence

of analyte. This background can be measured either as root-mean-square noise (N_{rms}, also denoted as σ) or peak-to-peak noise (N_{p-p}). N_{rms} is calculated as the standard deviation of the noise fluctuations on a background signal. Alternately, N_{p-p} is determined as the difference between the minimum and maximum deviations from a representative baseline. Noise is normally measured over a time span equivalent to at least 10 analyte peak base widths. An analyte peak (or signal) must be able to rise above the noise in order to be observed in a detector, so efforts to minimize noise are desirable.

The MDL of a detector is commonly determined as the amount of analyte exhibiting a signal response that is twice the N_{p-p} (S/N = 2). Alternatively, the limit of detection can also be expressed using the IUPAC definition from employing N_{rms} (or σ), where $S/\sigma = 3$. These S/N ratios correspond to the amount of analyte that gives the lowest discernable response in a detector (i.e. the MDL).

1.5.2 Selectivity

As previously described, selective detectors respond specifically to certain classes of compounds. This is incredibly practical when analyzing a complex sample since it can sense one analyte amidst a multitude of others. However, in practice, selective detectors may still elicit a very small response from other non-analyte compounds. Therefore, in order to measure the magnitude of selectivity of a detector, a calibration curve for both an analyte that the detector is selective for and one that represents the background matrix must be prepared. A comparison then of the mass of each that corresponds to their equal response in the detector determines the response selectivity. For example, in an FPD the selectivity for sulfur over carbon (S/C) is 10^{4-6} [33]. This indicates that an FPD requires 10^{4-6} × more carbon to

yield the same response observed for sulfur, and thus at analytically relevant levels, very little response is seen from any amount of carbon in this detector. Accordingly, when choosing and comparing detectors, the larger difference in mass required for an equal response leads to greater selectivity.

1.5.3 Linearity and Equimolarity

Another important characteristic of a detector is the response linearity. This refers to the range over which the detector response increases linearly with an increase in the amount of sample. A calibration curve is a convenient way to visualize a linear range, and an example of this is shown in Figure 1-4.

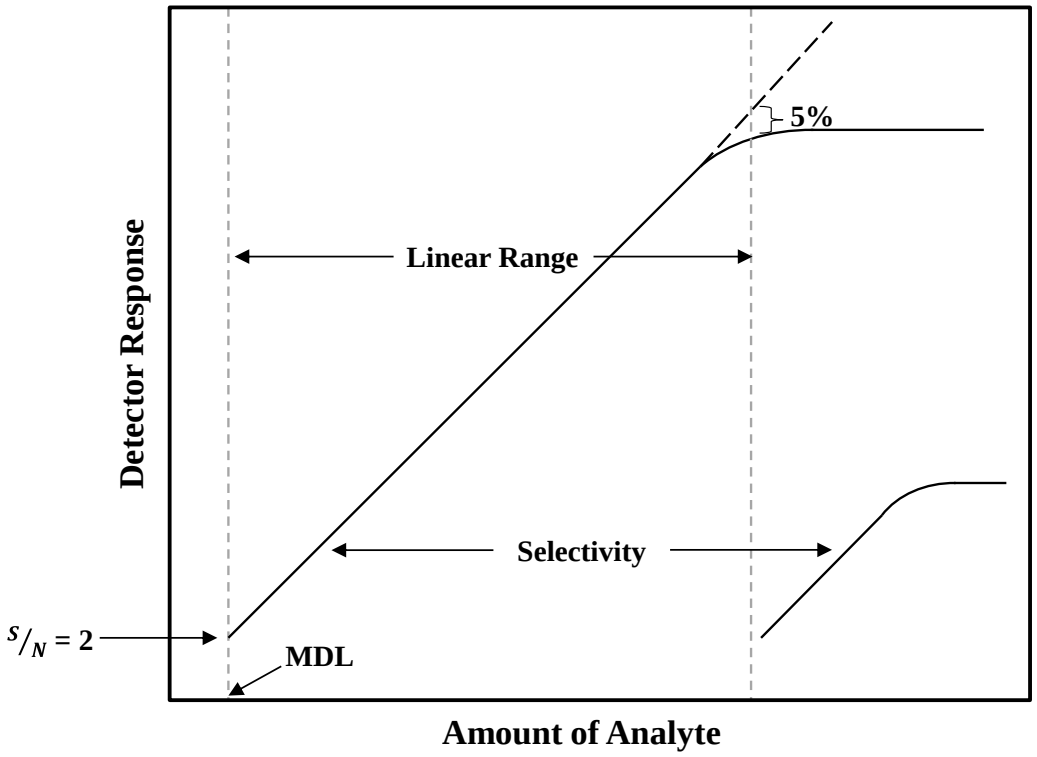

Figure 1-4: A representative calibration curve demonstrating linear range, minimum detectable limit, and selectivity.

As seen, the response increases linearly until the detector becomes saturated with analyte, where additional analyte can no longer induce an increased detector response. A 5% deviation from this linearity is conventionally considered the endpoint of the linear range.

In order to further understand the importance of a linear and uniform detector response, equimolarity must also be considered. An equimolar detector response indicates that equal molar amounts of different analytes will each yield the same response. However, practically this is not always the case. For instance, differences in the structure of a compound may cause the detector to respond slightly differently to it from other compounds without the same features. This also means that the calibration curves for different analytes may vary substantially in the same detector. As such, detectors that generate a more uniform response for a group of diverse compounds are commonly preferred since most analytes will produce the same calibration characteristics in such devices. If so, this means that one known analyte can be used to calibrate the detector for subsequent quantification of various other known/unknown analytes as needed.

1.6 Flame Based GC Detectors

1.6.1 Flame Ionization Detector

The flame ionization detector (FID) is one of the most widely used detectors for organic compound analysis in GC as it is a universal detector for carbon and is also very sensitive. The FID was developed simultaneously by McWilliam and Dewar and Harley et al. in 1958 [48,49], who each discovered a large amount of ions generated from organic carbon passing through a polarized hydrogen-air flame. The FID has long been commercialized and

is a common detector equipped on most GCs. A general design of an FID is shown in Figure 1-5.

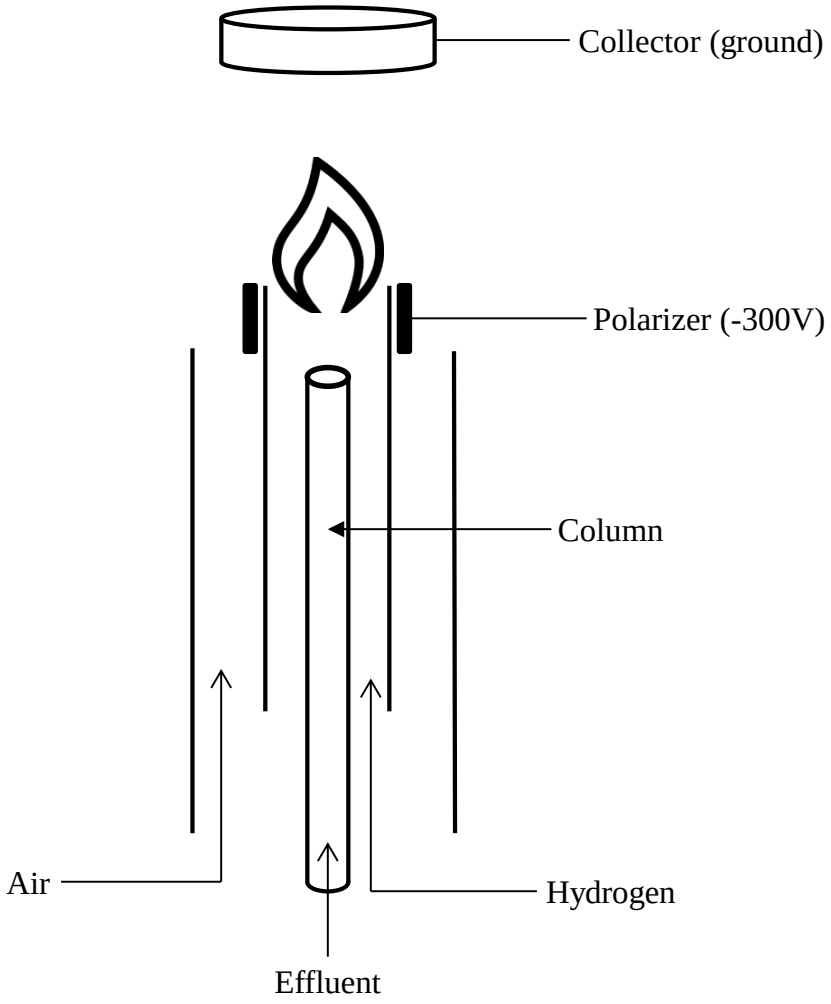

Figure 1-5: A basic schematic of a flame ionization detector.

As the FID uses a hot (2100 K) hydrogen-air flame, hydrocarbons thermally break down into methane, CH_4, just beneath the flame [46]. The methane then undergoes chemi-ionization reactions with hydrogen in the flame until it forms a CH· species. This radical then

reacts with oxygen in the flame, resulting in the production of CHO^+ and an electron, which is believed to provide FID response, as follows:

$$CH\cdot + O\cdot \rightarrow CHO^+ + e^- \qquad \text{Equation 5}$$

Since the collector is more positively charged than the polarizer, the negatively charged electron produced is attracted to it, and a current is generated that is proportional to the carbon present in the flame.

As the FID first processes all hydrocarbons into a single-carbon moiety (CH_4), the FID is said to have a fairly equimolar response, since the current generated is proportional to each gram of carbon analyzed [46]. Remarkably, it has been found that only one of every 10^5 carbon atoms in an FID will actually react to produce the CHO^+ ion. Despite the low conversion of carbon to CHO^+, the FID is still able to obtain low limits of detection, on the order of a few picograms of carbon per second (10^{-12} g C/s) [46]. Further, the linear range for an FID is also quite large and often observed to be around 10^7 [46].

Although the FID is largely universal to hydrocarbons, there are some carbon-containing species to which it does not respond. For example, CO, CO_2, CCl_4 and CS_2 give little-to-no FID response since they lack a CH fragment and therefore cannot form CHO^+ ions. As such, other partially functionalized carbon species can also exhibit a reduced response in the FID. Interestingly, some metals have also been found to respond in the FID, which suggests that any compounds that can similarly produce an electron in the polarized flame may possibly be able to garner a significant response from this detector [50–52].

Over recent years, in attempts to provide detection in portable micro-GC units, efforts to miniaturize the FID without compromising sensitivity and detection limits have been made [25,28,53–55]. To this end, a titanium-based micro-GC (µGC) platform with on-board µFID has recently been reported, allowing very successful separation and detection on one device [56]. This µFID shows a similar limit of detection, linear range, and sensitivity to a conventional FID [56], indicating that other flame-based GC detectors could be fabricated using a titanium substrate for miniaturization and be utilized in a similar fashion to the µGC-FID. However, this has yet to be explored and requires further investigation.

1.6.2 Flame Photometric Detector

In 1966, Brody and Chaney developed the flame photometric detector for the selective analysis of sulfur and phosphorous compounds [57]. In this detector, chemiluminescence is monitored in a cool (~500 °C) hydrogen-rich flame by a photomultiplier tube (PMT). Although sulfur and phosphorous are the main elements explored with the FPD, emission of light from tin, germanium, selenium, tellurium, manganese, ruthenium, and many others have also been observed in this detector and used for selective analysis [47,58–60]. A schematic of the FPD is shown in Figure 1-6.

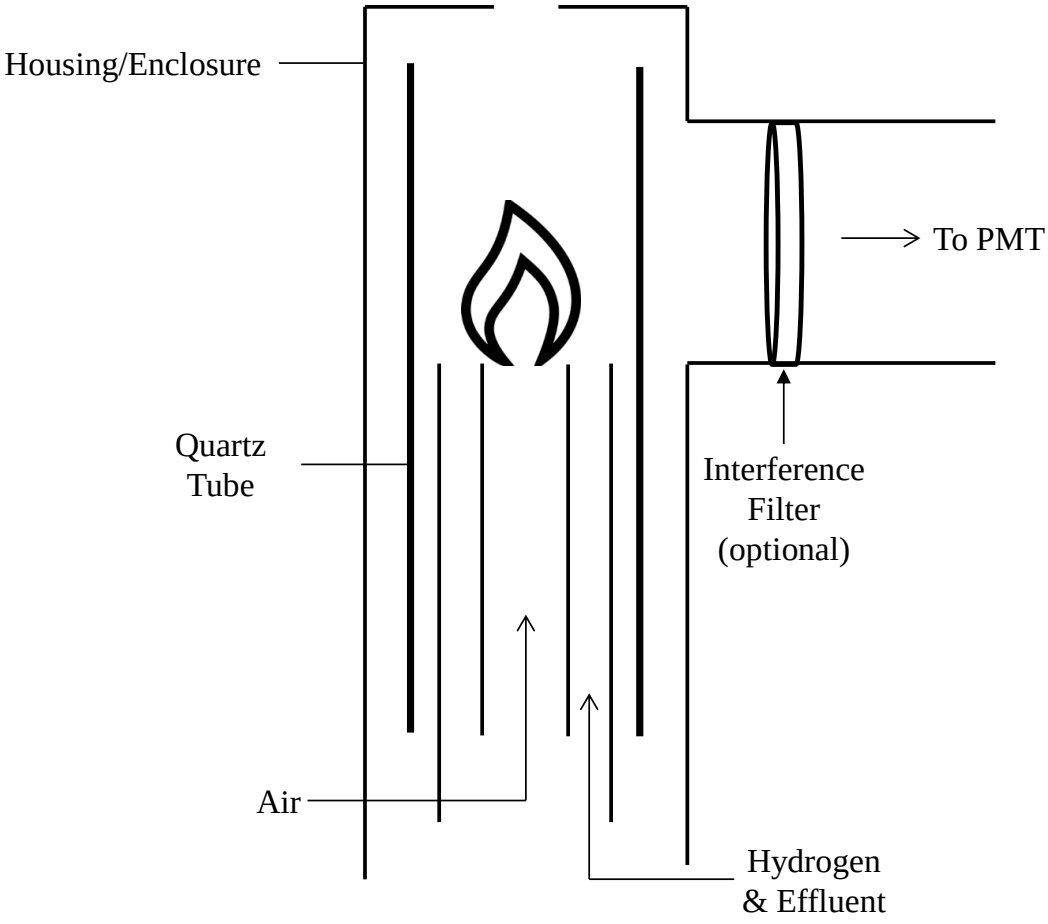

Figure 1-6: A basic schematic of a flame photometric detector.

The hydrogen flame contributes to the decomposition of the eluent analyte into luminescent species such as S_2 and HPO, for sulfur and phosphorous, respectively. The flame also provides the energy required to transition these species into an excited state for light emission. Although this excitation step is not fully understood, it is generally agreed upon that analyte species utilize the energy released (about 4.5 eV) from the recombination of hydrogen radicals present in the flame to form H_2 (Equation 6). When a chemiluminescent species is present, such as S_2, the released energy is used to excite this species, as demonstrated from Equation 7. This excited species can then emit light.

$$H\cdot + H\cdot \rightarrow H_2 + 4.5\ eV \qquad \text{Equation 6}$$

$$H\cdot + H\cdot + S_2 \rightarrow H_2 + S_2^{*} \qquad \text{Equation 7}$$

As such, the flame is kept fuel-rich to encourage hydrogen radical production in order to maximize the frequency of excitation events. This is in contrast to the FID flame, which functions in an oxygen-rich environment to produce CHO^{+}. It should be noted that this mechanism of excitation in the FPD is not species specific, as any chemiluminescent species (e.g. HPO) can utilize the energy released from the hydrogen radical recombination. Most importantly, as the excited state species returns to its ground state, the resulting emitted light is then monitored by a PMT for quantification.

Not surprisingly, the species-dependent light emission therefore has a great influence on the detector response. Analytes containing phosphorous generate HPO in the flame, while the major emitting species for sulfur-containing compounds is S_2. Thus, sulfur requires two sulfur atoms for emission, while phosphorous only needs one. This often produces a near quadratic (i.e. non-linear) response for sulfur in the FPD (Equation 8), while the response for phosphorous remains linear.

$$\text{e.g. Response} \propto [S]^{n}, \text{ where } n \cong 2 \qquad \text{Equation 8}$$

Since many species can chemiluminesce, an appropriate interference filter can be placed before the PMT in order to monitor only a particular wavelength/bandwidth of light. These filters can be specific to each chemiluminescent species and the colour of light they emit. Notably, S_2^{*} has a characteristic blue spectrum largely ranging from 320-460 nm, with

a maximum emission around 393 nm [33,46,47]. On the other hand, HPO^* has a green emission with its maximum at 526 nm. Thus, with the use of interference filters, these two species are easily isolated and distinguished from one another. Interestingly, the analysis of these compounds is often of great concern, particularly in complex mixtures such as petroleum products and biological samples [2,46,53,57,61–65], where selective detection is required.

The greatest advantage to using an FPD is that it generates a selective response for the analyte of interest and is insensitive to other potentially interfering species. As noted previously, a typical FPD has a S/C response selectivity of $10^{4\text{-}6}$, while that of P/C is 10^5 [33,47,60]. This highly selective nature over carbon demonstrates the applicability of the FPD for analysis of complex samples containing chemiluminescent species. Further, the MDLs for sulfur and phosphorous in the FPD are around 2-50 pg S/s and 0.1-2 pg P/s [33,47].

Despite the selective nature and good detection limits of the FPD, reports of a miniaturized FPD have been scarce [24,66]. This can largely be attributed to difficulties in miniaturizing the conventional burner and flame size without compromising sensitivity or stability. Further investigation into reducing and miniaturizing the FPD would therefore be beneficial to advance selective detection options in μGC.

Perhaps the biggest challenge that the FPD faces is the phenomenon of hydrocarbon response quenching. When a chemiluminescent analyte co-elutes with a hydrocarbon from the column and they enter into the detector flame together, the analyte signal can be severely reduced (i.e. quenched). Although the exact mechanism for this phenomenon is not known, it

is thought to be related to the combustion and breakdown of the hydrocarbon, where it consumes free hydrogen radicals in the flame (Equation 9) to form methane.

$$CH_3\cdot + H\cdot \rightarrow CH_4 \qquad \text{Equation 9}$$

This effect scavenges the hydrogen radicals and decreases the available energy for chemiluminescence. The result is a quenched analyte signal due to inadequate species excitation and corresponding emission. Consequently, emission can be nearly eliminated by even a small amount of hydrocarbon in the flame [67–69]. As such, complex mixtures with a matrix made up of numerous hydrocarbon components requires a high resolution column to prevent hydrocarbon co-elution; however this is not always possible for a complicated sample. Therefore, other means of separating an interfering hydrocarbon matrix from the analyte of interest are greatly desired.

1.7 Other GC Detectors

Quenching in the FPD can make the detector difficult to use for some applications, such as those in which the analysis of sulfur- or phosphorous-containing samples takes place. Therefore, other detectors for such samples have also been developed over the years.

1.7.1 Dual Flame Photometric Detector

The dual FPD (dFPD) has similar operating principles to the conventional single-flame FPD [70,71]. In this design, two hydrogen-rich flames are operated in series. The first flame serves to decompose and combust the compounds as they elute off the column. The

products of this flame are swept longitudinally into the second flame, where chemiluminescence of the analyte is monitored by a PMT. Thus, the dFPD has separated the two processes (decomposition and chemiluminescence monitoring) that occur in a single-flame FPD. This deconvolution of steps is important as it has been found that quenching can be reduced in a dFPD since carbon is present as a more oxidized and less-quenching form (e.g. carbon dioxide) in the second flame [72]. As such, the dFPD has led to success in decreasing the hydrocarbon quenching observed in a conventional FPD [70–72]. Unfortunately, the dFPD is also found to be significantly less sensitive than a single-flame FPD.

1.7.1.1 Multiple Flame Photometric Detector

Improvements on the dFPD have been found in the multiple flame photometric detector (mFPD), which utilizes five flames in series. Here, four initial 'worker' flames are used to homogenize the sample and ensure that all of the hydrocarbons have combusted and are decomposed into CO_2 [73,74]. This also helps break down compounds into their chemiluminescent emitter species and produces a more uniform and equimolar response. The products of the worker flames enter the fifth and final analytical flame for chemiluminescence with significantly reduced quenching and no reduction in sensitivity. Although this detector has shown great promise, it is not yet commercially available. Thus, other detectors are also utilized for selective detection of sulfur compounds.

1.7.2 Atomic Emission Detector

The atomic emission detector (AED) is another detector that can be used to overcome the difficulties of quenching in an FPD. The AED is a multi-element detector based on atomic emission lines. In essence, this detector works by transferring column effluent into a hot plasma, where compounds decompose into their individual atoms. These atoms are then

thermally excited and produce an emission of light that is monitored by a photodiode array. In this way, simultaneous emission from different atoms can be monitored. For sulfur detection, minimum detectability occurs near 1 pg S/s with a linear range of 10^4 [60]. By its operation, the AED is a quenching-free detector with a linear and selective response for various elements. However, the huge relative cost of the instrument and substantial requirements for additional maintenance are the largest hindrance for widespread usage of this detector. Thus, in terms of a sulfur-selective detector, the AED is not the most readily accessible option.

1.7.3 Sulfur Chemiluminescence Detector

The sulfur chemiluminescence detector (SCD) was first developed in 1989 by Benner et al., and is based on sulfur chemiluminescence induced from a reaction with ozone [75]. Sulfur compounds in GC effluent are first decomposed in a hot furnace where SO is produced. This is then carried into an ozone reaction cell under vacuum conditions, where SO is converted into excited SO_2, a species which then emits light. Thus, similar to the FPD, the SCD also utilizes unique sulfur chemiluminescent properties. The emission of SO_2^* occurs over a range of 280-460 nm [33,60].

The SCD is able to decompose eluting hydrocarbons without interfering with sulfur emission and detection, resulting in a non-quenched sulfur response. The SCD also has very good detection properties. For example, the detection limit for sulfur in an SCD is nearly 1 pg S/s, with a linear range of 10^{4-5}, and a selectivity for sulfur over carbon of 10^7. Further, the response is linear due to the light-emitting SO_2 species consisting of only one sulfur atom. However, as seen, the SCD is much more complicated than a simple FPD, as it requires an

ozone generator and a vacuum cell. Consequently, although the SCD is less expensive than the AED, it is still considerably more expensive when compared to an FPD and requires much more frequent maintenance.

1.8 Sample Preparation in GC

Another effective way to increase selectivity in chromatographic analysis is to invoke a selective sample preparation method. In every analytical process, there is a sample preparation step that prepares a sample for introduction into the measuring instrument, while hopefully reducing the background matrix presence. In its simplest form, sample preparation can be achieved by weighing a solid before dissolving it into a volume of solvent. Other common preparation techniques such as liquid-liquid extraction strive to selectively extract analyte from a complex matrix containing potential interferents into a less complicated matrix. Thus, sample preparation simplifies a sample which in turn simplifies its chromatographic analysis. Often, isolating analytes of interest from a bulk matrix and/or derivatizing compounds that are difficult to detect are preparation methods employed for GC.

Although liquid-liquid extraction is commonly used for sample preparation, it regularly requires large amounts of organic solvent which becomes hazardous waste after use. One technique that reduces this waste is solid-phase micro-extraction (SPME). In SPME, a syringe is used to house a fused silica fiber coated with an extracting polymer [76]. The fiber is exposed to the sample (either liquid or gas) and extraction of the analyte of interest takes place without the use of organic solvent. The fiber can then be removed and injected straight into a GC for analysis. This is often an easy way to help reduce matrix effects and simplify analyses. However, similar to other common extraction techniques,

SPME can suffer from non-selective extraction, meaning other compounds in addition to the analyte of interest are transferred to the fiber [76]. To this end, simultaneous in-fiber derivatization with SPME has been noted to somewhat further increase selectivity during extraction [13,77]. Nevertheless, SPME requires optimization of polymer composition, exposure time, etc., which can make this a lengthy sample preparation process [76]. Thus, other selective sample preparation techniques, especially for sulfur-containing compounds in complex matrices, are desired.

Derivatization in GC is another way in which samples can be prepared for analysis. Analytes that may have poor chromatographic peak shapes, have low/no volatility, reduced signal, or are thermally labile can be chemically derivatized to increase their ability to be analyzed chromatographically [78]. For example, derivatization of thiol compounds, a type of organosulfur compound, can help increase their retention on a column to separate them further from interfering components that may have been co-eluting with the thiols prior to derivatization [79]. As a result, the post-derivatization separation demonstrates an increase in selectivity. Therefore, derivatization can sometimes allow quantification of analytes in other complicated matrices, such as pharmaceutical formulations and biofluids [12,80–84]. Despite these improvements to analyses, derivatization can also be very lengthy, prone to errors, and often requires specialized reagents [78].

Research is ongoing to increase the speed, convenience, and selectivity of sample preparation methods. It is well known that sample preparation is the most time consuming step in an analytical process, accounting for up to 80% of the time spent on a particular analysis. Also, various reagents and solvents can produce waste that requires special disposal, so efforts to minimize these reagents are of benefit. Thus, novel methods of

selectively preparing samples for analysis, particularly those containing sulfur analytes, are of continual interest.

1.9 Statement of Purpose

This thesis describes several novel means of improving the selective analysis of organosulfur compounds in GC using an FPD. As described, there are many routes for increasing selectivity in a GC analysis. One such way is using a selective detector, such as the FPD, which is commonly used to detect sulfur compounds. This detector is highly selective and exhibits good detection limits (i.e. picogram level), while being cost-effective, robust, and simple to operate. However, as noted previously, the FPD is prone to hydrocarbon quenching when analyzing complex samples. Therefore, even greater means of increasing selectivity are required to generate quenching-free results for the analysis of sulfur compounds in an FPD. Further, the FPD has not yet been miniaturized into a format for simple μGC use.

As noted, column chemistry primarily drives the selectivity for compound retention. In Chapter Three, an environmentally friendly water stationary phase is examined for separations of organosulfur compounds. Previous investigations with this phase in GC demonstrated its separation potential for moderately polar compounds [39,43–45]. As organosulfur compounds are typically separated on non-polar columns, it is of interest to study their separation characteristics on a polar water stationary phase. Additionally, the improved separation between analyte and organic matrix reported earlier with a water stationary phase suggests that this phase may increase selectivity for sulfur over hydrocarbons to prevent co-elution and quenching in the FPD. This method of separation is

therefore investigated as an alternative for sulfur-selective GC analysis where the FPD is employed.

Another way to avoid FPD quenching is to simplify the sample to reduce background interference prior to GC analysis. As an important class of sulfur compounds, thiols are often prepared from petroleum and foodstuff samples by various techniques such as derivatization, liquid-liquid extraction and SPME [79,85–87]. On a much greater scale, the selective removal of thiols from industrial Canadian petroleum process streams in the 1860s was performed by using an aqueous 'Doctor Solution', containing plumbite (PbO_2^{2-}) [88]. This process inspired recent reports of using lead (II) oxide (PbO) for a similar purpose [89,90]. However, plumbite and PbO have never been explored for use as an analytical extraction technique for thiols. Thus, Chapter Four explores the use of these reagents as a novel selective sample preparation extraction technique for thiols to simplify their later analysis by GC-FPD.

The modification of a water stationary phase to suit certain applications has been reported previously [43–45,91]. For example, using an aqueous acid, base, or chiral solution was found to give good separation and peak shape for the phase-selected class of analyte. Thus, for sulfur-selective analysis, it is of interest to examine a short column with a plumbite stationary phase coating (as a new extension to the work in Chapter Four) prior to a conventional GC column. Chapter Five investigates the use of a thiol 'trap-and-release' setup in GC to increase the on-line separation control between thiol compounds and interfering components for analysis with an FPD.

As the FPD is a robust, sensitive, simple, and very widely used detector, investigations into miniaturizing the FPD for use in μGC are of continual interest. Although

there has been progress made in decreasing burner sizes and flow rates required for FPD operation, many μGC devices are unfortunately made of silicon wafers that are prone to fracturing and breakage, especially at high temperatures such as those of a flame [92]. However, recently a titanium-based μGC-FID device has been reported. Thus, the use of titanium as a stronger and more durable μGC substrate could help integrate an FPD into such a device. Chapter Six describes and characterizes a novel titanium microfluidic device that contains a μGC column with an on-board μFPD.

The seventh chapter contains a brief summary of this work and presents thoughts on directions for this work in the future.

CHAPTER TWO: EXPERIMENTAL

2.1 Analysis of Sulfur Compounds Using a Water Stationary Phase in Gas Chromatography with Flame Photometric Detection

2.1.1 Instrumentation and Operation

An HP 5890 Series II GC (Hewlett-Packard, Palo Alto, CA, USA) equipped with an FPD was used in these experiments. The GC system is depicted in Figure 2-1 and is similar to that described previously with an FID [39]. Briefly, high purity helium carrier gas (Praxair, Calgary, AB, CAN) is bubbled through HPLC-grade water (Burdick & Jackson, Muskegon, MI, USA) and saturated with vapor using a reservoir made from a 1/4" Swagelok cross-union (Calgary Valve and Fitting, Calgary, AB, CAN) connected to a capped stainless steel (SS) tube (4.6 mm i.d. x 5 cm) that resides inside the oven [39]. It is important to emphasize here that this water only serves to saturate the carrier gas and preserve the water phase, which is firmly stationary against the capillary wall and does not move [37]. The carrier gas then passes through a SS pre-heating coil (1/16" o.d. x 250 μm i.d. x 168 cm; Chromatographic Specialities, Brockville, ON, CAN) before entering the injector, which was typically maintained at 220 ºC with a split ratio of 7:1.

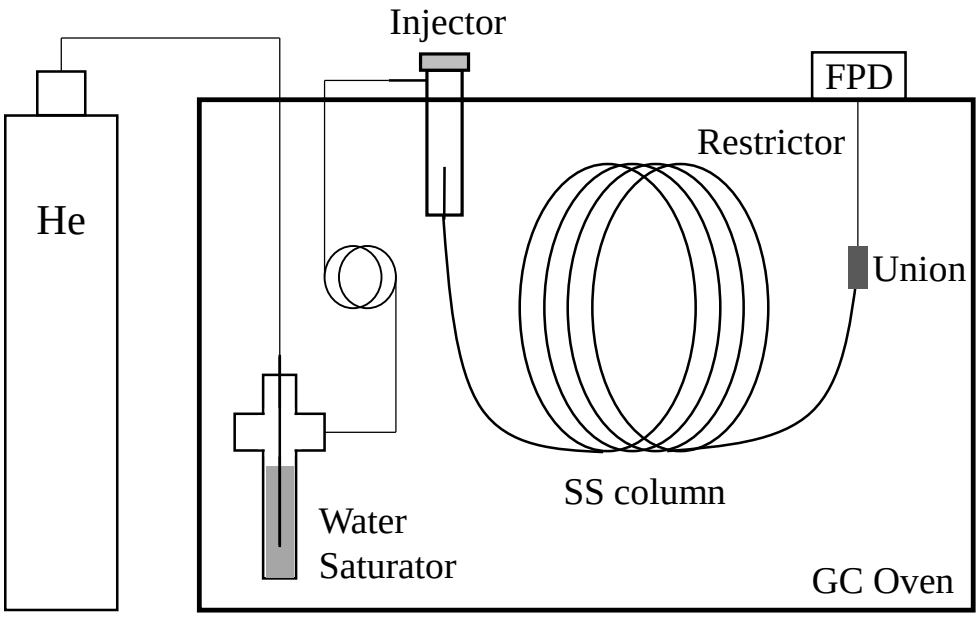

Figure 2-1: Schematic diagram of the water stationary phase GC-FPD system.

The SS capillary column employed (1/16" o.d. x 250 μm i.d. x 30 m; Chromatographic Specialties) was coated with an HPLC-grade water stationary phase (Burdick & Jackson) using a previously established technique [39]. This coating methodology typically yields a phase thickness of about 4 μm [37]. It was then placed inside the oven with the inlet directly connected to the injector. A fused silica restrictor (75 μm i.d. x 50 cm; Biotaq, Gaithersburg, MA, USA) was connected to the column outlet by a zero dead volume union (Vici-Valco, Houston, TX, USA) and was led directly into the detector where it was situated just below the flame.

The carrier gas velocity was normally maintained at 22 to 26 cm/s. The detector temperature was kept at 320 ºC with flame gases set to 40 mL/min hydrogen (Praxair) and 7 mL/min oxygen (Praxair). Note that although oxygen is used here, air should be useful as an alternative as well. All FPD emission was monitored using an R-1104 PMT (Hamamatsu,

Bridgewater, NJ, USA) with a 393 nm optical interference filter (11 nm bandpass; Oriel Instruments, Stratford, USA). It should be mentioned that a useful linear sulfur emission at 750 nm has also been reported [93], and can readily be observed in this system as well. However, since this study was directed toward the vast majority of FPD users that still access the quadratic response at 393 nm and experience the interference problems at that conventional wavelength, it was invoked here. For some comparison experiments, a DB-1 column (250 µm i.d. x 30 m; 0.25 µm thickness; Agilent Technologies, Mississauga, ON, CAN) was employed in a conventional unhydrated manner.

Data acquisition was performed using PeakSimple Chromatography Software with a Model 202 Four Channel Data System (SRI Instruments, Torrance, CA, USA). The PMT was operated through an external power supply/electrometer constructed in-house by the University of Calgary Chemistry Electronics Shop.

2.1.2 Reagents and Supplies

A variety of standard sulfur-containing organic compounds were examined in this study. They include: 2-propanethiol, tetrahydrothiophene (each 97%; Fluka Analytical, Oakville, ON, CAN), tert-butylthiol, 1-propanethiol, 1-butanethiol, dimethyl sulfide, carbon disulfide, diethyl disulfide, dimethyl disulfide, thianaphthene (each 99%; Sigma-Aldrich, Oakville, ON, CAN), 2-butanethiol, diethyl sulfide (each 98%; Sigma-Aldrich), dipropyl sulfide (97%; Sigma-Aldrich), diisopropyl disulfide (96%; Sigma-Aldrich), and 1-hexanethiol (95%; Sigma-Aldrich).

Standard solutions were normally prepared in hexanes (a mix of isomers; EMD Chemicals, Gibbstown, NJ, USA), except for those in the quenching experiments, which

were instead prepared in octane (98%; Sigma-Aldrich) or a commercial automotive fuel (purchased from a local vendor). Other applications had sulfur solutions prepared directly in wine, milk, or urine samples that were all obtained locally. The urine sample was collected from a healthy volunteer after informed consent was obtained, and all related experiments were conducted in compliance with the relevant laws and institutional protocols established under the auspices of the University of Calgary Biosafety Committee. All other details are outlined in the text.

2.2 A Rapid Analytical Method for the Selective Quenching-Free Determination of thiols by GC-FPD

2.2.1 Chemicals and Reagents

The solid yellow massicot form of PbO (99%; Sigma-Aldrich) was used in these extractions. Also used was a 0.06 M PbO_2^{2-} solution, made from saturating 1 M sodium hydroxide (97%; EMD Chemicals) with the solid PbO. Nitric acid (68-70%; VWR International, Edmonton, CAN) diluted to 1 M with HPLC-grade water (Burdick & Jackson) was used to recover the thiols. Test analytes included 2-propanethiol, tetrahydrothiophene (each 97%; Fluka Analytical), tert-butylthiol, 1-butanethiol, dimethyl disulfide, thianaphthene (each 99%; Sigma-Aldrich), 2-butanethiol, diethyl sulfide (each 98%; Sigma-Aldrich), dipropyl sulfide (97%; Sigma-Aldrich), diisopropyl disulfide (96%; Sigma-Aldrich), and benzenethiol (99%; Eastman Chemical, Kingsport, TN, USA). Standard analyte solutions were made in n-hexane (99%; Sigma-Aldrich) at varying concentrations as noted in the text. Pentane, cyclohexane (each 99%; Sigma-Aldrich), heptane (96%; Sigma-

Aldrich), octane (98%; Sigma-Aldrich), benzene and toluene (each 99%; EMD Chemicals) were used to prepare a model petroleum condensate sample matrix. A natural gas sample was obtained in-house, while commercial gasoline was acquired from local vendors.

2.2.2 GC Analysis

A Shimadzu 8A GC-FPD instrument (Shimadzu Corporation, Kyoto, Japan) was used to analyze samples. A megabore DB-5 column (30 m x 530 µm i.d.; 1 µm thickness; Agilent Technologies) was employed for separations using a high purity helium (Praxair) carrier gas. The optimum flow was 3 mL/min, but was occasionally set to 11 mL/min for faster analyses. Note the GC conditions used are "fit-for-purpose" (i.e. not designed for a given application), and only used to demonstrate the concept of the sample preparation. High purity hydrogen and oxygen (both Praxair), at respective flows of 40 and 7 mL/min, supplied the flame gases. Signal response was monitored by a Hamamatsu photomultiplier tube (R-268P; Hamamatsu, Bridgewater, NJ, USA) without an interference filter. For certain work, an adjacent flame ionization detector (FID) was also used with 300 mL/min air and 100 mL/min hydrogen. PeakSimple Software (SRI Instruments) was used to acquire data.

2.2.3 General Procedure

Normally, a standard solution of sulfur analytes in hexane (1 mL) was placed in a glass vial at room temperature and solid PbO (0.04 to 0.08 g) or PbO_2^{2-} solution (0.5 to 1.5 mL; 0.06 M) was added to it. The mixture was then briefly shaken to rapidly remove the thiols by precipitating the solid lead thiolate complex according to either Reaction 1 or 2:

$$PbO + 2RSH \rightarrow Pb(SR)_2 + H_2O \qquad \text{(Reaction 1)}$$

$$PbO_2^{2-} + 2RSH \rightarrow Pb(SR)_2 + 2OH^- \qquad \text{(Reaction 2)}$$

Following this, the remaining hexane layer was typically removed by hand using a pipet, or alternatively by careful evaporation with a low stream of high purity N_2 (Praxair) across the surface. A new organic layer of equal or reduced volume (as appropriate to the experiment) was then added in its place using a pipet. The trapped thiols were recovered from the lead thiolate complex by adding sufficient 1 M HNO_3 to neutralize the solution and protonate the thiolates, which were reconstituted into the new organic layer as a result. This step was also visually confirmed by the disappearance of the yellow thiolate complex according to Reaction 3:

$$Pb(SR)_2 + 2HNO_3 \rightarrow 2RSH + Pb(NO_3)_2 \qquad \text{(Reaction 3)}$$

Specific conditions for several applications that were performed are given below.

2.2.3.1 Natural Gas

A capped 1 L Erlenmeyer flask was thoroughly flushed and filled with a natural gas sample spiked with 104 ppm of tert-butylthiol. A gas-tight syringe was used to withdraw 40 mL of this sample and it was dispensed through a 5 mL solution of PbO_2^{2-} placed in a glass vial. The solid yellow thiolate complex immediately formed atop this aqueous layer. Hexane (1 mL) was then added to the vial and the solution was neutralized with 1 M HNO_3 to capture the thiol analyte. The organic layer was then analyzed by GC for its thiol content.

2.2.3.2 Petroleum Condensate

A model condensate sample was prepared by combining pentane, hexane, heptane, cyclohexane, benzene, toluene (4:4:4:1:1:1 ratio) and spiked with 610 ng/µL of 1-butanethiol. A 1 mL aliquot of the sample was added to a vial containing 1.5 mL of PbO_2^{2-} solution and the mixture was shaken briefly to form the thiolate complex. The organic layer was removed by evaporation with N_2 and 1 mL of fresh hexane solvent was added. This solution was then neutralized with 1 M HNO_3 to recover the thiol as above prior to GC analysis of the hexane layer.

2.2.3.3 Gasoline

A 1 mL volume of a gasoline sample spiked with 600 ng/µL of 1-butanethiol was placed in a vial. A 0.04 g portion of solid PbO was added to the sample and it was allowed to equilibrate and form the thiolate complex. The gasoline matrix was then removed by pipet and it was rinsed 3 times with equal washings of hexane. A final 1 mL aliquot of hexane was then added to the vial and the thiol compound was released as above using 1 M HNO_3, prior to GC analysis.

2.2.3.4 Garlic

A bulb of garlic (36 g) was coarsely chopped and placed inside of a capped, N_2-purged 125 mL Erlenmeyer flask and allowed to equilibrate for several hours, during which time it was analyzed at specified points. At each interval, 10 µL of headspace was taken by syringe and analyzed directly by GC. Following this, 40 mL of headspace was removed using a gas-tight syringe and it was dispensed through a 1.5 mL PbO_2^{2-} solution, forming the thiolate complex. Next, 1 mL of hexane was added to this solution and it was neutralized with 1 M HNO_3 as above to recover the thiol prior to analyzing the organic layer. Any other

details are outlined in the text.

2.3 Trap-and-Release System for the Determination of Thiols by GC-FPD

2.3.1 Reagents

Similar to Chapter 2.2.1, a 0.06 M PbO_2^{2-} solution was used for trapping thiol compounds. The thiol tested was 1-butanethiol (Sigma-Aldrich) in an n-hexane (Sigma-Aldrich) solvent. Diethyl sulfide (Sigma-Aldrich) was also tested in this system, as a non-thiol compound for comparisons. The releasing acid in this study was formic acid (96%; Sigma-Aldrich).

2.3.2 Instrumentation and Set-up

A Shimadzu 8A GC-FPD instrument (Shimadzu Corporation) with a megabore DB-5 column (30 m x 530 µm i.d.; 1 µm thickness; Agilent Technologies) was employed for separations using high purity helium (Praxair) as carrier gas (Figure 2-2). Oven temperature was typically 30 °C. A 50 cm length of fused silica (250 µm i.d.; Biotaq) was coated with PbO_2^{2-} solution and was used as the trap column. Another fused silica shunt (20 cm x 250 µm i.d.; Biotaq) inserted into the injector was connected to the trap through a ZDV union (Vici-Valco). The other end of the trap was connected through another ZDV union to the analytical column. The trap was outside of the oven to allow for the same conditions as the offline method as described in Chapter 2.2.3 (i.e. room temperature reaction), and also for ease of coating and changing the trap when required. Other modifications to this set up are

mentioned in the text. Data acquisition was performed using PeakSimple Software (SRI Instruments).

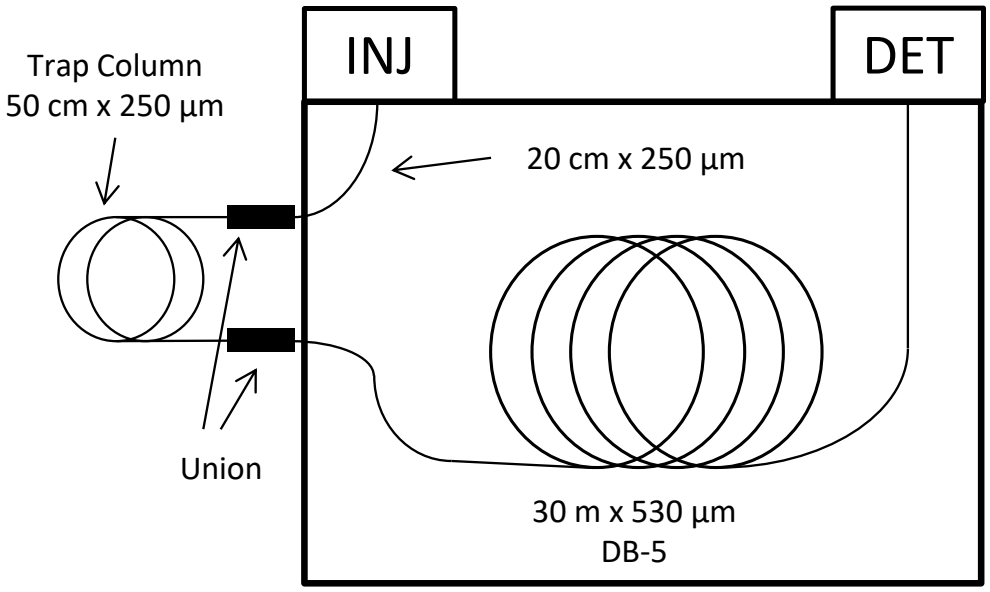

Figure 2-2: Schematic diagram of the Trap-and-Release GC-FPD system.

2.4 Micro-Flame Photometric Detection in Miniature Gas Chromatography on a Titanium Tile

2.4.1 Instrumentation

A Shimadzu GC-8A instrument (Shimadzu Corporation) was employed to perform injections. The injector temperature was kept constant at 200 ºC and a split ratio of 1:100 was commonly used. A 15 cm length of 250 µm i.d. fused silica tubing (Biotaq) was led from the injector and connected to the carrier gas inlet of the Ti µGC tile by a gas tight Vespel fitting (see below). High purity helium (Praxair) was used as the carrier gas with a typical flow rate

of about 0.1 mL/min. High purity oxygen and hydrogen (both Praxair) were each employed for FPD operation. These flame gases were similarly delivered through lengths of 250 µm i.d. fused silica tubing (Biotaq) attached to the tile by gas tight Vespel fittings at their respective inlets. With these connections in place, the Ti µGC tile was positioned adjacent to the GC mainframe where injections were performed, while separation and detection were accomplished on-board the µGC device.

2.4.2 Ti µGC-FPD Device

The Ti µGC tile employed in this work was obtained from Waters Corporation (Milford, MA, USA) and its construction has been previously described in detail [56]. A schematic of the device is depicted in Figure 2-3. Briefly, two rectangular Ti tiles (each 7.5 cm x 15 cm x 660 µm thick) were joined together to form a single Ti device. One of the tiles had been etched with a channel such that the resulting device contained a 5 m long x 100 µm i.d. serpentine column that was subsequently coated with OV-101 stationary phase [56]. At the column outlet, a channel for flame gases (5 cm x 228 µm i.d.) was etched along the width of the tile. The hydrogen inlet was incorporated at the junction of the column outlet and this channel while the oxygen inlet was added to the terminal end of the channel. In the middle of its length, a 1.44 mm i.d. hole was bored through the monolithic tile to create a flame cavity. Carrier gas was incorporated at the column inlet.

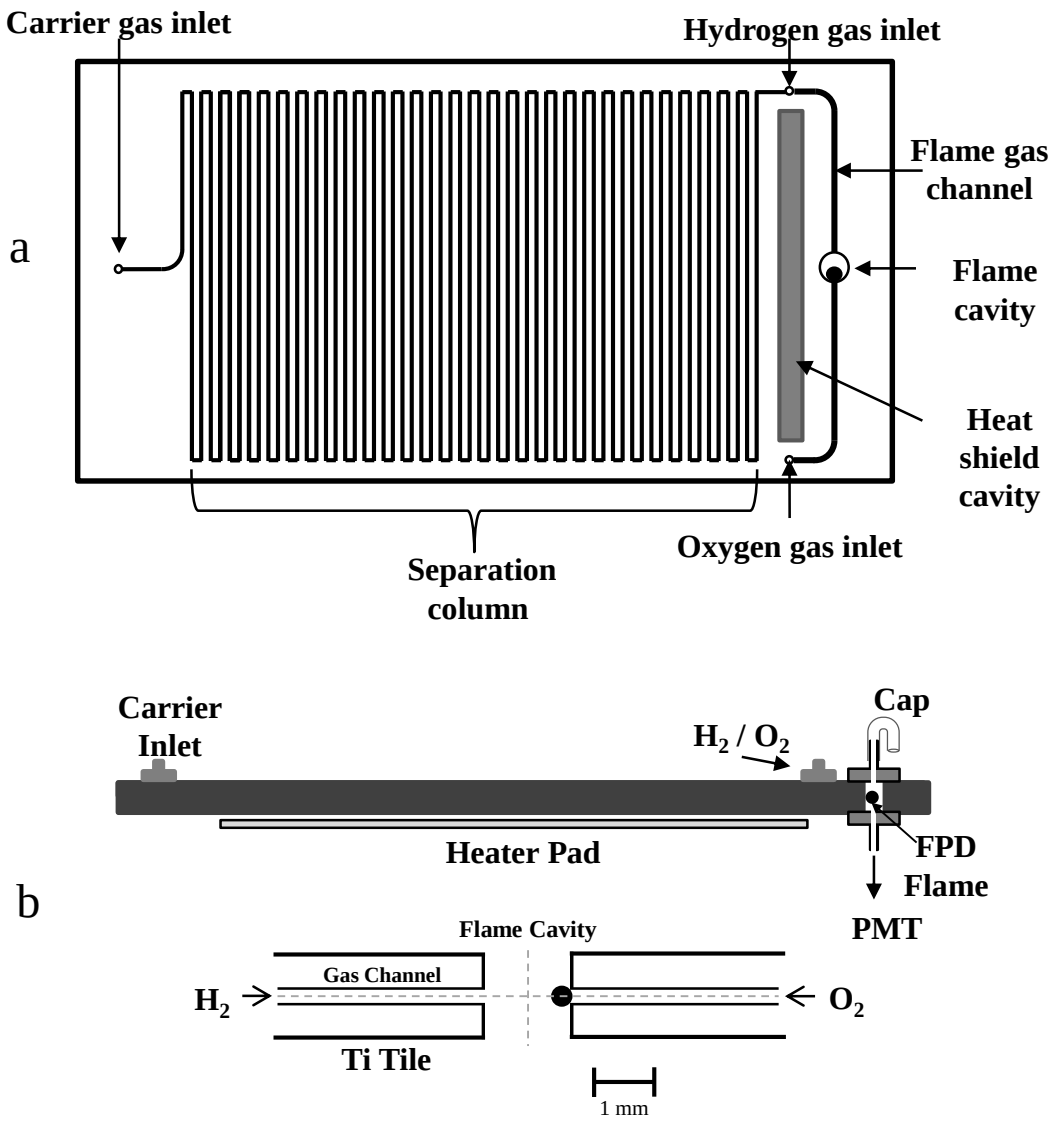

Figure 2-3: Schematic diagram of the Ti µGC-FPD device showing the a) top down view, b) side view (upper) and alignment of the channels with respect to the flame cavity (lower)

Each flow inlet was secured by a custom made 316 stainless steel gas tight fitting (9.0 mm o.d. x 2 mm i.d.) that was bolted onto the Ti tile. The fittings were threaded to accept a one-piece Vespel nut/ferrule assembly (0.4 mm i.d. x 13 mm long) to hold the fused silica

gas transfer line in place. This allowed the formation of a zero dead volume interface between the gas inlet hole on the tile and the tubing outlet. Between the separation column and the flame cavity, a 3.5 cm long x 0.3 cm wide rectangular piece was excised from the tile to thermally isolate the column and shield it from the heat of the detector flame. The temperature of the column was regulated by a 76 mm x 102 mm Minco Thermofoil Heater (model 5466; Minco Products Inc, Minneapolis, MN, USA) that was adhered to the column side of the Ti device. Temperature control was maintained by a standard variable transformer (120 V supply, 10 A max; model 3PN 1010, Staco Inc., Dayton, OH, USA) that allowed the device to be readily and repeatedly maintained at temperatures up to 100 ºC (1.8% RSD; n=5) for well over an hour.

To enhance FPD operation, the flame cavity was bounded by stainless steel fittings (3 mm o.d. x 1 mm i.d. x 6.5 mm long) on both sides of the tile cavity (Figure 2-3b). This helped maintain a hydrogen-rich atmosphere to support chemiluminescence in the flame. The FPD operated at counter-current flows of 7 or 10 mL/min oxygen (for sulfur or phosphorous analysis respectively) and 40 mL/min hydrogen. Analyte emission from the flame was transmitted through a sealed quartz light guide (3 mm o.d. x 17 cm) fixed to one end of the FPD flame cavity, and was delivered to a photomultiplier tube (PMT; R-268P; Hamamatsu) placed at the other end that was used to monitor the signal. Selective sulfur analysis was achieved by placing a 393 ± 11 nm interference filter (Oriel Instruments) in front of the PMT, while phosphorous analysis utilized a 527 ± 10 nm filter (Melles Griot, Rochester, NY, USA). The PMT was also occasionally operated in open mode (no filter) for other analyses. The opposite side of the flame cavity was fitted with a tiny removable light tight aluminum

cap for venting of flame gases and ease of viewing as required in experiments. The signals were acquired and processed through PeakSimple Software (SRI Instruments).

2.4.3 Reagents and Supplies

Diethyl sulfide (98%), diethyl disulfide (99%) and trimethyl phosphite (99%) were purchased from Sigma-Aldrich while tetrahydrothiophene (97%) was obtained from Fluka Analytical. These were used as test analytes and prepared in n-hexane (99%; Sigma-Aldrich) to achieve standard solutions. Hexane and benzene (99.9%; EM Science, Gibbstown, NJ, USA) were used to gauge hydrocarbon response in the detector. A garlic bulb obtained from a local vendor was prepared for headspace analysis of allyl mercaptan by coarsely chopping the bulb (32 g) and placing it inside of a capped, N_2-purged, 125 mL Erlenmeyer flask. After equilibrating for 1 hour, 10 µL of headspace was taken by syringe and analyzed directly with the device. In-house natural gas was also analyzed. The sample was prepared by thoroughly flushing a capped, 1 L Erlenmeyer flask and filling it with a natural gas sample containing 130 ppm of tetrahydrothiophene. From this, 10 µL of sample was withdrawn and injected onto the tile for µGC-FPD analysis. Any other details are noted in the text.

CHAPTER THREE: ANALYSIS OF SULFUR COMPOUNDS USING A WATER STATIONARY PHASE IN GAS CHROMATOGRAPHY WITH FLAME PHOTOMETRIC DETECTION

3.1 Introduction

As discussed, a common approach used for the analysis of volatile organic compounds containing sulfur is GC-FPD. However, the signal quenching that occurs when analytes co-elute with hydrocarbons decreases the observed response and can compromise analytical results [94]. One such means of overcoming this barrier has been the pursuit of better separation between hydrocarbons and sulfur compounds to prevent co-elution and response quenching [95]. Currently, many sulfur compounds are separated using conventional non-polar (e.g. dimethylpolysiloxane) [96–103] or polar (e.g. porous layer open tubular) [104] columns. However, the general effectiveness of these columns is still largely hindered by the limited resolution achievable for most complex mixtures. As a result, separation columns that can yield higher selectivity for sulfur compounds over other hydrocarbons in such matrices could potentially further facilitate GC-FPD utilization and would be beneficial to explore.

Previous investigations with a water stationary phase for use in capillary column GC have demonstrated unique selectivity toward moderately polar compounds. Of note, retention has been shown to be primarily based on analyte water solubility and minimally dependant on volatility [39]. Thus, non-polar hydrocarbons display almost no retention in this method, while functionalized compounds are relatively well-retained. As of yet, an extensive examination of organosulfur compounds on the water stationary phase has not been reported.

In this chapter, the potential of a water stationary phase for analyzing organosulfur compounds is explored. The system compatibility with selective detection from an FPD is also demonstrated. Several analytes and their retention characteristics are examined and FPD performance when coupled with the water phase is investigated. Various system applications will be presented and discussed. The combined selectivity from a selective column and detector is found to provide a relatively simple means for direct, quenching-free, and sensitive analyses of such sulfur compounds in complex mixtures.

3.2 General operating characteristics

Initial efforts were aimed at establishing the FPD performance characteristics within the assembled system (see Chapter 2.1.1). For example, although no interference was anticipated, it was uncertain if the water-laden carrier gas might adversely impact the detector's background emission and analytical properties, as the FPD had never before been coupled with this phase. However, upon probing this further, it was indeed found that the FPD yielded favorable and appropriate response behavior. For instance, experiments revealed that with and without the water phase present in the system, the background flame emission intensity remained very low in either case and differed by only 4% over a wide range of system operating temperatures. This stability was also observed with various carrier and flame gas flows. Of note, as flows were considerably varied during optimizations, the system noise changed very little with and without the water present and only altered on average by a factor of about 1.3. Therefore, no appreciable interference was noted in the detector from the added water vapor present.

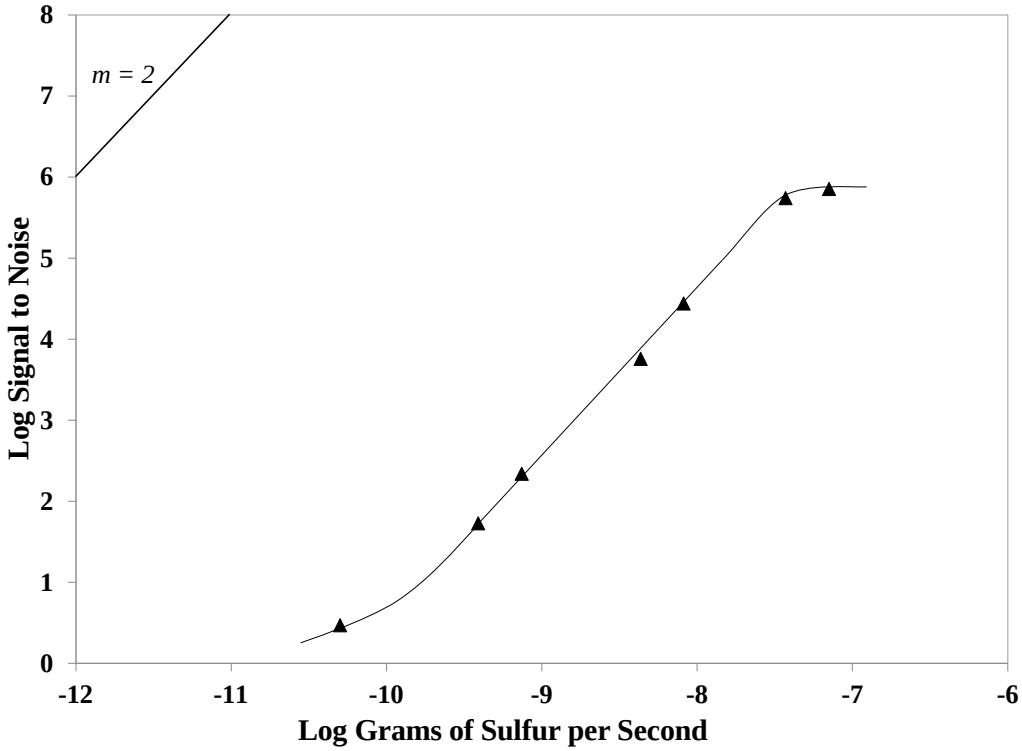

Figure 3-1: Calibration curve for dimethyl sulfide response using the water stationary phase GC-FPD system.

Accordingly, good sulfur response was observed with the system. In terms of performance characteristics, the calibration curve of dimethyl sulfide is shown in Figure 3-1. As seen, the response obtained increases pseudo-quadratically over about 3 orders of magnitude (roughly 30 pgS/s to 30 ngS/s) and yields a minimum detectable limit near 30 pgS/s. Similar results were obtained with other analytes as well. This response was also quite selective over hydrocarbons, as no signal was observed for dodecane or benzene below amounts of about 150 µg injected on column. This translated into a formal selectivity for sulfur over carbon of about 3×10^4. In all, these values agree quite well with those of conventional GC-FPD methods and most modern commercial manufacturers [57,105,106].

Therefore, the results indicate that the water stationary phase system can readily interface with an FPD for the analysis of organosulfur compounds.

3.3 Retention characteristics of sulfur analytes

In order to better understand the relative retention characteristics of the system, a number of organosulfur analytes were examined with it. Table 3-1 shows an example of this with the retention time observed for the various analytes under isothermal conditions of 30 ^{o}C. As seen, the compounds are listed in increasing elution order and they show varying degrees of retention. However, a few interesting trends can be noted from the data.

For example, many analytes show a "normal phase retention pattern" akin to that observed in HPLC, where more polar compounds are more strongly retained, similar to earlier work with the water stationary phase [37–39]. Of note, this is demonstrated by the elution of sulfides, where the less polar dipropyl sulfide elutes before the increasingly more polar diethyl and dimethyl sulfides. Similarly, the disulfide series elutes in an analogous fashion. Furthermore, in addition to analyte polarity, these elution patterns also trend closely with greater analyte water solubility in many cases. For instance, dimethyl sulfide is nearly 2 orders of magnitude more water soluble than dipropyl sulfide [107]. As well, dimethyl disulfide is near 10-fold more water soluble than diethyl disulfide [107,108]. Note that while this property may also imply a potential relationship between analyte retention and Log Kow partitioning, very few values (i.e. only 5) are available for the analytes studied here. Nonetheless, of those obtained, a good linear relationship between Log Kow and retention was found, with an R^2 correlation of 0.9. However, this parameter needs more data in the future to establish a verifiable trend (if any).

Table 3-1: The retention* of various organosulfur analytes on the water stationary phase.

Compound	t_r (min)	Boiling point (°C)	Structure
hexane	2.26	68.72	
carbon disulfide	2.30	46.2	
tert-butylthiol	2.50	64.2	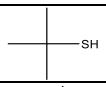
2-propanethiol	3.02	52.6	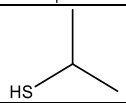
2-butanethiol	3.05	85.0	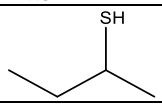
1-propanethiol	3.16	67.7	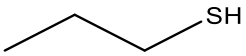
dipropyl sulfide	3.58	142.8	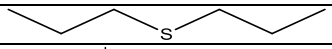
isopropyl disulfide	3.84	177	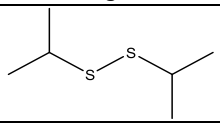
diethyl sulfide	3.88	92.1	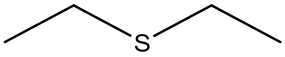
1-hexanethiol	4.09	152.7	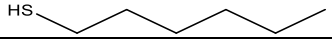
dimethyl sulfide	4.15	37.32	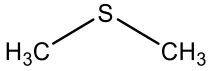
diethyl disulfide	4.21	154.0	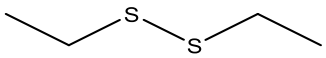
dimethyl disulfide	5.24	109.72	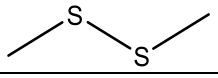
1-butanethiol	5.33	98.4	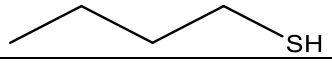
tetrahydrothiophene	12.29	121.1	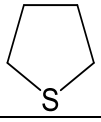
thianaphthene	25.76	220.9	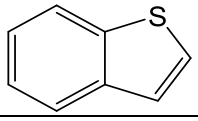

*Column temperature is 30 °C and carrier flow is 2.5 mL/min.

In contrast to this, analyte boiling point does not seem to correlate well with retention. For example, also included in Table 3-1 is the boiling point for each compound. It can be seen that as retention times increase, there is no apparent trend in the corresponding analyte boiling point. For instance, even though dimethyl sulfide possesses the lowest boiling point of 37 ºC, it is more retained than a number of other higher boiling point analytes, including several thiols, sulfides, and even diisopropyl disulfide, which boils at 177 ºC. Additionally, several other similar cases can be seen where this occurs as well. Therefore, in many instances, increasing polarity and water solubility appear to be key factors in promoting sulfur analyte retention on the water stationary phase, while boiling point is less relevant. This also agrees well with previous findings for other hydrocarbons on this phase [39].

It should be noted that certain thiols did not exhibit this retention behavior. As seen, 1-propanethiol was found to elute before 1-butanethiol. Even more odd, 1-hexanethiol eluted between these analytes. However, of the compounds examined, the latter was also the only one to yield a very poor, broad peak shape. This may be due to potential interactions with the stainless steel column wall, as it is well known that some thiols can strongly adhere to such surfaces [109]. In fact, when probing this further, 1-hexanethiol did show some retention on dry stainless steel tubing, whereas other analytes did not. Therefore, it appears possible that such interactions could potentially influence the retention behavior of certain thiols in this system. Still, aside from the adverse separation characteristics noted for 1-hexanethiol, good peak shape and retention behavior was generally noted for the other compounds investigated here. Figure 3-2 illustrates this with the separation of some different organosulfur species using the assembled GC-FPD system.

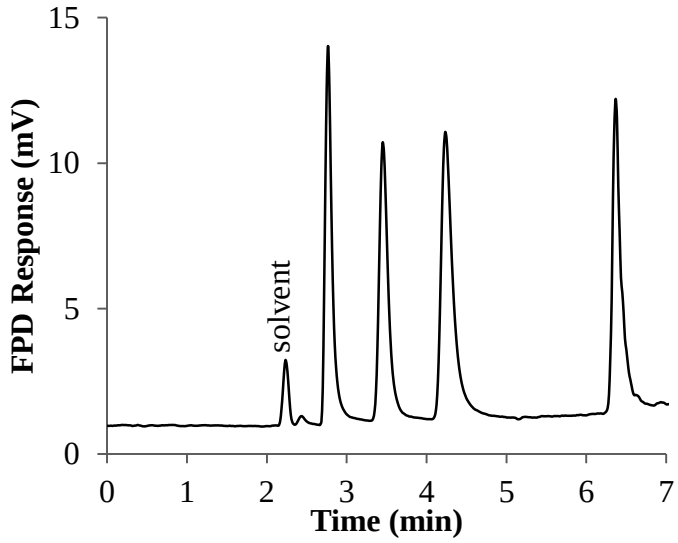

Figure 3-2: Chromatogram showing the separation of various sulfur analytes using the water stationary phase GC-FPD system. The temperature program is 30 ºC for 2 min, then 20 ºC/min to 70 ºC, and then 47 ºC/min to 140 ºC. The elution order is 2-propanethiol, diethyl sulfide, dimethyl disulfide, and tetrahydrothiophene.

3.4 Reduced FPD quenching

Since addressing FPD quenching was a primary motivation for this study, it was of interest to examine how this may be impacted by the current method. In particular, since most non-polar hydrocarbons are essentially unretained on the water stationary phase, it was anticipated that this might be able to offer beneficial selectivity in cases where peak co-elution can lead to detrimental FPD response quenching. Figure 3-3A demonstrates this issue for a dimethyl disulfide standard solution in octane on a conventional DB-1 column.

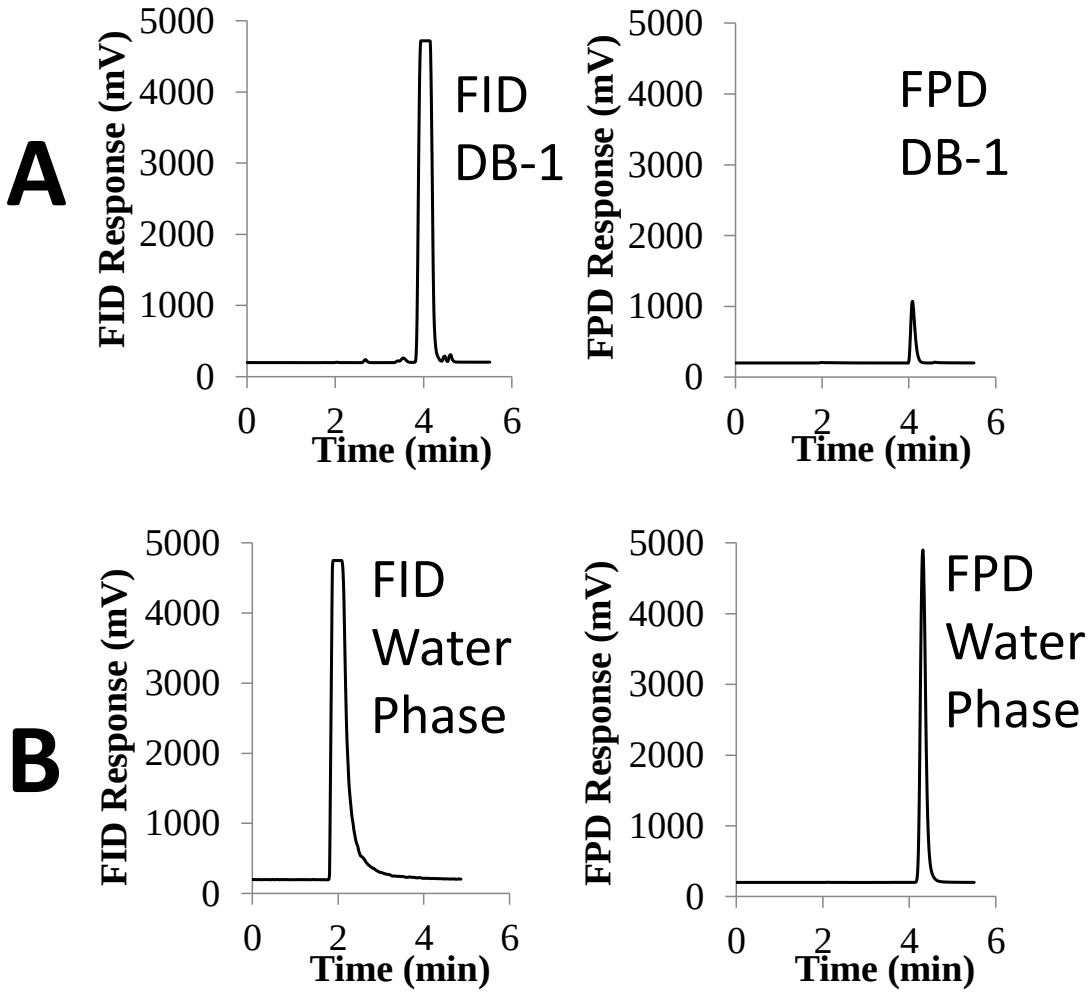

Figure 3-3: The FID (left) and FPD (right) traces of 220 ng of dimethyl disulfide in octane solvent on (A) a conventional DB-1 column and (B) the water stationary phase. Oven conditions are (A) 50 ºC for 2 minutes, then 10 ºC/min to 100 ºC, and (B) 30 ºC.

As seen from the octane solvent in the FID trace (left) and the dimethyl disulfide peak in the FPD trace (right), the two co-elute and fully overlap. As a result, the sulfur response obtained is severely quenched and the peak intensity shown is diminished to just 29% of its anticipated value. This is determined by referencing signals against an identical unquenched analyte standard in a non-overlapping hexane solvent on the same column. By comparison,

Figure 3-3B shows the same analysis with the water stationary phase system. As shown, the FID trace (left) displays rapid elution and low retention of the non-polar octane solvent on the phase, still yielding similar hydrocarbon response (within a factor of 1.3) to that obtained in Figure 3-3A. Conversely, though, the sulfur analyte is retained and well separated from octane. As a result, no hydrocarbon response quenching is observed in the FPD analysis. Therefore, in complex matrices containing numerous hydrocarbons, this retention behaviour may be potentially useful for alleviating FPD quenching of sulfur analyte signals.

To examine this, a gasoline sample spiked with diethyl sulfide, dimethyl disulfide, and tetrahydrothiophene was also analyzed on a conventional DB-1 column and the water stationary phase. As seen from the FID chromatogram of the DB-1 trial (Figure 3-4A), the hydrocarbon matrix continually elutes across the 10 minute period displayed. The 3 sulfur test analytes were also found to elute within this same range. As a result, significant analyte signal quenching was observed for this sample in the FPD. Table 3-2 displays the response erosion that was measured for each analyte, and indicates that about half of the signal was lost due to quenching from overlapping hydrocarbons. In contrast to this, the water stationary phase promotes rapid elution of these same non-polar gasoline components (Figure 3-4B), and prevents hydrocarbon co-elution and interference with FPD sulfur response as a result.

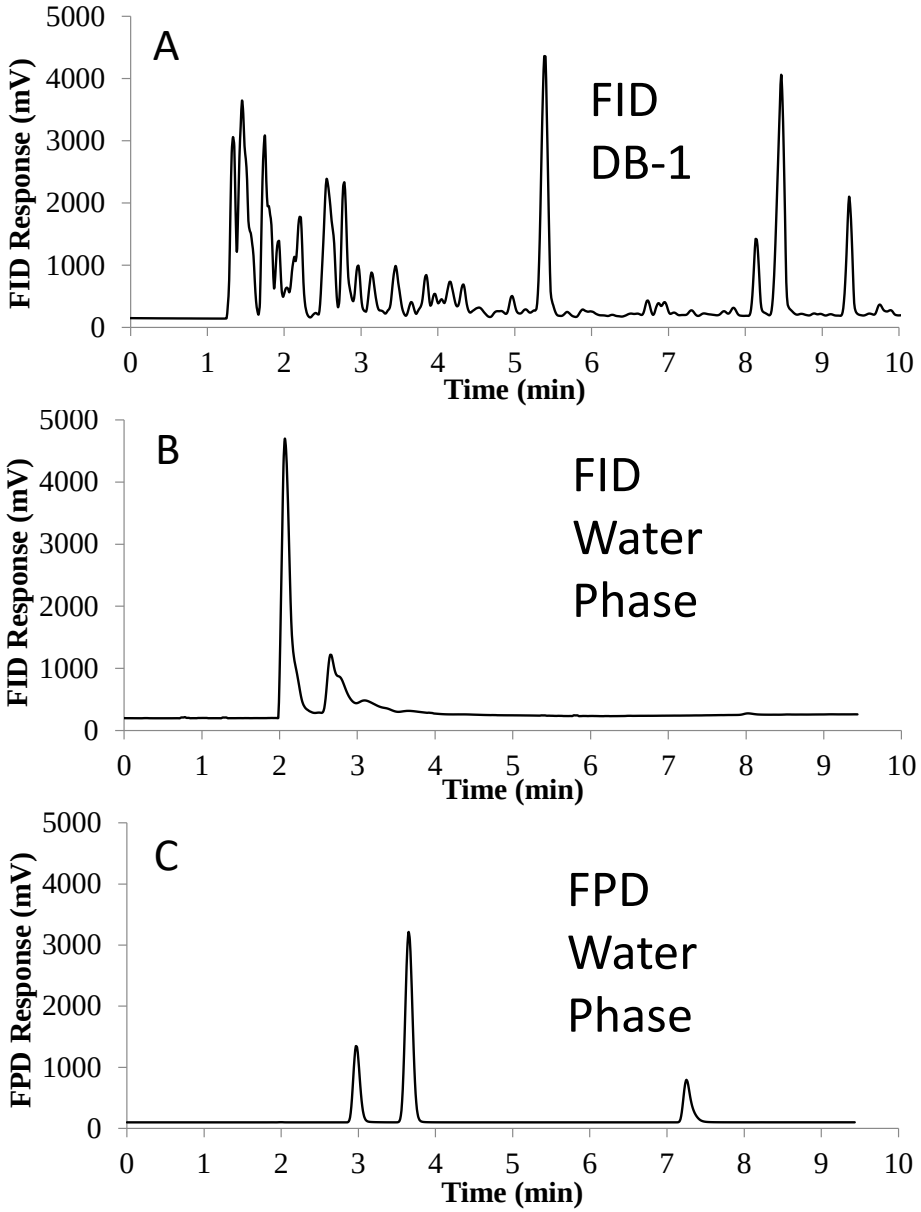

Figure 3-4: The FID chromatograms of gasoline spiked with 120 ng of diethyl sulfide, dimethyl disulfide, and tetrahydrothiophene on (A) a conventional DB-1 column and (B) the water stationary phase. The unquenched FPD sulfur signals arising from the latter water phase trial are also shown in (C). Oven conditions are (A) 30 °C for 1.5 minutes, then 5 °C/min to 120 °C, and (B, C) 30 °C for 4.5 minutes, then 20 °C/min to 100 °C.

Table 3-2: Preservation[a] of FPD sulfur response in gasoline analyzed on different columns

Analyte	Conventional DB-1	Water Stationary Phase
Diethyl sulfide	48 ± 9 %	97 ± 3 %
Dimethyl disulfide	57 ± 9 %	105 ± 11 %
Tetrahydrothiophene	45 ± 9 %	109 ± 14 %

[a] As a percentage of the original unquenched response of a reference standard in hexane; n = 3.

Of note, the data in Table 3-2 demonstrate that the sulfur signal is essentially fully preserved when the same sample is analyzed on the water stationary phase. Figure 3-4C further illustrates this with the unquenched FPD sulfur signals obtained from this trial. Therefore, the large bias of the water phase against retaining non-polar hydrocarbons can allow for such components in complex matrices to be completely separated from target analytes and greatly facilitate FPD sulfur analyses.

3.5 Sulfur analysis in other complex matrices

In an analogous fashion, the water stationary phase can also simplify the analysis of other complex matrices that contain a variety of more polar sample constituents. For example, it has been shown previously that highly polar matrix components are often fully retained on the water stationary phase, while more mobile target analytes can be eluted and quantified [39]. Further, there is no subsequent concern for column fouling from the retained species since the water stationary phase can be readily discarded and replenished on demand.

Therefore, it was of interest here to also analyze for sulfur in some other challenging matrices using this system.

The first of these was a red wine sample spiked with dimethyl sulfide and dimethyl disulfide. The analysis of these compounds is important since they are often found in wine and can be indicators of bad flavouring if present in high concentrations [110]. However, wine also contains many other components such as sugars, polyphenols, and proteins that increase the turbidity of the product. These can often make GC quantification of the sulfur-containing flavour compounds difficult and they frequently necessitate the use of multiple sample preparation steps prior to analysis [111]. As seen from Figure 3-5, direct injection of the neat wine sample on the water stationary phase results in two prominent peaks for these target analytes on an otherwise smooth background with no other apparent matrix interference. This was also supported by FID examinations of the same sample, which were similar in appearance and indicated that many of the other polar and/or high molecular weight components present in the wine remained highly retained on the water phase and did not interfere with the sulfur analysis at hand. Incidentally, while the presence of sulfur dioxide might also be anticipated in such a sample, it was found here to be very highly retained. For example, it did not elute after an hour of observation, even at 100 ^{o}C using the 30 m column. Therefore, if it were a target analyte in future investigations using this method, the employment of a shorter column could be beneficial.

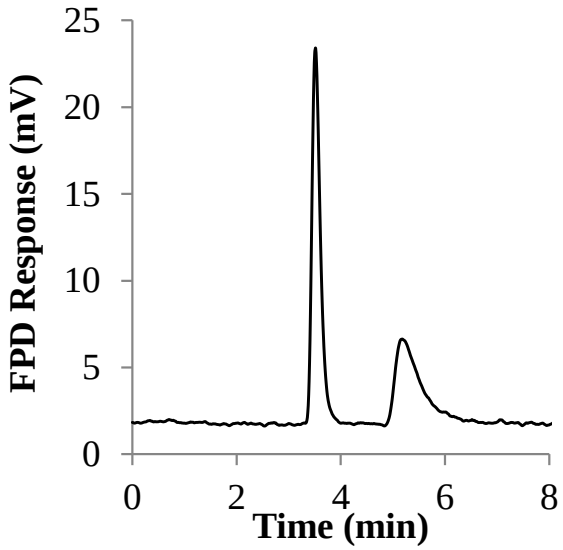

Figure 3-5: The FPD chromatogram of dimethyl sulfide (15 ng) and dimethyl disulfide (30 ng) in an undiluted red wine sample directly injected onto the GC water stationary phase. Oven temperature is 30 °C.

The second sample investigated was milk, which is subject to similar quality issues when high concentrations of sulfurous compounds are present [20,112]. Additionally, milk can be a very challenging matrix since it is a heterogeneous solution often containing various casein proteins, significant amounts of large triglycerides, and abundant sugars such as lactose, all of which can complicate GC analysis [20,112]. As shown in Figure 3-6, when a neat injection of milk containing dimethyl sulfide was analyzed on the water stationary phase, a prominent analyte peak is again observed on an essentially unobstructed background (i.e. no response from large hydrocarbon concentrations breaching the detector selectivity). Therefore, as with the red wine sample, many of the large, polar components in milk appear to be highly retained by the phase, allowing for a relatively simple analysis of the sulfur analyte. This was further confirmed by FID examination of the sample, which showed a very

similar trace with the addition of some minor unretained hydrocarbons that eluted early in the separation and did not interfere.

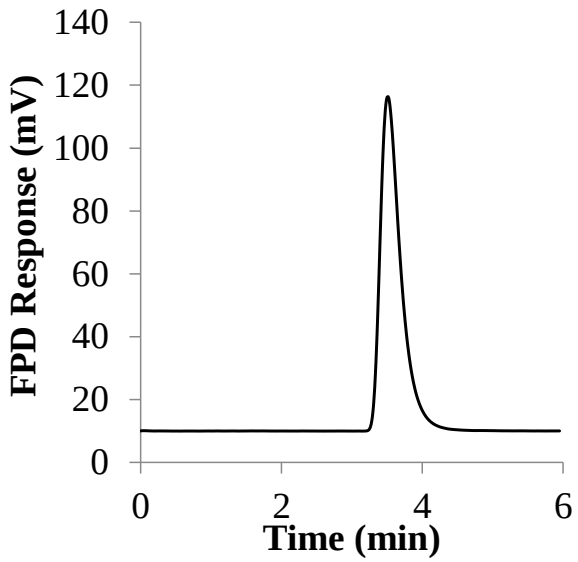

Figure 3-6: The FPD chromatogram of dimethyl sulfide (30 ng) in an undiluted milk sample directly injected onto the GC water stationary phase. Oven temperature is 30 ^{o}C.

A final investigation focused on the analysis of urine, which is an important area of research that can facilitate the diagnosis of a number of health issues. For example, decreased levels of urinary dimethyl sulfide have been correlated to instances of breast cancer [113], while increased dimethyl disulfide concentrations have also been noted as an indicator of skin cancer [114]. Currently, GC analysis of these analytes in such complex matrices can be difficult as urine often contains thousands of metabolites in each sample, including larger components such as steroids, protein hormones, and collagen cross-linker metabolites [115].

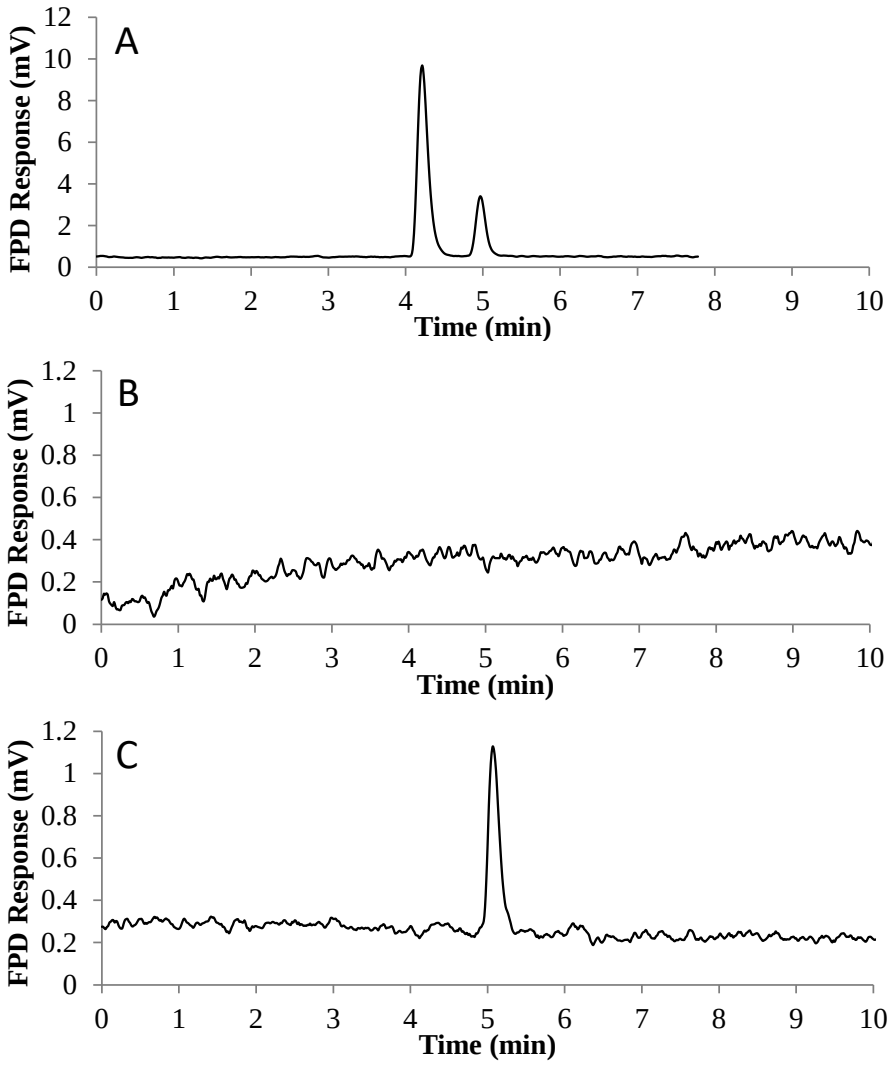

Figure 3-7: Direct injections of urine in the water stationary phase GC-FPD system. The samples are (A) urine spiked with dimethyl sulfide (15 ng) and dimethyl disulfide (30 ng), (B) unspiked urine obtained before consuming asparagus, and (C) unspiked urine obtained after consuming 500 g of asparagus. Oven temperature is 30 °C.

Figure 3-7A demonstrates the chromatogram of a urine sample spiked with dimethyl sulfide and dimethyl disulfide that is injected directly into the water stationary phase system. As seen, these important organosulfur markers are well separated and produce good peak

shapes with no apparent background interference from the sample matrix (i.e. no response from large hydrocarbon concentrations breaching the detector selectivity). Again, this is because most of the other components present in urine are heavily partitioned into the water stationary phase and do not elute from the system. As before, FID examination of the same sample also further attested to this as little else was detected beyond the target analytes.

Given the strong signals obtained for the above spiked sample, another experiment was performed in efforts to monitor the endogenous formation of such target analytes. Asparagus is well-known for the pungent odour that it can create in the urine after consumption, which is due in part to the presence of sulfur compounds such as dimethyl disulfide that evolve during digestion [116]. Therefore, to examine if the system could be able to distinguish such an event at more biologically relevant concentrations, urine was obtained from a healthy individual before and after eating about 500 g of asparagus. As seen in Figure 3-7B, prior to ingesting the asparagus, no sulfur compounds appear in the urine, which was directly injected into the system. However, after eating the asparagus and collecting the urine several hours later for analysis, Figure 3-7C shows that there is an obvious presence of dimethyl disulfide that arises as a result. This was also evident from the relative odour of each sample. Of particular note, approximately 680 µg of this analyte was determined in the urine sample, which agrees very well with previous reports of near 770 µg of dimethyl disulfide being detected in the same volume of urine by headspace analysis [116].

Finally, it should also be noted that these separations reproduced quite well as repeat injections of the above samples yielded retention times that differed by only about 0.4% RSD (n=3). Therefore, overall the water stationary phase GC-FPD system provides reliable

performance that can potentially simplify the analysis of such complex samples by largely preventing matrix interference and reducing the need for sample preparation.

3.6 Conclusions

The analysis of various organosulfur compounds using a water stationary phase GC-FPD system has been described. The FPD demonstrated good compatibility with the phase and yielded figures of merit similar to those of a conventional GC-FPD system. The retention of a number of organosulfur compounds was examined on the column. Many of the analytes showed increasing retention as a function of water solubility and polarity. In all cases, analyte boiling point was generally a poor predictor of analyte retention. By comparison, most non-polar hydrocarbons are uniquely unretained on the water stationary phase. As a result, the FPD response for sulfur analytes was not subject to conventional signal quenching by co-eluting hydrocarbons, which greatly assists the analysis of complex samples such as petroleum products. Conversely, many large polar molecules are heavily retained on the water stationary phase. Accordingly, this can equally simplify the analysis of complex aqueous samples since they can be directly injected into the system and the sulfur analytes present can be determined with little matrix interference. These results suggest that this GC-FPD water stationary phase system could provide a useful alternative method for analyzing organosulfur compounds in complex matrices.

CHAPTER FOUR: A RAPID ANALYTICAL METHOD FOR THE SELECTIVE QUENCHING-FREE DETERMINATION OF THIOLS BY GC-FPD

4.1 Introduction

As seen in Chapter Three, the analysis of organosulfur compounds present in complex samples can be challenging. One such class of organosulfur compound that can be difficult to analyze is organic thiols. The analysis of thiols is an important area due to their inherent properties and prevalence in various sectors [104]. For example, owing to their negative effects on oil refinery equipment and the environment, their concentration in petroleum products is routinely regulated [117,118]. Further, thiols are often found in many foodstuff products, where they strongly impact smell and flavor [119,120]. Thus, frequent quality control analysis of thiols is required in matrices such as gasoline [88,121–125], condensate [126–128], natural gas [129–131], and foods/beverages [85,86,119,120,132–137]. However, due to the highly complex nature of many of these samples, the use of GC-FPD for such analyses can be limited.

To this end, sample preparation methods for thiols can be very helpful as an effective way to facilitate the continued use of GC-FPD and avoid quenching during analysis. For instance, petroleum and foodstuff samples are often prepared for thiol analysis by various extraction techniques [79,85–87]. In fact, on a much greater scale, the selective removal of thiols from large industrial process streams has been a significant interest for many years. For example, as early as the 1860s, Canadian petroleum producers employed a caustic 'Doctor Solution' containing plumbite ion (PbO_2^{2-}) in bulk refinery feedstocks to selectively complex thiols and form lead thiolates, which were then converted into less odorous disulfides after

reaction with powdered sulfur [88,122,138]. Even more recently, high concentrations of thiols have also been removed from such large scale petroleum streams using an analogous reaction with lead oxide (PbO), which forms a solid lead thiolate product that is filtered off by gravimetric means [89,90]. The separated thiols can then be recovered in the process by the addition of acid. Even though such bulk procedures are typically quite long (i.e. 1-2 hours) [89,90], they do demonstrate the effective removal of thiols in large industrial applications. Perhaps surprisingly, given their highly selective nature and potential benefit, similar approaches have never been developed and examined for their use in analytical methods.

This chapter presents a rapid analytical technique for the selective GC-FPD determination of thiols that employs primary facets of both of these industrial thiolate-trapping and acid-release approaches. The method is simple and inexpensive and greatly reduces hydrocarbon matrix components such that it can allow for FPD operation without quenching interference. The properties and characteristics of this technique are discussed and applications to various complex samples are demonstrated.

4.2 General Optimization

Initial experiments revealed that either solid PbO particles or PbO_2^{2-} (plumbite) solutions could be used to efficiently isolate thiols from samples for analysis. Figure 4-1 helps illustrate the typical observations of this process with the removal and recovery of a thiol standard from solution using PbO.

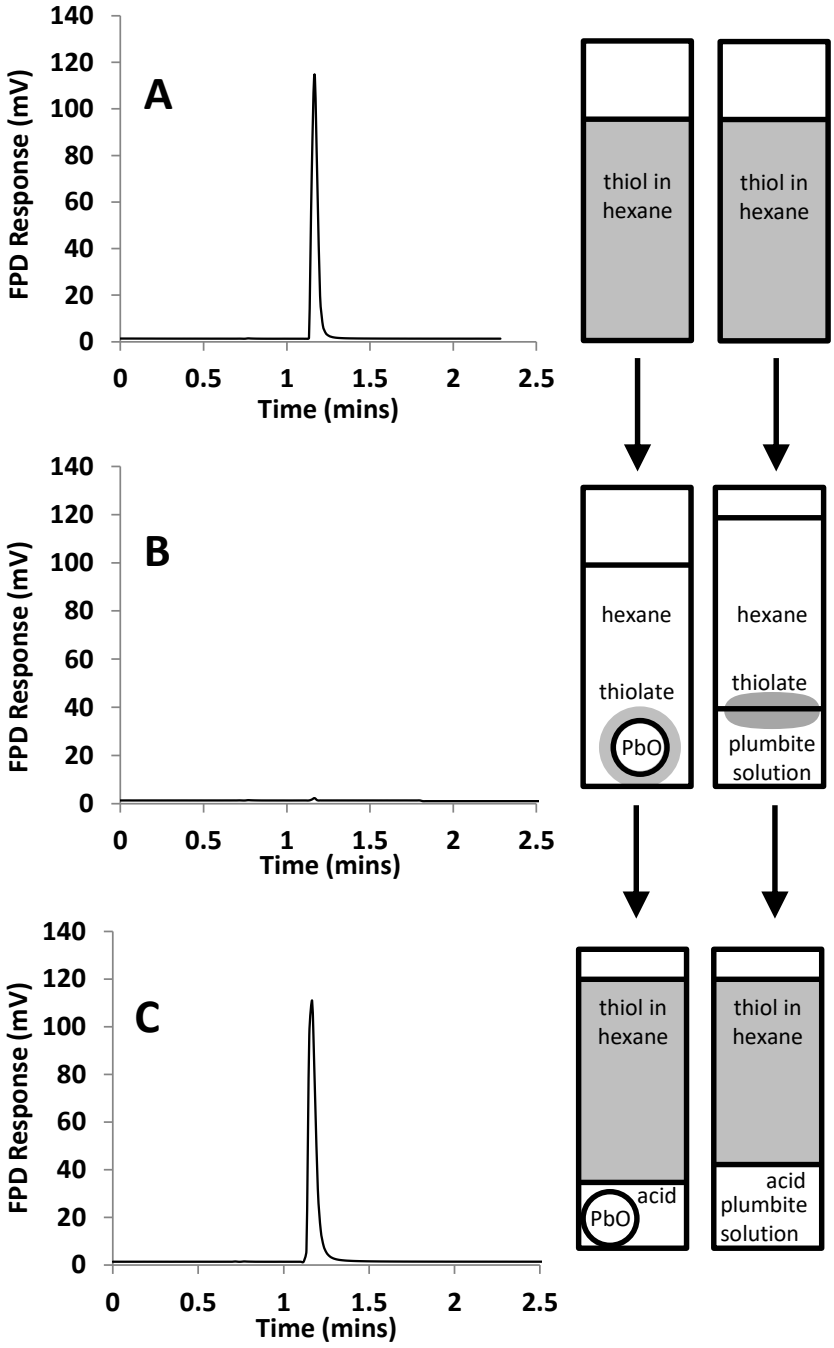

Figure 4-1: The analysis of a standard solution of 1-butanethiol (600 ng/µL) in hexane A) before adding PbO, B) after adding PbO, and C) after adding nitric acid (1 M) to the solution in B). Schematic illustrations of the process are shown adjacently for the use of solid PbO addition (left) and plumbite solution (right).

Figure 4-1A shows the analysis of the thiol standard in hexane before addition of PbO, and displays a prominent analyte peak. After addition of PbO (Figure 4-1B), analysis of the hexane layer indicates that the thiol has been effectively removed (>99%) from the solution by forming an insoluble lead thiolate complex on the particle surface. Note, this compares favorably to corresponding industrial-scale procedures, which typically remove about 80% of thiols present after an hour of treatment [89,90]. Following this, after addition of acid to the solution, the thiol is released from the complex and fully recovered back into the hexane layer (Figure 4-1C). This again is consistent with industrial-scale trials, which typically recover about 80% of the initial thiols removed [89,90]. Note that while the data here in Figure 4-1 was generated using solid PbO, very similar results were obtained when using plumbite solution to form a thiolate layer at the interface between the aqueous and organic solvents (also depicted in the figure). Therefore, it appeared that either lead substrate could provide a potentially effective route for isolating thiols for analysis.

Next, a closer examination was made of the relative ability of these substrates to extract thiols. Since thiolates have been formed in bulk hydrocarbon matrices using both red (litharge) and yellow (massicot) PbO [88,89], the two forms were compared to better reveal any differences in their extraction characteristics (Figure 4-2). While both demonstrated the ability to extract thiols, it was found that the red form was nearly 10 times slower at removing the analytes. Of note, while yellow PbO often quantitatively extracted thiols in about 25 min, the red form frequently took up to 4 h to achieve the same result. While the exact reason for this is not clear, it could be related to differences in the available lattice forms (orthorhombic or tetragonal) of the two species on the PbO particle surface [139].

Regardless, because yellow PbO had preferable properties, it was employed in subsequent trials.

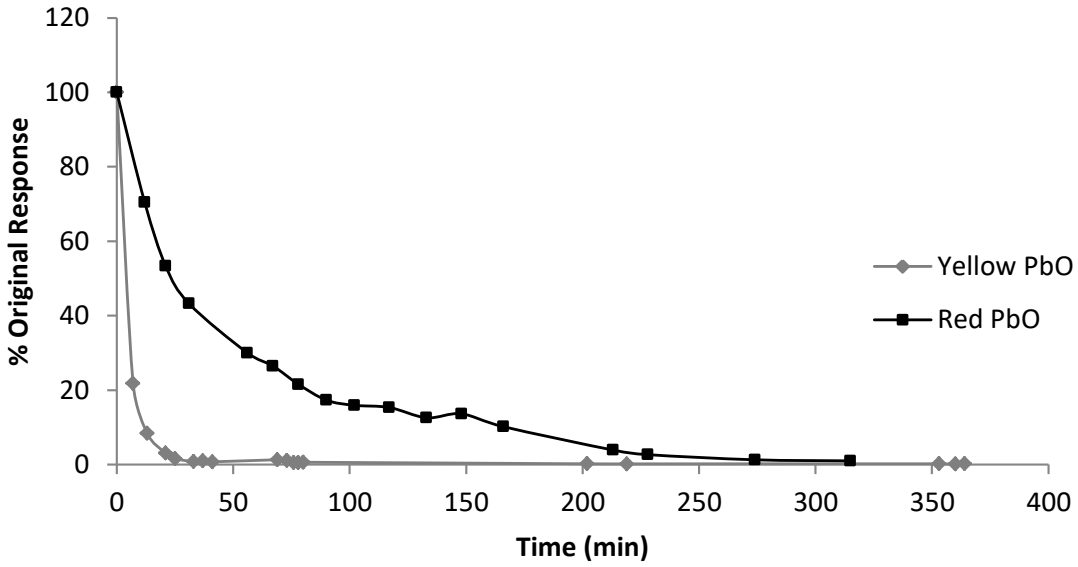

Figure 4-2: The percent of response remaining for 1-butanethiol (600 ng/µL) after the addition of yellow (♦) and red (■) PbO.

Since alkaline plumbite solution has also been used to remove thiols in bulk processes industrially [140], it was further compared here to the solid PbO substrate, shown in Figure 4-3. It was found that plumbite solution was particularly rapid at extracting thiols and was often near 10 fold faster than even the solid yellow PbO form. This is likely due to the relative mobility of the analyte and substrate in solution, which can enhance formation of the lead thiolate complex. As a result, thiols were reproducibly extracted from samples in a very short time using the plumbite solution. For example, 98 ± 1% (n = 3) of a 1-butanethiol standard in hexane (600 ng/µL) was extracted after only 2 minutes of contact with plumbite solution. Thus, similar to industry, both solid PbO and plumbite solution can each efficiently

extract thiols on an analytical scale, and appear to do so quite readily. Given the relatively rapid nature of the plumbite solution, it was primarily used here going forward.

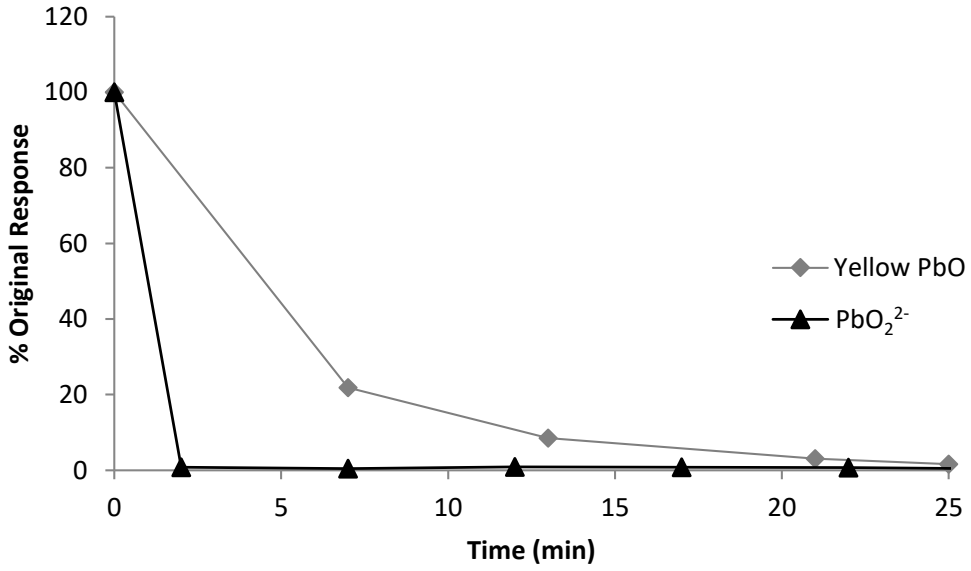

Figure 4-3: The percent of response remaining for 1-butanethiol (600 ng/µL) after the addition of yellow PbO (♦) and PbO_2^{2-} (▲).

Accordingly, a number of parameters were examined for their impact on thiol extraction efficiency using the plumbite solution. These included the volume (0.5 – 1.5 mL) and the concentration (0.06 – 0.015 M) of the plumbite solution used, and the concentration of analyte being extracted (60 – 1000 ng/µL). In general these variations did not greatly alter the overall extraction efficiency, and most trials yielded greater than 90% thiol removal after only 2 minutes. However, when the plumbite concentration was below about 0.03 M, it often took several minutes longer to achieve complete removal of the thiol from solution. Therefore, this is important to optimize and was normally maintained at 0.06 M in these experiments. The same was also true when analyte concentrations were low (near 60 ng/µL),

likely due to reduced contact between the thiol and substrate in solution. To offset this, it was found that increasing the plumbite solution volume could improve the extraction efficiency of more dilute analyte solutions, even though it had little effect for more concentrated solutions. Specifically, it was determined here that an analyte to plumbite solution volume ratio of 1 to 1.5 gave optimum results for analyte concentrations at or below about 60 ng/µL, and while not necessary, also worked well for most other scenarios. Therefore, while thiol extractions using 0.5 to 1 mL of 0.06M plumbite solution were typically adequate and quite efficient (i.e. for 1 mL of analyte solution), in certain cases where greater contact with the substrate was useful, larger volumes were employed.

4.3 Extraction Selectivity

The selectivity of this thiol extraction method was also examined. Figure 4-4A shows the results of extracting various different analytes from solution using the standard approach of adding plumbite and then monitoring the analyte concentration in the organic layer over time. As can be seen, the non-thiol analytes investigated were essentially unaffected by the addition of the plumbite solution and fully remained in the organic layer over the course of the trial. Conversely, the various thiols investigated were quantitatively removed from solution within about 2 minutes of the plumbite addition and did not return thereafter. Thus, the extraction of thiols by plumbite appears to be highly selective. Similar behavior was also noted for solid PbO addition.

Next, various thiols were extracted using plumbite solution and then the ability to recover them from the resulting thiolate complex was explored by adding acid to the mixture. Figure 4-4B displays the typical results of these experiments.

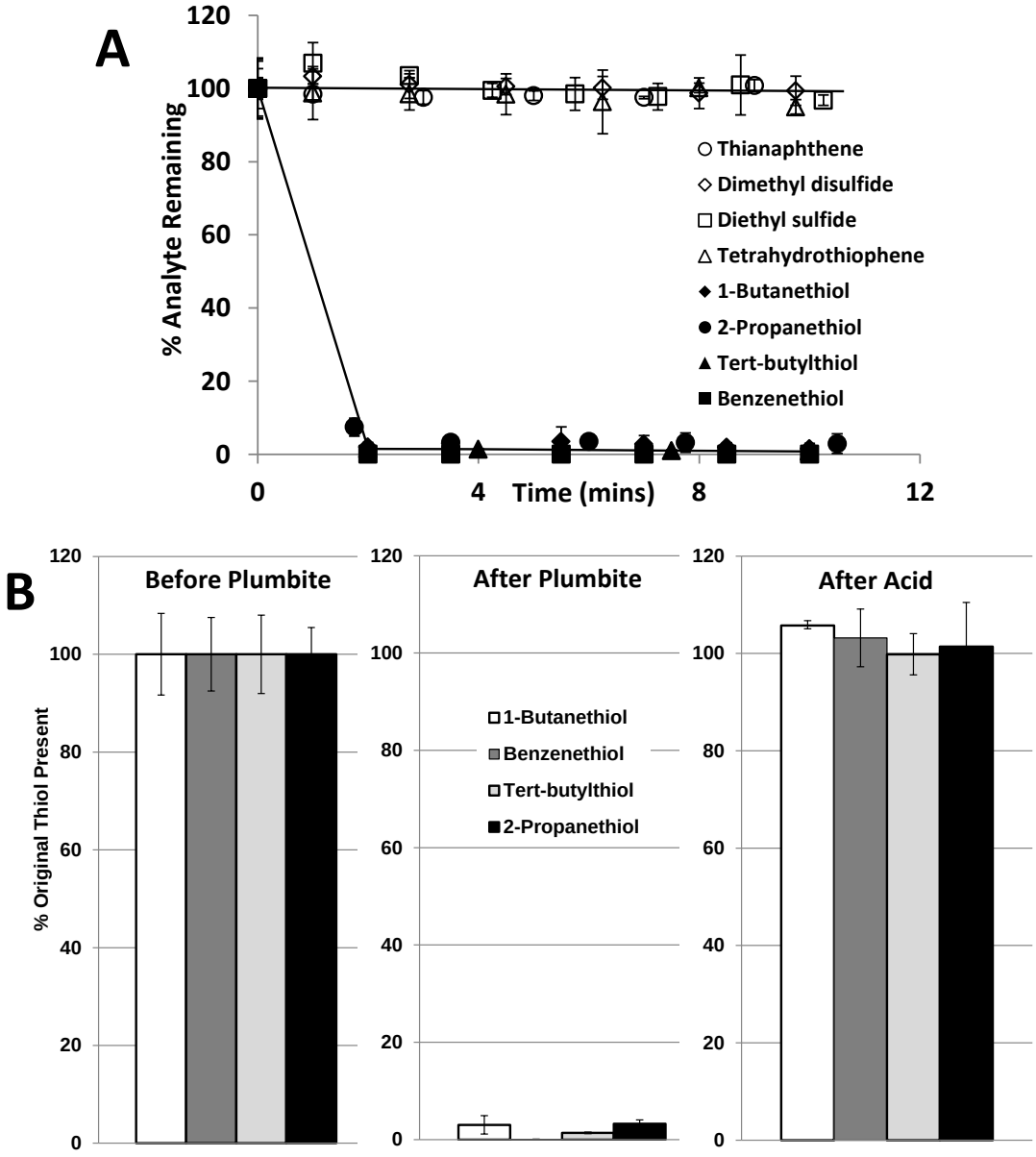

Figure 4-4: A) Extraction efficiency of plumbite solution for various sulfur analytes as a function of time. Trials were done with 1 mL analyte standard solutions in hexane extracted with 0.5 mL of 0.06 M plumbite solution. B) Thiol content in solution before (left) and after (middle) plumbite addition, and then again after nitric acid (1 M) addition (right) for various analytes. Average time to measurement was 3.5 min and immediately after plumbite and acid addition respectively

For this, before the addition of plumbite (left plot), the average signals of the thiols present in the organic layer were measured and then used to represent 100% of the total thiol present. As seen, only a few minutes after the addition of the plumbite solution (middle plot), the amount of thiol present in the organic layer is greatly reduced (< 3% remaining) as a result of the high efficiency of the thiolate complex formation. Finally, immediately upon the addition of acid to this solution (right plot), the thiol is released from the lead complex and quantitatively transfers back to the hexane layer. Thus, the process provides an efficient and reversible means of thiol removal. As such, it offers potential for highly selective extractions that can target thiols in solution and isolate them from sample matrices.

In order to test this latter concept, an experiment was performed with a mixture of thiol and non-thiol sulfur analytes in hexane. Figure 4-5A shows the chromatogram of this mixture, which displays prominent peaks for each analyte. Upon the addition of plumbite solution (Figure 4-5B), it can be seen that the thiol signals disappear and only the non-thiol analyte signals remain, consistent with that expected from Figure 4-4A. Following this, the organic layer was carefully removed from atop the aqueous plumbite solution and solid thiolate complex. It was replaced with an equivalent volume of pure hexane and acid was then added to release the thiols from the complex and transfer them back into the organic layer. As expected from the results in Figure 4-4B, it is seen from the analysis of this layer (Figure 4-5C) that the thiol signals are restored to yield a selective chromatogram without any detectable signals from the other analytes originally present. Therefore, this approach may provide a highly selective means of analyzing thiols and also distinguishing them from other sulfur analytes, which is useful in sample characterization [79].

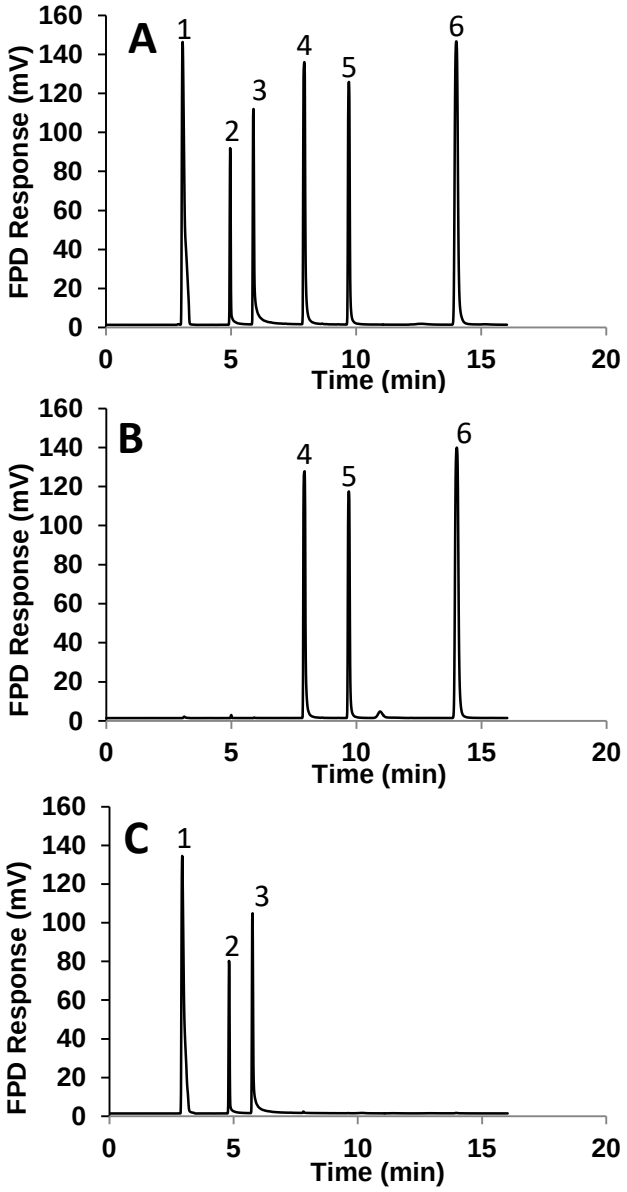

Figure 4-5: Analysis of a mixture of sulfur analytes in hexane (about 520 ng/µL each) in order of A) before and B) after plumbite addition, and C) after subsequent removal/replacement of the organic layer with an equal volume of hexane and the addition of nitric acid (1 M). Analytes are 2-propanethiol (1), 2-butanethiol (2), 1-butanethiol (3), tetrahydrothiophene (4), dipropyl sulfide (5), and isopropyl disulfide (6). Conditions: 30 °C for 2 min, then 10 °C/min to 100 °C; Carrier gas at 3 mL/min.

4.4 Signal Enhancement

Considering the selective nature of the thiol extraction method, it was further investigated for its ability to facilitate situations where the analyte signal may be obscured. The first of these concerned the chromatographic co-elution of analytes, where the signals interfere with one another. Figure 4-6A demonstrates this with the chromatogram of a mixture of diethyl sulfide and 1-butanethiol in hexane. As seen on the expanded scale shown, two prominent peaks appear for the analytes, which are notably overlapped at their base. The mixture was then treated with plumbite solution as above and the solution was reanalyzed. As seen (Figure 4-6B), this results in the removal of the 1-butanethiol peak leaving the diethyl sulfide peak for analysis and free from interference. Following this, the hexane layer containing the diethyl sulfide was carefully removed and replaced with an equivalent volume of pure hexane and acid was added to release the thiol into the fresh organic layer. As seen from the analysis of this layer (Figure 4-6C), the result is a chromatogram of the sole thiol peak restored from the original pair without overlap. Thus, this approach can help resolve such co-eluting analytes.

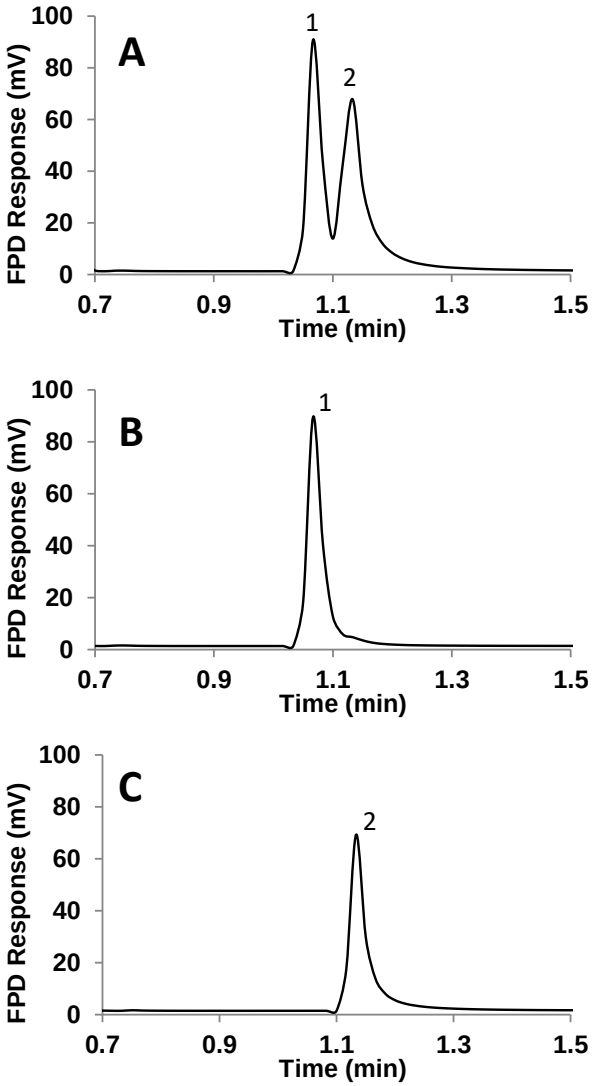

Figure 4-6: Analysis of a mixture of diethyl sulfide (1) and 1-butanethiol (2) in hexane (600 ng/µL each) in order of A) before and B) after plumbite addition, and C) after subsequent removal/replacement of the organic layer with an equal volume of hexane and the addition of nitric acid (1 M). Temperature is 70 °C and carrier is 11 mL/min.

Another signal enhancement involved analytes present below their detection limit. For example, Figure 4-7A shows the analysis of a dilute solution of 1-butanethiol in hexane. As shown by the arrow in the figure, no peak is detected at the expected analyte retention

time of 1.1 min, just after the hexane solvent peak at around 45 seconds. Following this, a 5 mL aliquot of this same solution was treated with 7 mL of the plumbite solution in order to remove all of the thiol present. The hexane layer was then carefully removed and replaced with 250 µL of pure hexane and acid was added to release the thiol into the organic layer. As seen from its analysis (Figure 4-7B), a strong signal now appears in the same retention window due to the 20 fold concentration factor invoked. Thus, this approach may also facilitate sample preconcentration.

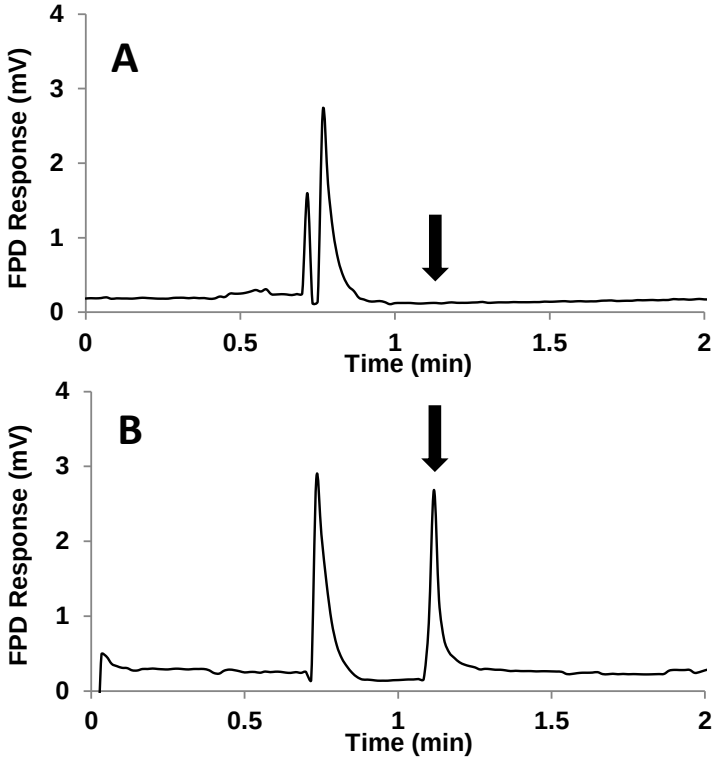

Figure 4-7: Analysis of a 6 ng/µL solution of 1-butanethiol in hexane A) before plumbite addition, and B) after plumbite addition, removal/replacement of the organic layer, and the addition of nitric acid (1 M). 7 mL of plumbite solution was added to 5 mL of analyte solution. After organic layer removal, it was reconstituted into 250 µL of hexane for analysis. The temperature is 70 ºC and the carrier gas is at 11 mL/min.

4.5 Applications

To examine the utility of this method, both lead substrates were used to analyze various samples. The first was a commercial gasoline containing 1-butanethiol. Figure 4-8A presents an FID trace of the sample, which contains a complex multitude of hydrocarbons.

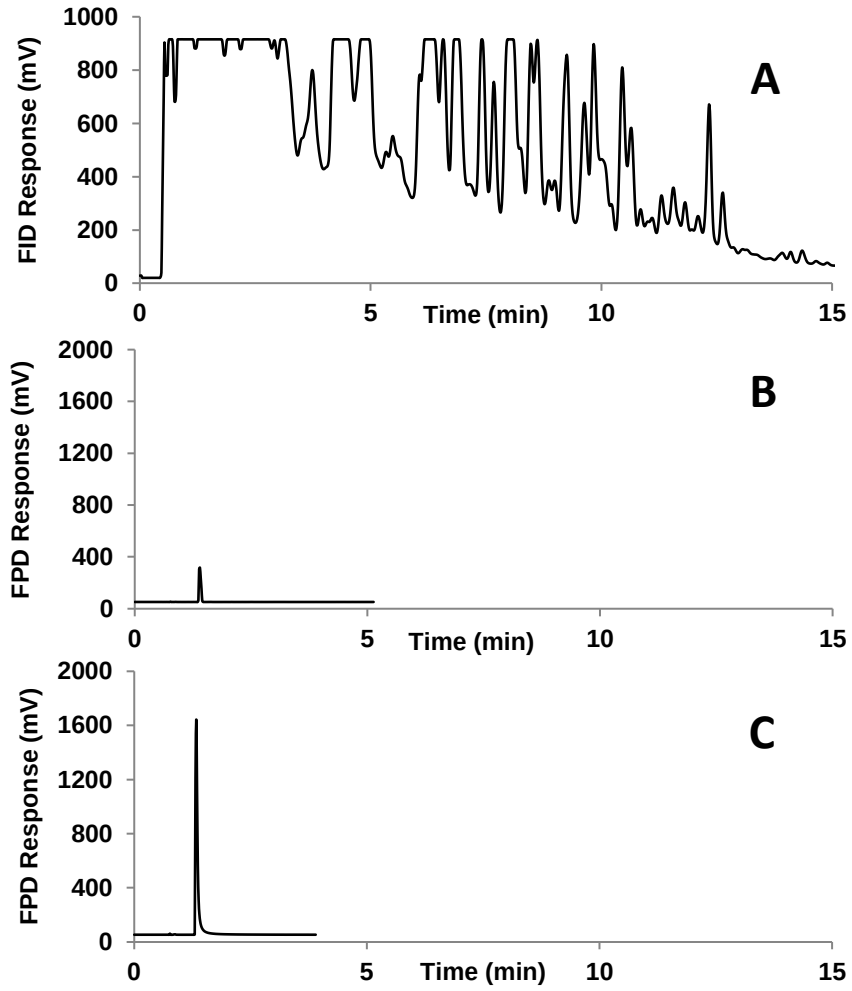

Figure 4-8: Chromatograms of a gasoline sample containing 1-butanethiol (600 ng/µL) as detected by an A) FID, B) FPD, and C) FPD after thiolate formation, removal/replacement of the gasoline with an equal volume of hexane, and the addition of nitric acid (1 M). Solid PbO addition is used to form the thiolate. Conditions used are 50 °C for 2 min, then 10 °C/min to 250 °C; Carrier gas is at 11 mL/min.

By comparison, the selective FPD trace of the sample (Figure 4-8B) displays a lone peak for the thiol at 1.4 minutes, which also co-elutes with the most abundant hydrocarbons present (shown by the off scale FID signals). As a result, the analytical signal is diminished due to severe response quenching. Of note, comparison with a reference standard indicates that hydrocarbon interference has eroded the signal to 16% of its expected value. Following this, solid PbO was added to the fuel sample, where the thiolate complex readily formed on the solid surface and facilitated the subsequent careful removal of the gasoline from the solid. This was replaced with an equivalent volume of hexane and then treated with acid to again release the thiol. Analysis of this solution is shown in Figure 4-8C. As seen, a much stronger thiol signal appears and is restored to 97% of its expected value as a result of removing the co-eluting hydrocarbon interference.

Similar results were also obtained from a model petroleum condensate sample containing a prescribed assortment of target hydrocarbons and 1-butanethiol, seen in Figure 4-9A. Specifically, the signal of 1-butanethiol was quenched to 27% of its expected value due to significant overlap between the heptane portion of the sample and the sulfur analyte, signified by the arrow in the figure. Using the same approach as above, but this time with plumbite solution, the signal was subsequently restored to 94% of its expected value by removing the bulk of the hydrocarbon matrix and replacing it with hexane. Figure 4-9B demonstrates the strong prominent analyte signal obtained from analysis of this solution. Therefore, the ability to isolate thiols from complex petroleum matrices using either solid PbO or plumbite solution treatments can greatly simplify their GC-FPD analysis.

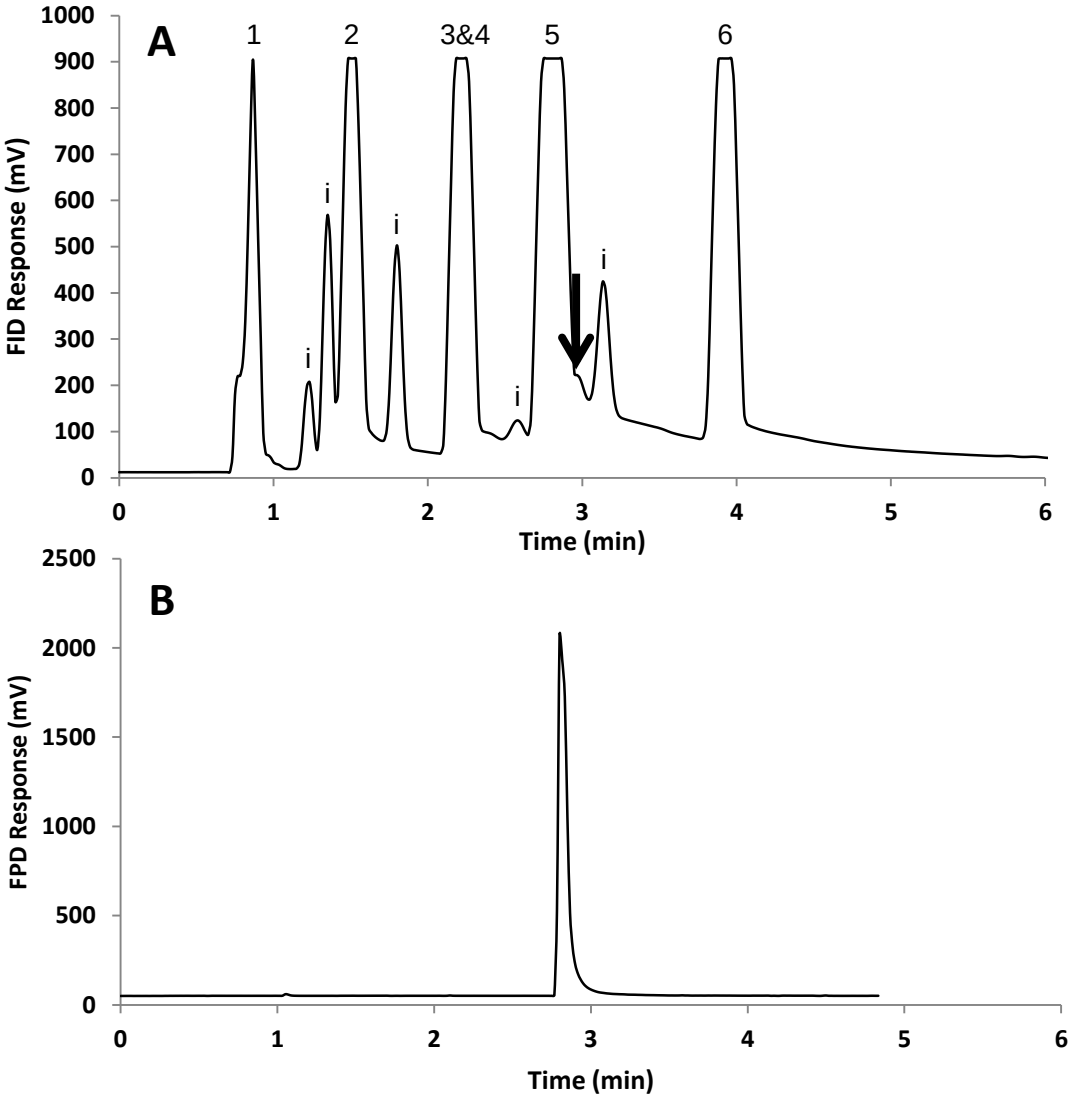

Figure 4-9: A) The FID trace of a model condensate containing 1-butanethiol (600 ng/uL) and B) the FPD trace of the same sample after thiolate formation, removal/replacement of the condensate with an equal volume of hexane, and the addition of nitric acid (1 M). Hydrocarbons included are (1) pentane, (2) hexane, (3) cyclohexane, (4) benzene, (5) heptane, and (6) toluene, amongst various solvent impurities (i). The arrow in the FID trace represents the elution time of 1-butanethiol.

The method was also examined with gas phase matrices. In particular, a natural gas sample containing tert-butylthiol was next evaluated. Using similar protocol as before, and carefully passing 40 mL of the gas through 5 mL of the plumbite solution, it was found that the thiol present was readily trapped in the solution. Acidification then transferred the thiol into a 1 mL aliquot of hexane added to the sample and produced a significantly enhanced signal as a result of the concentration factor. Of note, 77% of the thiol was recovered from the gas sample and the signal was enhanced by a factor of near 3300, a result of the increased analyte concentration and the well-known square law response of the FPD [93]. Reasons for the somewhat lower thiol recovery are unconfirmed, but are likely due to gas bubbles escaping the solution unreacted from the simple syringe approach used here for the purpose of demonstration.

Still, such a concentration effect can be quite useful in monitoring trace quantities of analytes. For example, another gas phase sample examined was the headspace above freshly cut garlic. Since garlic contains many sulfur compounds that can impart flavor and potential health benefits, it is of great interest to analyze [141]. For this, a garlic bulb was cut into pieces that were placed in a sealed flask and the headspace was monitored over time. Figure 4-10 shows the analysis of this sample using the same approach as above for natural gas. Figures 4-10A, B, and C show the progression of the first three hours of thiol evolution from the sample.

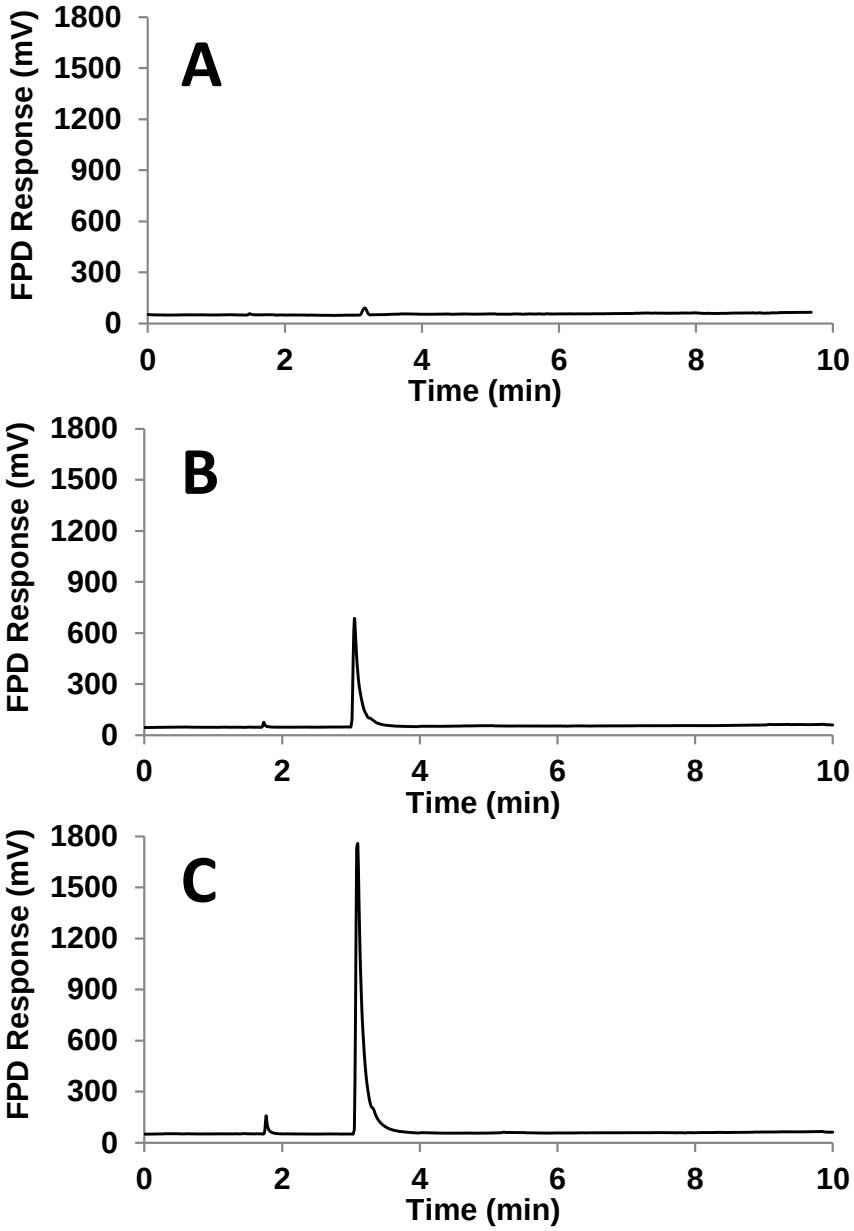

Figure 4-10: Chromatograms showing the analysis of a headspace sample above freshly cut garlic. 40 mL of headspace was passed through a plumbite solution, then 1 mL of hexane was added and it was acidified with 1 M nitric acid. Analyses are done A) 1, B) 2, and C) 3 hours after cutting the garlic. Analytes in elution order are methyl mercaptan and allyl mercaptan. Conditions are 30 ^{o}C for 2 min, then 10 ^{o}C/min to 250 ^{o}C; Carrier gas flow is 11 mL/min.

As seen, two prominent species emerge over this period, from trace quantities after 1 hour (Figure 4-10A) to a more abundant presence after 3 hours (Figure 4-10C). These were confirmed by GC-MS to be methyl mercaptan and allyl mercaptan, which are well known and important components of garlic [132,142], and the only prominent mercaptans found in the headspace over such samples [132]. By comparison, when directly analyzing the headspace without the thiolate extraction method, the untreated sample yielded little evidence for these analytes (Figure 4-11). This indicates that when this sample is not preconcentrated, the signal for these analytes is not able to rise above the noise for detection. Of note, no other sulfur compounds were observed over the three hours that the headspace of this garlic sample was monitored, likely due to their low concentration and thus limited response in the untreated method. Therefore this method appears to have a reasonable ability to work with both solution and gas phase samples and can provide useful signal enhancement for thiols.

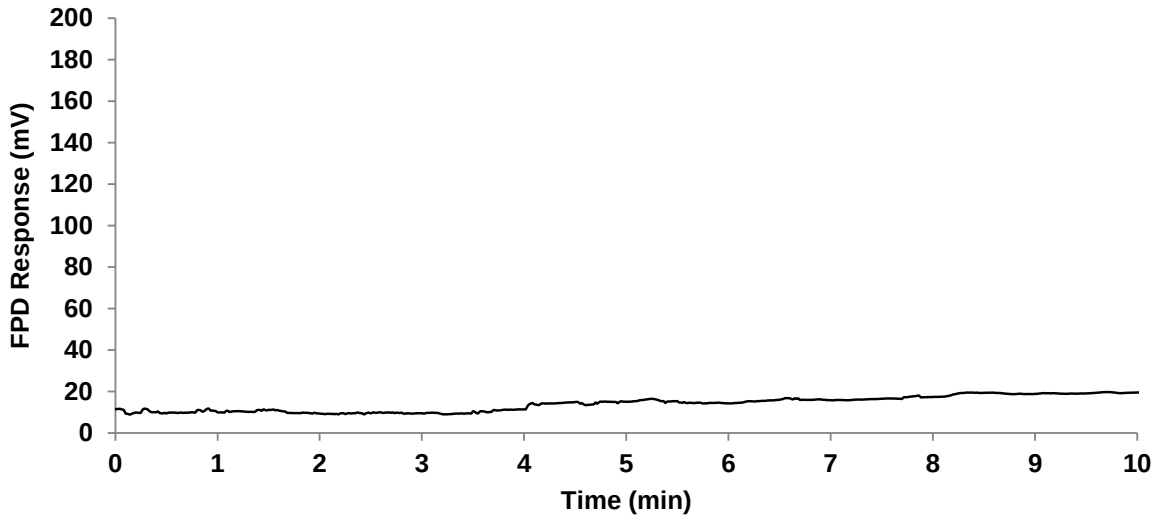

Figure 4-11: The direct analysis of 10 µL of headspace above freshly cut garlic after 3 hours without any sample treatment. Same conditions as in Figure 4-10.

4.6 Conclusions

The use of solid PbO and plumbite solution substrates, traditionally employed in industry to trap thiols, can provide a relatively rapid and efficient analytical tool for usage in the determination of thiols in a variety of samples. The method is highly selective, simple, inexpensive, adaptable, and allows for GC-FPD analysis of thiols without quenching interference. The method is also potentially amenable to the trapping of longer-chain thiols for analysis [89,90], and may be useful in the determination of thiols in biological samples in the future [143]. Therefore, results indicate that this approach could be a useful means of isolating thiols from complex matrices for their subsequent analysis.

CHAPTER FIVE: A SELECTIVE CHROMATOGRAPHIC SYSTEM FOR THE DETERMINATION OF THIOLS BY GC-FPD

5.1 Introduction

The sample extraction technique described in Chapter Four also presents a potentially effective and simple way to selectively analyze thiols by GC-FPD. The data in Chapter Four shows that through the use of an aqueous plumbite solution, this technique resulted in thiol extractions that occurred nearly instantaneously. However, due to the offline nature of this method, extra time (up to two minutes) and sample handling was required to prepare the sample for injection into the GC for analysis. To this end, it would be even further beneficial to extrapolate this technique into a selective online 'trap-and-release' GC system and minimize the total analysis time, while still maintaining the advantages of the quenching-free analysis seen previously.

In Chapter Three, a water stationary phase in a capillary column was established with great promise for sulfur separations. Accordingly, as a water-based solution, plumbite also has the potential to be used as a stationary phase in a capillary column format. Thus, a plumbite phase used as a pre-column trap could generate an in situ precipitation reaction of thiols into solid lead thiolates. This would allow non-thiols to pass through the trap unaffected and separate as normal on the subsequent analytical column, but prevent thiol compound elution until they are later released through the injection of acid into the system. The advent of such a trap and release method could potentially also help avoid co-elution of thiols with various hydrocarbons, and thus the resulting response quenching in an FPD.

This chapter presents an investigation into the potential of a selective chromatographic system using a trap column coated with plumbite solution and subsequent release through injection of acid. This method is highly selective for thiols and presents the potential opportunity to control their elution in GC. The general operating properties of this system and characterization of the trap column phase are discussed.

5.2 Establishing the Trap Phase

Initial efforts were aimed at testing if thiols could be selectively extracted and released in situ with a plumbite stationary phase pre-column trap. Previous work has shown separations using a water stationary phase inside of capillary tubing. As such, plumbite was established here as a stationary phase in fused silica tubing prior to a megabore analytical column. Preliminary results indicated that this plumbite phase was indeed very effective at trapping thiols injected into the system, while other compounds passed through and separated on the column unaffected. For instance, upon injection, thiol peaks never appear after nearly an hour of monitoring, while sulfide species eluted as normal. Thus, the subsequent release of the trapped thiols was explored next.

The plumbite phase must be neutralized by an acid to allow conversion of the trapped thiolate back into the original thiol. Although nitric acid was effective for neutralization in the offline method in Chapter Four, it is also corrosive to capillary columns and was thereby avoided for this in situ technique. Instead, formic acid was introduced for release of thiols, as it is relatively volatile and does not exhibit the same corrosion effects as nitric acid. To confirm its ability to convert thiolate into original thiol, formic acid was then tested as the acid in the offline extraction technique, described in Chapter Four. From this, it was found

that formic acid could also readily be used for neutralization of the phase and conversion into thiols. Further, when applied to the plumbite stationary phase, formic acid demonstrated good ability in neutralizing the phase and releasing the trapped thiols. Of note, thiol peaks would appear only after injection of acid. Thus, formic acid was used moving forward.

Next, the length of the plumbite phase pre-column trap was examined and optimized. Since plumbite reacts nearly instantaneously with thiols, it was expected that even short lengths of column would be effective at trapping thiol. As such, lengths between 30 and 50 cm were examined. Some typical results are shown in Figure 5-1. Initial observations suggested that all lengths of pre-column trap surveyed were effective at trapping the thiol. As can be seen from the figure, the thiol is expected to elute at 4 minutes (without plumbite present; Figure 5-1 top), but using a plumbite pre-column trap resulted in no observed signal around that same time range (Figure 5-1 middle, bottom), indicating successful trapping with the phase. The addition of formic acid (noted by the arrows) then demonstrates a release of thiol from the trap, as a signal is then detected around 7 minutes after this acid injection. However, the 35 cm length trap showed the detection of multiple peaks after the acid addition. Also, this length indicates insufficient recovery of thiol, as the response given is a tenth of that expected (in Figure 5-1 top). In addition, the shorter 30 cm length of trap behaved similarly with multiple peaks eluting after the addition of acid. It is not clear why this occurs, but it may be related to the manner in which the analyte band spreads in the trap prior to release. In contrast, the 50 cm length trap (Figure 5-1 bottom) showed one distinct peak that resembles the expected response of the analyte (in Figure 5-1 top). This indicates excellent conversion between thiolate to thiol in the release step of this technique. Further, up

to 1000 ng of 1-butanethiol could be trapped with a 50 cm length of trap. As such, a 50 cm length of trap was chosen for all future experiments.

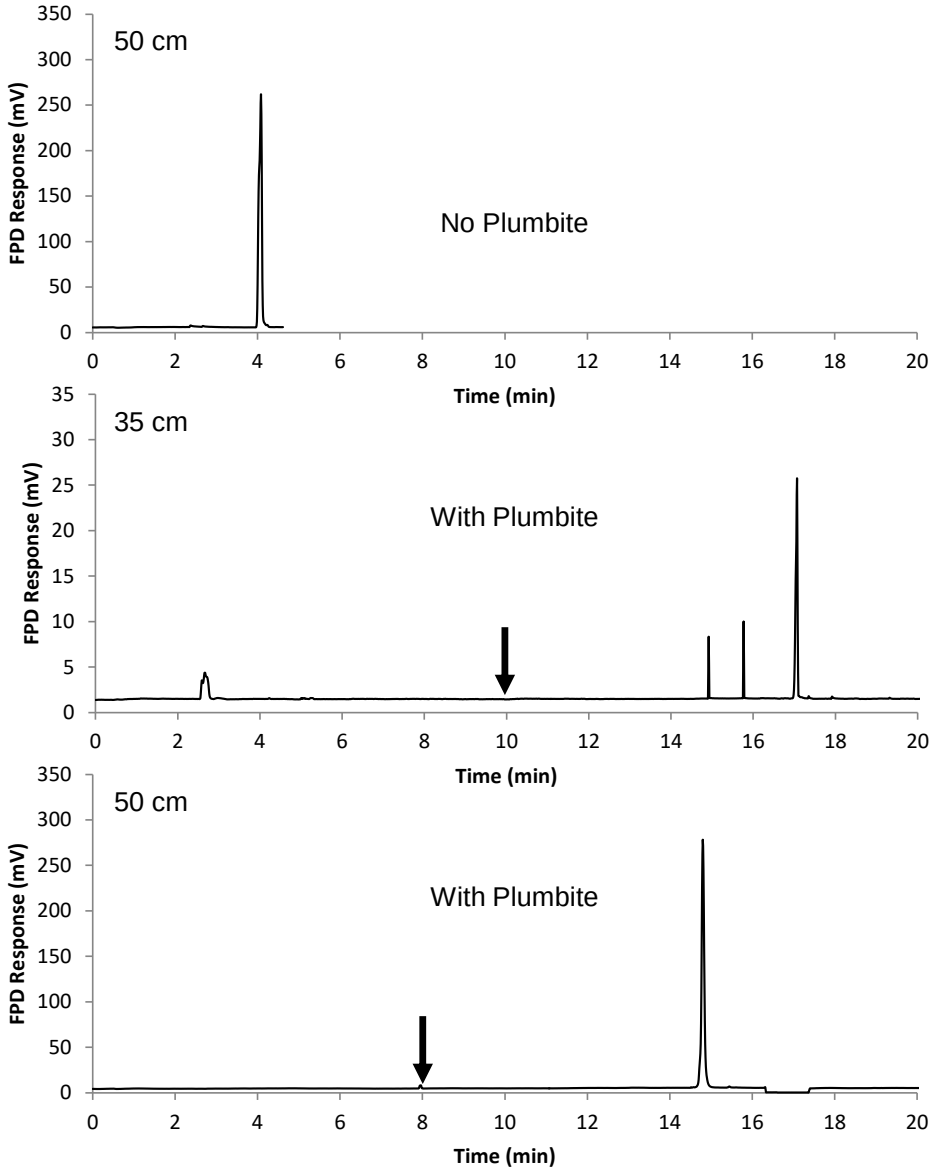

Figure 5-1: The analysis of 1-butanethiol (419 ng) using 50 cm (top, bottom) and 35 cm (middle) lengths of the pre-column trap. Arrows indicate injection of 10 µL of formic acid (14 M) for release. Oven is 30 °C for 0.5 mins, then 35 °C/min to 70 °C, with carrier gas at 3.6 mL/min.

It should be noted that another early observation with the fused silica pre-column trap was that it was unable to be reused. Even after thoroughly washing with water prior to reusing, the efficiency of trapping thiol decreased on the same piece of fused silica. Thus, a fresh fused silica shunt was used for each plumbite trapping analysis.

5.3 Selectivity

Similar to the results discussed in Chapter Four, the plumbite pre-column trap was selective for thiol compounds, while non-thiol compounds were unaffected. Figure 5-2 demonstrates this for the analysis of both 1-butanethiol and diethyl sulfide. As expected without plumbite present, 1-butanethiol elutes as normal near 4 minutes. When plumbite is added to the trap column, the thiol is effectively trapped until after the addition of acid (noted by the arrow). As such, the strong peak at 15 minutes indicates neutralization of the phase and full elution of the thiol. In contrast, the chromatograms of diethyl sulfide with and without the presence of the plumbite phase pre-column trap are almost identical in retention and peak height. This shows that diethyl sulfide is unaffected by the plumbite trap. In addition, the analysis of diethyl sulfide also shows a hexane solvent void time marker in both chromatograms, indicating (as anticipated) that hydrocarbons are also not affected by the trap. Thus, this trapping selectivity shows the potential for selective analysis of complex matrices containing thiols, as hydrocarbons and other non-thiols could separate and elute as normal through the GC, while thiols present in the sample would remain trapped until their later controlled release by the addition of acid.

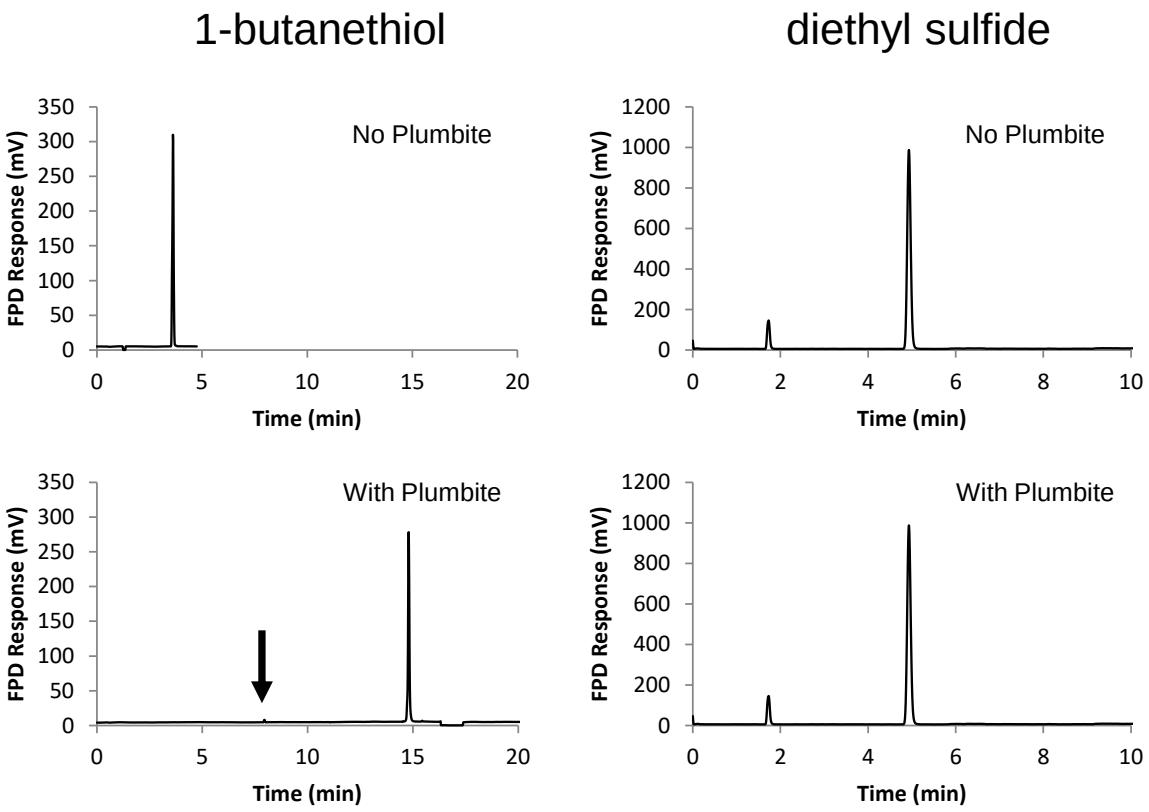

Figure 5-2: The elution of 1-butanethiol (419 ng; left) and diethyl sulfide (265 ng; right) with (bottom) and without (top) a plumbite pre-column trap. The arrow indicates the addition of 10 µL of formic acid (14 M) for release. Conditions for 1-butanethiol: 30 °C for 0.5 mins, then 35 °C/min to 70 °C, with carrier gas at 3.5 mL/min. Conditions for diethyl sulfide: 30 °C with carrier gas at 7 mL/min.

5.4 Reproducibility and System Modifications

Despite the selective nature of the online trap, the main reoccurring issue encountered was the poor reproducibility from trial-to-trial. In fact, elution reproducibility for all of these tests was low and often multiple injections of formic acid did not yield the expected single-peak thiol release. Furthermore, consecutive analyses frequently generated very different

results. For example, Figure 5-3 demonstrates the back-to-back analysis for 1-butanethiol, each using a freshly coated trap. As can be seen, while both analyses trap the thiol well, only in the first attempt is the thiol fully eluted and recovered. This unpredictability was common and each trial was very difficult to reproduce. Thus, the system could not be reliably used in its current format.

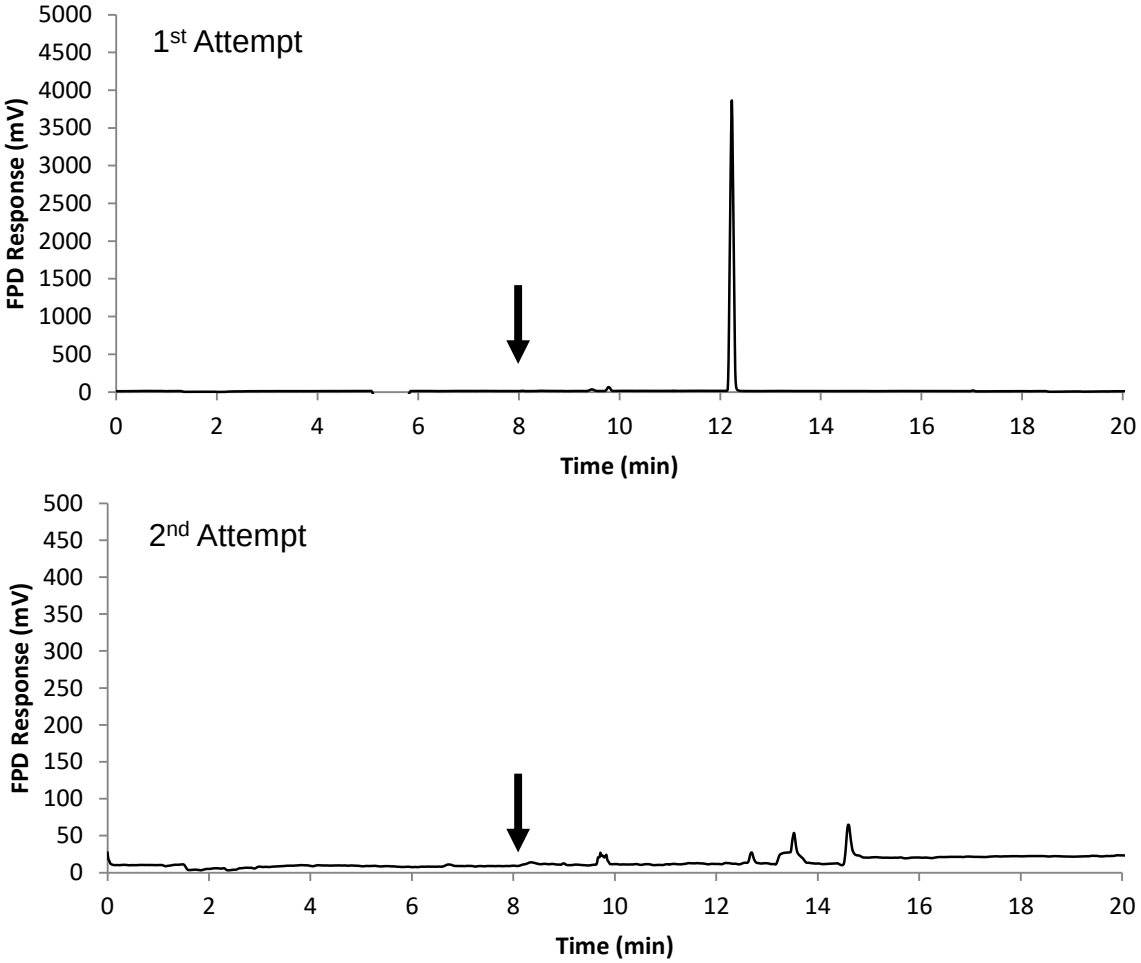

Figure 5-3: The consecutive analysis of 1-butanethiol (525 ng) with a plumbite phase pre-column trap. Arrows indicates injection of 10 µL of formic acid (14 M) for release. Conditions: 30 °C with carrier gas at 4.7 mL/min.

In order to attempt to better reflect the conditions from the reliable and effective offline method described in Chapter Four, the system was modified to allow room temperature neutralization of the plumbite phase. As such, an additional union was added to allow for injection outside of the oven. This circumvents the need to use the hot injector for the introduction of acid and instead allows liquid acid to be added directly to the plumbite phase pre-column trap. However, in this format it was found that the while the plumbite continued to trap the thiol well, room temperature additions of liquid acid did not help to reproducibly release the thiol as hoped. Further, liquid injections of hexane (previously used as a solvent in Chapter Four) were also ineffective at helping to elute the thiol through the system.

To investigate reasons for the unpredictability in response, the pre-column trap, analytical column, and detector were visually observed after each trap-and-release attempt. The pre-column trap was repeatedly found to be completely void of any liquid. This means that the arrangement did not well retain the plumbite phase and it was carried into the column. Additionally, the outlet of the analytical column (that enters the detector/heating block), and the detector itself contained black spots. These are suspected to be from the reaction product between plumbite and formic acid, which is lead formate. At elevated temperatures (> 190 °C), lead formate decomposes [144], which may help explain why only the hot detector and a small portion of the column contained the black product. However, a decrease in detector temperature did not resolve this issue overall, as the contaminant passing through the detector decomposed in the flame instead, resulting in an unstable flickering flame response.

To this end, restrictions on the pre-column trap were also examined in an attempt to prevent the plumbite stationary phase from escaping into the column or detector. Various lengths of fused silica shunts (of 50 and 100 μm i.d.) were explored for restriction use post-trap and post-analytical column. Unfortunately, under the conditions tested, these restrictive shunts were not able to prevent the plumbite phase from escaping the pre-column trap and into the analytical column. Thus, other means of preventing the plumbite from entering the column were also explored.

One such way to address the movement of plumbite in the system is to use a drying agent after the pre-column trap. In this manner, water (from plumbite and/or acid) in the pre-column trap can be absorbed by the agent and prevent its progression through the system. As such, a small amount of drying agent was added to the system through a union. $CaCl_2$ was found to be ineffective at preventing water from passing through to the analytical column, with liquid visibly observed inside the inlet of the column. Conversely, $MgSO_4$ and Na_2SO_4 were very effective at absorbing water from the pre-column trap. However, both of these agents also absorbed the thiol and its elution/release could not occur. Thus, while the plumbite pre-column approach has shown potential effectiveness at trapping/releasing thiols injected into the system, the lack of reproducibility that could not be overcome led us to abandon this approach.

5.5 Solid Lead (II) Oxide (PbO) for Trap-and-Release

As PbO(s) was also useful in Chapter Four for the selective removal of thiols from solutions, it too was examined here for trap-and-release. Instead of a coated pre-column trap, a short fused silica shunt filled with a small amount of PbO was inserted in its place. Once

again, initial results indicated excellent trapping efficiency of injected thiols with no effect on non-thiols, as expected. However, releasing the thiol was found to be difficult. Figure 5-4 demonstrates the PbO trap. The asterisk in the figure indicates where the expected elution of thiol without PbO present would take place near 4 minutes. As no peak is observed at this time, this demonstrates that PbO is an effective trap for the thiol. However, the addition of formic acid (shown by the arrow) did not release the thiol for its subsequent elution and separation on the analytical column. In fact, up to 50 µL of formic acid (14 M) was added to the system in some trials with no elution of thiol. Further, the addition of more formic acid extinguishes the detector flame, so extra amounts of acid could not be used in this regard. It should be noted that in this setup, black spots were again present near the analytical column outlet and inside of the detector.

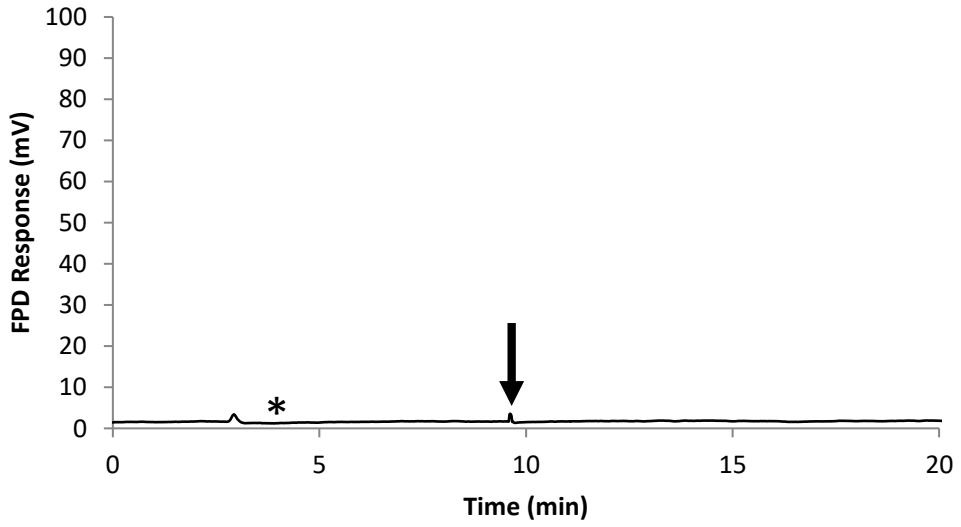

Figure 5-4: The analysis of 1-butanethiol (419 ng) using a solid PbO trap. Arrow indicates 10 µL injection of formic acid (14 M) for release. Asterisk shows typical thiol elution time without PbO. Conditions: 30 °C with carrier gas at 3.9 mL/min.

To further attempt thiol elution with the PbO trap shunt in-line, a stronger acid was employed. In Chapter Four, liquid nitric acid (1 M) was used to neutralize the PbO and plumbite solutions, and as such it was investigated here. However, it was ineffective in this regard as no significant peaks arose from this attempt at thiol release. Moreover, after adding 7 µL of nitric acid, there was no trace of PbO remaining in the shunt. It is unclear why the release of thiol was not observed and thus this requires further investigation to better understand.

5.6 Conclusions

A plumbite phase pre-column trap was employed to demonstrate a trap-and-release system for controlling the analysis of thiols in GC. The plumbite trap showed excellent selectivity for thiol compounds, which allows all non-thiols to elute and separate as normal while thiols are converted into thiolate on the pre-column trap until their subsequent release and conversion back to thiol by the addition of formic acid. Further, solid PbO also showed great selectivity for trapping thiols. However, release of the thiol in both of these methods was frequently difficult and unreproducible and therefore requires further optimization and investigation. Still, the data proves that the overall idea of trap-and-release has great potential and could be powerful for controlling thiol separations in GC. Thus, if the reproducibility issues can be addressed in the future, it could lead to a very beneficial method.

CHAPTER SIX: MICRO-FLAME PHOTOMETRIC DETECTION IN MINIATURE GAS CHROMATOGRAPHY ON A TITANIUM TILE

6.1 Introduction

Throughout this thesis, GC has been utilized as the primary analytical method for the determination of VSCs. Due to its widespread employment in various areas [7,9,15,145], continuous advancements are being made to improve the speed and performance of GC methods [146,147]. For example, miniaturization of such instruments can afford many benefits including increased analysis speed, reduction of resource consumption and instrument portability [29,31,148–150].

Microfluidics has been a very effective tool in this regard. Of note, since the first miniaturized microfluidic GC (μGC) device was reported [14], many developments have been made in this field [29,151]. One area of on-going interest in μGC is the adaptation of detection methods. Unfortunately, although the FPD is a widely used and highly desirable GC detector, reports of incorporating this selective detector into μGC devices have been scarce [66]. This can largely be attributed to difficulties in miniaturizing the conventional diffusion burner and flame size to function within the reduced channel dimensions of a μGC device without severely compromising sensitivity or stability. Further, the FPD flame is normally enclosed to help establish the optimal hydrogen-rich atmosphere that drives analyte chemiluminescence, and this is challenging to achieve in small cavities like those of a microfluidic device [24]. Lastly, popular device materials such as silicon wafers are fragile [92] and often susceptible to fracture and breakage from contact with the hot flame. Thus,

novel materials and microfluidic detector designs that can help address these issues and successfully incorporate FPD sensing into μGC analyses are useful to investigate.

Earlier explorations with counter-current micro-flames have been able to help miniaturize flame-based GC detectors while maintaining similar performance [24,25,28,152]. Briefly, this method directly opposes low flows of fuel and oxidant gas streams to establish micro-flames that can be supported/stabilized on a reduced burner within a small enclosure. For instance, this technique has enabled flame-based photometric and ionization detectors to be operated inside of conventional capillary GC columns [24,28] and a few modifications/adaptations of the method have even been used to demonstrate flame operation with quartz-based microfluidic devices [55,66,153]. These efforts indicate that further exploration of integrating the FPD within a microfluidic device by this approach using other materials would be useful.

Recently, titanium (Ti) tiles which are strong, lightweight, thermally conductive and simple to coat for separations have been employed in μGC devices [56,154]. For these reasons and also due to their relative inertness and monolithic architecture, microfluidic Ti devices are increasingly being sought for various analytical tasks such as liquid chromatography, electrophoresis, and other applications [155–158]. Owing to their robust structure and electrical conductivity, it was found that Ti tiles provide an excellent substrate for the incorporation of an FID into a μGC device [56]. The Ti μGC-FID was durable, functional, and performed on par with a conventional FID. Since the FPD is similarly a flame-based GC detector, it would be of great interest to investigate if Ti tiles could also provide a useful platform for the incorporation of an FPD into μGC devices.

This chapter investigates a novel Ti μGC-FPD device that uses a counter-current flame approach to incorporate the FPD into the microfluidic tile. The general operating properties of the Ti μGC-FPD device are discussed and the optimal FPD parameters are established. Additionally, the performance of this miniaturized FPD for analyzing sulfur and phosphorous compounds is presented, and the Ti μGC-FPD device is demonstrated in analytical applications.

6.2 General Operating Characteristics

In contrast to fragile components such as quartz [66] that have been used previously to support μGC devices and detectors, Ti tiles can provide a relatively very robust substrate for such endeavors. Indeed, initial observations of the Ti μGC-FPD device explored here were that it was quite sturdy and not prone to breakage or cracks. For example, the gas inlet and flame cavity fittings used with this tile have been replaced multiple times without causing any defects in the structure from the bolting used to make gas-tight connections. In addition, there have been no observed effects on analytical performance from routine handling of the device, including occasionally dropping it. Further, extensive flame operation did not produce any signs of surface fatigue or fracturing, as is common in quartz substrates. Thus, similar to earlier results reported for a Ti μGC-FID device [56], Ti generally appears quite compatible as a platform material for use in μGC devices, and particularly those employing flame based detectors.

With regard to detector stability, preliminary experiments demonstrated that the FPD flame could be readily lit in the device with the fittings in place surrounding the flame cavity. Direct ignition was routinely achieved by presenting a spark at the open end of the cavity

with hydrogen and oxygen flowing. The FPD flame established could then be operated stably and hydrogen-rich for hours without any visual fluctuation or disturbance. Further, the resulting flame was relatively tiny (~250 µm wide, similar to earlier reports [56]) and it resided on the oxygen flow inlet to the cavity (Figure 6-1). This is normal for a hydrogen-rich flame [152] and additionally confirms that the cavity fittings employed effectively isolated the flame from atmospheric oxygen. Of greater interest to FPD operation was the intense chemiluminescence that was visually observed for various analytes as they passed through the flame cavity in the tile. For example, as anticipated [47] sulfur and phosphorous compounds produced characteristic bright blue and green emissions respectively (Figures 6-1, 6-2), while carbon compounds yielded almost nothing (Figure 6-3).

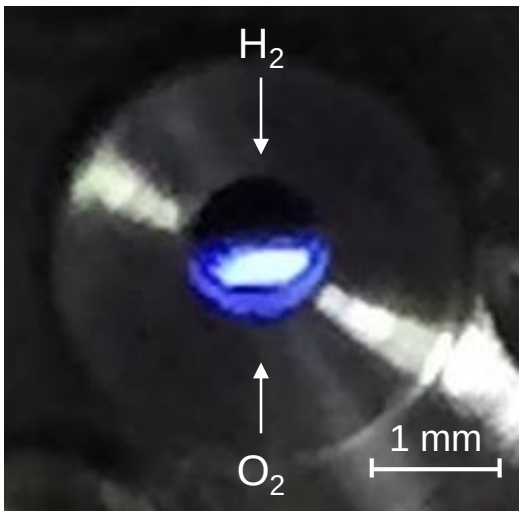

Figure 6-1: Image of the detector flame in the Ti µGC-FPD device as sulfur passes through the flame cavity.

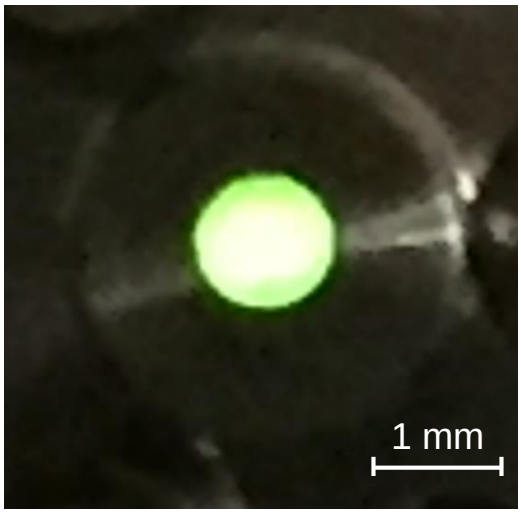

Figure 6-2: Image of the detector flame in the Ti µGC-FPD device as phosphorous passes through the flame cavity.

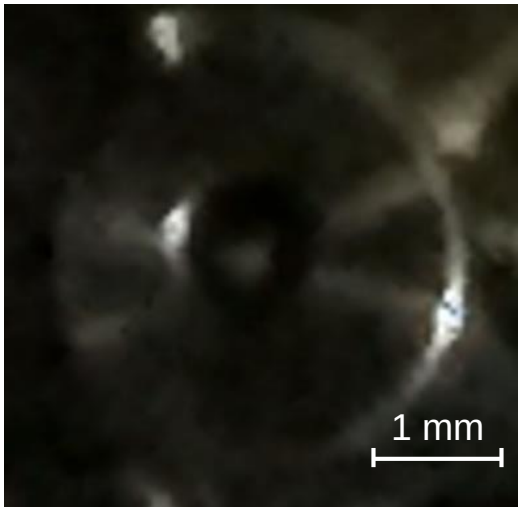

Figure 6-3: Image of the detector flame in the Ti µGC-FPD device as carbon passes through the flame cavity.

As well, similar to a conventional FPD, the chemiluminescence could extend well beyond the visible flame region (e.g. Figure 6-1) and even fill the cavity (e.g. Figure 6-2) depending on the mass flow of the analyte present. In this way, both sulfur and phosphorous

analytes were seen to fill the cavity with chemiluminescence when analyte flows were large. Thus the selective emissions observed qualitatively agreed well with those anticipated for an FPD and were further explored for their analytical properties.

6.3 Ti µGC-FPD Device Properties

A similar approach for column design and coating to that used previously for Ti tiles was also adopted here [56,154]. In particular, a 100 µm wide and deep channel dimension was used to obtain reasonable separation efficiency. Further, this was coated with a standard non-polar OV-101 phase since it has demonstrated good chromatographic utility previously in µGC applications involving Ti and also ceramic platforms [32,56,154]. However, while some earlier Ti µGC devices employed a dual-spiral column design [154], a serpentine column configuration was used here since it was more amenable to interfacing with the on-chip FPD. Further, it readily facilitated the incorporation of a heat shield cavity to help thermally isolate the detector flame from the separation column.

Initial trials indicated that the device produced quite reasonable GC separations with good detector response. For example, Figure 6-4 shows a chromatogram of a mixture of diethyl sulfide, dimethyl disulfide and tetrahydrothiophene in hexane as separated on the Ti µGC-FPD device. As seen, these compounds are well resolved from each other on the relatively short 5 m column employed, and they each display fairly good peak shape with the device providing a plate height of 0.8 mm for tetrahydrothiophene under these conditions. Even more, the trace shows a very stable FPD response profile, a smooth baseline, and prominent analyte signals with no significant response from the hexane solvent. Overall, these attributes align well with those expected of conventional GC-FPD systems [47].

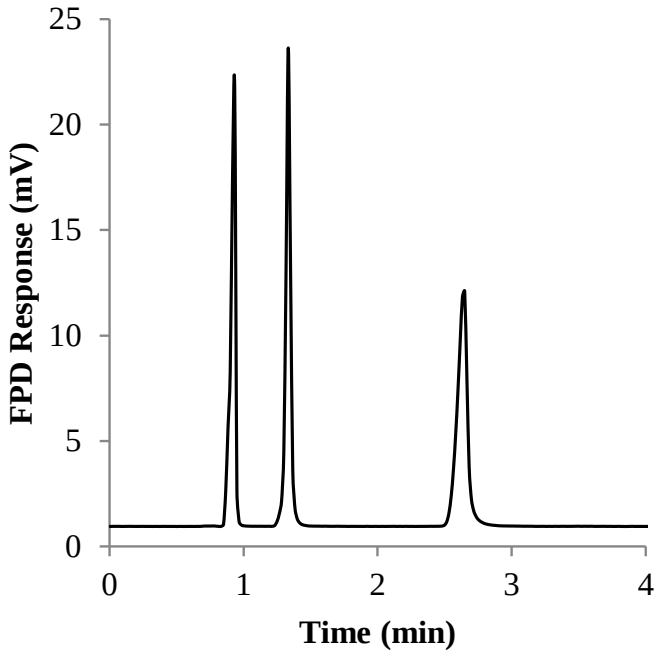

Figure 6-4: Separation of diethyl sulfide, dimethyl disulfide, and tetrahydrothiophene (in order of elution; each 40 ng) on the Ti µGC-FPD device. Column temperature is 52 °C.

In order to maximize the performance of the on-chip FPD, efforts were next made to optimize the flame gas flows. A range of hydrogen and oxygen flows were examined in the device to determine those that achieve the highest analyte signal-to-noise ratios and best system performance. In general, optimal operating flow rates were normally found between about 5 to 14 mL/min of oxygen and 30 to 60 mL/min of hydrogen. These are fairly modest relative to most conventional FPDs, which can require over 200 mL/min of gas depending on the design [47]. Note that while either oxygen or air could be used, similar to a conventional FPD [47], the former is noted to yield more compact flames. Further, these optimal gas flows should also be scalable with channel dimensions, as has been shown previously with counter-

current flames [24]. Over the range investigated it was found that the noise (peak-to-peak) was fairly consistent and changed little, normally residing between about 0.004 and 0.007 mV. By comparison, the chemiluminescent analyte signal was more notably affected in this regard. For example, phosphorous response was most impacted this way as changing the oxygen flow by 4 mL/min could lead to a near 5 fold change in signal intensity. Ultimately it was found that the optimal flow rate for sulfur response in the device was obtained with 7 mL/min of oxygen and 40 mL/min of hydrogen. Conversely, the phosphorous response was maximized with 10 mL/min of oxygen and 40 mL/min of hydrogen. These values agree well with those from other counter-current FPD flame applications [25,73,93,159], and are decidedly hydrogen-rich in character as would be expected for FPD operation [47]. For instance, the hydrogen to oxygen ratio invoked resides between 4 and 6 to 1, similar to a conventional FPD. As well, a slightly higher oxygen flow was found preferable for phosphorous response, which is consistent with the fact that its primary emitting species (HPO^*) is oxygenated whereas that of sulfur (S_2^*) is not [47].

Using these optimal conditions, the performance and analytical figures of merit for the Ti μGC-FPD device were probed further. Figure 6-5A shows how the response of sulfur and phosphorous (examined as diethyl sulfide and trimethyl phosphite respectively) changes as a function of injected analyte concentration.

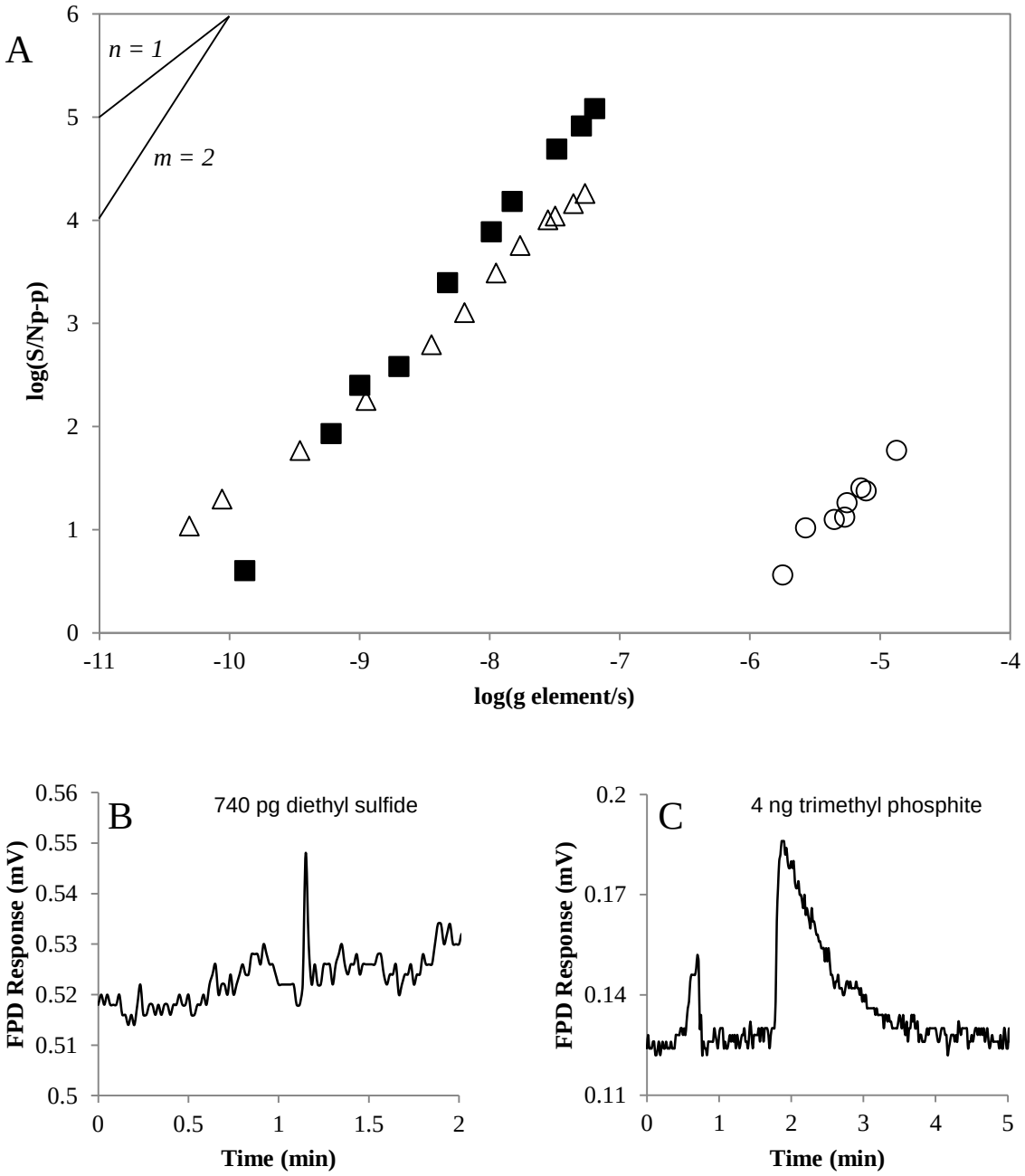

Figure 6-5: (A) Response of the Ti µGC-FPD device toward different amounts of diethyl sulfide (■), trimethyl phosphite (Δ), and benzene (○) in the open mode under optimal conditions. Peak traces for (B) 740 pg of diethyl sulfide and (C) 4 ng of trimethyl phosphite on the device are also shown.

As can be seen, over a range of about 3.5 orders of magnitude investigated, sulfur response increases pseudo-quadratically with concentration, while phosphorous responds linearly. This is because the diatomic nature of the S_2^* emitter (vs HPO^* for phosphorous) is thought to theoretically yield a square-law response, but often varies slightly in practice [47]. This yields a detection limit of about 70 pg S/s for sulfur with the Ti μGC-FPD device, which is 50 times lower than previous reports of coupling an FPD to a μGC system [66]. Alternately, the device also yields a detection limit near 8 pg P/s for phosphorous, which is about 1.5 times lower than, and more similar to, that reported previously [66]. Further, these values also agree well with those anticipated from a conventional FPD [47]. Note that these values were both determined at the conventional signal-to-noise ratio of 2, where noise is measured as peak-to-peak fluctuations of the baseline over at least 10 analyte peak base widths. Therefore, the Ti μGC-FPD device provides quite reasonable operating sensitivity. Figure 6-5B and C further confirm these values with peaks of sulfur and phosphorous analytes near their detection limit. Also seen is the relatively more tailed peak shape of the phosphorous compound, which is a commonly observed chromatographic trait for such analytes [24,66,152], and as such is not ascribed uniquely to the Ti channel properties. Since other phosphorous compounds can yield better peak shape [47], this may be useful to further explore in the future.

In terms of repeatability, the Ti μGC-FPD device was also found to be quite consistent in performance. For example, since the adhesive heating pad arrangement employed yielded stable device temperatures over long periods, this translated into reliable analyte retention times that only varied within about 0.7% RSD (n=10). Further, in terms of detector output, analyte peak areas were also quite consistent. For instance, signals from

repeated injections of diethyl sulfide produced an RSD of 3.7% (n=10), which is similar to the range and behavior expected from a conventional FPD [47,93]. Therefore, this indicates that the Ti µGC-FPD device is very stable in routine operation.

Figure 6-5A also includes the Ti µGC-FPD device response toward carbon (as benzene) to help gauge the natural (i.e. without an interference filter) selectivity of the system with respect to sulfur and phosphorous. As seen, carbon response is relatively very low. In fact, in our experience, only hydrocarbon masses of about 10 µg or larger were normally detectable in the system. As a result, this provides a natural selectivity of about $10^{4.3}$ and 10^{5} for sulfur and phosphorous response, respectively, over hydrocarbon response. This finding is reasonable given the selective nature of the FPD and agrees well with conventional GC-FPD methods [47,104,160,161].

Since routine FPD operation often employs interference filters to enhance selectivity in monitoring sulfur and phosphorous analytes, they were also examined here. Figure 6-6 illustrates the results with a standard mixture of diethyl sulfide and trimethyl phosphite in hexane as analyzed on the Ti µGC-FPD device, both with and without characteristic interference filters employed. As seen, in the open mode without any filter (Figure 6-6A), both sulfur and phosphorous compounds are readily observed due to their respective chemiluminescence. Conversely, the hexane injection solvent at 0.75 minutes (i.e. carbon response) is practically undetected. Of note, closer examination of Figure 6-6A revealed that it only gave a signal of about 0.02 mV that is near the noise level. To discern the HPO^{*} emission band from the phosphorous compound, a 527 nm (10 nm bandpass) filter was used with the PMT. Subsequent analysis of the same mixture rendered a lone trimethyl phosphite peak in the chromatogram, as seen in Figure 6-6B. Similarly, a 393 nm (11 nm bandpass)

filter used to isolate a characteristic S_2^* emission band from the sulfur compound also resulted in the diethyl sulfide peak being solely observed (Figure 6-6C).

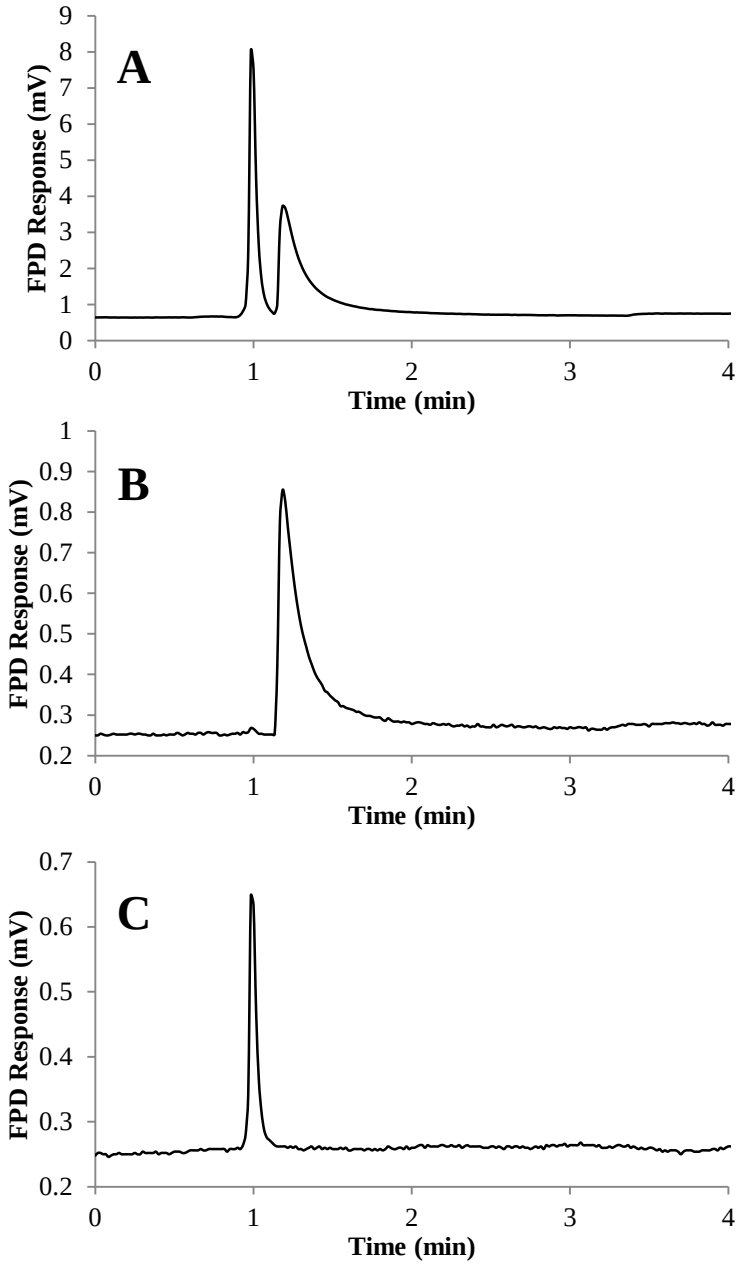

Figure 6-6: The Ti µGC-FPD analysis of (in order of elution) diethyl sulfide and trimethyl phosphite in hexane using a PMT with A) no filter (open), B) a 527 nm filter, and C) a 393 nm filter. Column temperature is 35 °C.

Further, in both Figure 6-6B and C, no signal at all was detected from the hydrocarbon injection solvent. It is worth noting that because of the extensive range of the S_2^* spectrum, a very minor interference can be seen in the phosphorous channel in Figure 6-6B at the diethyl sulfide retention time. However, this is commonly observed in the conventional FPD [47], and only amounts to 0.17% of the original signal in Figure 6-6A. Thus, together this confirms that the Ti μGC-FPD device can readily invoke the familiar selectivity enhancements (over hydrocarbons and other elements) expected from the conventional FPD [47] when interference filters are used to further isolate sulfur and phosphorous emissions.

6.4 Applications

To help illustrate the analytical utility of the device, some samples were analyzed. The first was a natural gas sample containing the common additive tetrahydrothiophene. This sulfur compound is often used as an odorant for natural gas and is therefore important to monitor [162]. Figure 6-7 presents a chromatogram of this sample as analyzed on the Ti μGC-FPD device and displays a singular sulfur peak corresponding to about 5 ng of the compound. As seen, the analysis yields a good sharp signal for this analyte in a short amount of time.

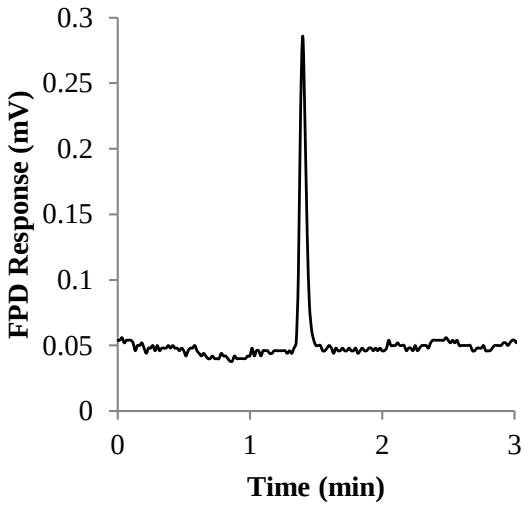

Figure 6-7: Chromatogram from the Ti µGC-FPD device showing the analysis of a natural gas sample containing tetrahydrothiophene. Column temperature is 35 °C.

The second sample tested was the headspace over minced garlic. Literature reports that one of the most abundant and important compounds found in garlic headspace is allyl mercaptan [132,142] and so it was also investigated here with the Ti µGC-FPD device. As seen, analysis of the headspace after an hour of equilibration with the garlic readily detected the early-eluting allyl mercaptan species (Figure 6-8), which represented nearly 1 ng of the analyte present. Therefore, the Ti µGC-FPD device demonstrates a simple operation and good sensitivity that can allow for useful selective analyses.

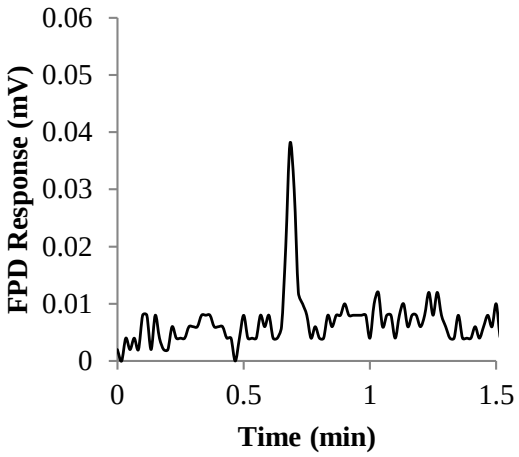

Figure 6-8: Chromatogram from the Ti µGC-FPD device showing the analysis of allyl mercaptan in the headspace over garlic an hour after mincing. Column temperature is 35 °C.

6.5 Conclusion

The properties of a novel Ti µGC-FPD device are demonstrated. The design is favorable for on-chip separation and detection, and provides robust and reliable FPD analysis. The separation column employed allows for fairly rapid µGC-FPD analysis with reasonable peak shape and resolution. Using relatively low optimal flow rates, the detector yields good detection limits, repeatability, and selectivity. It should also be noted that a linear sulfur response mode in the FPD has been reported [93] and therefore it would be interesting to explore in this Ti device in future investigations. Results indicate that Ti platforms, such as those used in this device, can be a useful alternative for supporting µGC analyses with a portable FPD sensor on-chip. As such, the Ti µGC-FPD device may be a beneficial approach for miniaturizing conventional GC-FPD systems and could also perhaps lead to other useful detector adaptations.

CHAPTER SEVEN: SUMMARY AND FUTURE WORK

7.1 Summary

This thesis describes the development of novel strategies for the analysis of organosulfur compounds in gas chromatography with flame photometric detection. Due to the importance of regular monitoring for quality control purposes, analytical methods that can selectively determine organosulfur compound identities and amounts are desirable. In GC, these analyses often employ selective detectors such as the rugged and simple FPD. However, the FPD can suffer from response quenching when a chemiluminescent analyte (i.e. sulfur) co-elutes with a hydrocarbon. As such, further development of methods that avoid or reduce quenching for FPD use are beneficial.

One such way to avoid FPD quenching is to invoke increased selectivity for GC separations through a water stationary phase column, which was investigated here for sulfur separations for the first time. With this stationary phase, various classes of sulfur compounds such as thiols, sulfides, disulfides, and ring species were retained and separated on the phase, while non-polar alkanes exhibited no retention. This inherent selectivity for sulfur compounds over hydrocarbons prevents their co-elution and enables the use of the FPD. The separation of a complex gasoline matrix spiked with three sulfur components demonstrated this, with no detector quenching observed when using the water stationary phase. In contrast, the same analysis using a conventional non-polar DB-1 column showed significant sulfur response quenching in the FPD. Overall, these experiments have shown the potential for further use of a water stationary phase for GC-FPD analysis of organosulfur compounds.

Next, a selective sample preparation method for the extraction of thiols was presented to simplify solutions prior to GC-FPD analysis. This method uses solid PbO or plumbite (PbO_2^{2-}) solution to convert thiols into solid lead thiolates. These reagents were both found to have excellent selectivity toward thiol compounds. Further, plumbite was able to extract thiols ten times faster than PbO. To this end, extraction efficiencies near 100% were achieved for 1-butanethiol, benzenethiol, tert-buylthiol, and 2-propanethiol in less than four minutes of contact with plumbite, with most of the extraction taking place within the first two minutes. Conversion of solid thiolate back into the original thiol was rapidly achieved through the addition of acid to neutralize the plumbite solution. Using this method, thiols were selectively extracted and fully reconstituted into a fresh and simple solvent to avoid co-elution and FPD quenching from other matrix components. These results suggest that this method could be very useful as an analytical tool for the determination of thiols in complex matrices.

The utility of this extraction method was then extended by using plumbite as a stationary phase for the potentially selective chromatographic analysis of thiols. Using a plumbite pre-column stationary phase, thiols injected into the GC system could be easily converted into solid thiolates and trapped on the phase, while non-thiol compounds eluted as normal. As expected, the plumbite phase was selective only for thiol compounds, and the conversion of thiol to solid thiolate was instantaneous. However, releasing the thiol into its original form for analysis was difficult and unreliable. Reproducibility from trial-to-trial was unpredictable despite various troubleshooting attempts, such as using restriction or drying agents to prevent plumbite from entering the analytical column. Alternatively, solid PbO was tested. Similar results were obtained in this format, showing both excellent selectivity toward

thiols and also the lack of repeatable release. However, overall the data still indicates that this method has the potential to be powerful for controlling thiol elution in GC.

This thesis also described the first on-board FPD in a µGC device. The Ti µGC-FPD showed good separation and peak shape, as well as excellent chemiluminescence from sulfur and phosphorous compounds. As such, the limits of detection obtained from this device were similar to a conventional FPD and were comparatively much lower than previous reported limits from an FPD coupled into a µGC system. The use of interference filters for flame emission was demonstrated and a few applications were examined to show the usefulness of this device. Overall, this initial study with the Ti µGC-FPD device indicates the potential for selective detection in a µGC format that could be further beneficial in field analysis.

7.2 Future Work

7.2.1 FPD Analysis of Other Chemiluminescent Compounds Using a Water Stationary Phase

Since the FPD is a selective detector for chemiluminescent compounds, it would be of interest to analyze various other light-emitting compounds using the water stationary phase. A natural extension of the work presented in Chapter Three is to analyze phosphorous-containing compounds, as their analysis is frequently performed with an FPD. Preliminary results with phosphites on the water phase indicated their reactivity and incompatibility. However, phosphates are much more stable in water and have not yet been explored in detail. Thus, a study of their retention characteristics on the water stationary phase could be valuable and help elucidate their behaviour on the phase. Moreover, the analysis of various

phosphorous-containing pesticides and insecticides are of interest due to their presence in a wide range of environmental samples. For example, chlorfenvinphos is a potent insecticide with high water solubility that would be of interest to monitor in groundwater leaching experiments. This analysis can be difficult due to the complex nature of these samples. To this end, the water stationary phase could be very beneficial for the examination of such compounds. Further, the selectivity of the water phase for moderately polar compounds over non-polar or highly polar hydrocarbons could help avoid FPD response quenching with matrix materials. Therefore, it would be advantageous to explore this and numerous other phosphorous-bearing analytes.

Other chemiluminescent compounds would also be interesting to investigate using the water stationary phase. For example, tetraethyl tin can be used as a biocide and thus its analysis is important in biological aspects [163]. As tetraethyl tin has low water solubility and biological components are often highly soluble in water, the water stationary phase could provide good separation of the two and therefore lead to improved detection. Thus, examination of the water stationary phase for this and other chemiluminescent species (e.g. Fe, Cr, Ni, Mn, etc.) may lead to novel and useful methods for analyzing various metals by this GC-FPD approach.

7.2.2 Subtraction Chromatography Using PbO or Plumbite

The selective chromatographic system described in Chapter Five demonstrated the possibility of a controlled trap-and-release thiol analysis. Although further investigations are necessary to understand the in situ process, this method does however indicate the potential for subtraction chromatography. In subtraction chromatography, chromatograms are

subtracted from one another to determine differences between analyses. For example, an unknown solution may demonstrate a chromatogram with multiple peaks. Using the in situ thiol trapping method with PbO or plumbite, the injection of the same sample can show a similar analysis but with no thiol peaks present. Thus, the subtraction of these two chromatograms would eliminate the common peaks that were observed in each chromatogram, and show only the thiol compounds. This distinguishes which of the unknown peaks were from thiols. Therefore, it would be useful to explore the extraction technique employed in this thesis for subtraction chromatography to determine with certainty the presence of thiols in unknown solutions.

7.2.3 Further Investigations into the Ti µGC-FPD Device

The µGC-FPD presented in Chapter Six showed great potential for a miniaturized analytical device selective for sulfur and phosphorous. However, only a few compounds have been characterized on this device as the existing on-board heater has a limiting maximum temperature of 100 °C. Since most conventional GC columns can be heated to 250 °C or higher, it would be of great interest to investigate other suppliers that can provide a larger temperature range for this device. In turn, more complex matrices could be analyzed. This would be a very beneficial trait for a portable analytical device. For example, a small, lightweight, low reagent consumption device would be useful for the oil and gas industry to perform regular selective analysis for sulfur compounds at various points along a pipeline to ensure quality control. Additionally, the use of a higher temperature separation device could also be beneficial for military personnel detecting chemical warfare agents in the field, as these compounds often have moderately high boiling points.

Further characterization of the FPD response in this device would also be interesting to explore for elements such as arsenic, tin, selenium, and others. Such elements can garner a significant response in the FPD, so it is valuable to examine. Additionally, interference filters may be required to differentiate between such chemiluminescent compounds. Thus, there is still much to investigate with this device. Overall, the ability to selectively analyze multiple light-emitting species is beneficial and could potentially extend the applicable range of this analytical device to numerous industries.

REFERENCES

[1] X. Labandeira-Villot, Market instruments and the control of acid rain damage generating industry, Energy Policy. 24 (1996) 841–854. doi:10.1016/0301-4215(96)00062-6.

[2] M.H. Whittaker, A.M. Gebhart, T.C. Miller, F. Hammer, Human health risk assessment of 2-mercaptobenzothiazole in drinking water, Toxicol. Ind. Health. 20 (2004) 149–163.

[3] R. Avagyan, I. Sadiktsis, C. Bergvall, R. Westerholm, Tire tread wear particles in ambient air - a previously unknown source of human exposure to the biocide 2-mercaptobenzothiazole, Environ. Sci. Pollut. Res. 21 (2014) 11580–11586. doi:10.1007/s11356-014-3131-1.

[4] T. Sorahan, Cancer risks in chemical production workers exposed to 2-mercaptobenzothiazole., Occup. Environ. Med. 66 (2009) 269–73. doi:10.1136/oem.2008.041400.

[5] X. Lu, C. Fan, J. Shang, J. Deng, H. Yin, Headspace solid-phase microextraction for the determination of volatile sulfur compounds in odorous hyper-eutrophic freshwater lakes using gas chromatography with flame photometric detection, Microchem. J. 104 (2012) 26–32. doi:10.1016/j.microc.2012.04.001.

[6] R.J. McGorrin, The significance of volatile sulfur compounds in food flavors, in: M.C. Qian, X. Fan, K. Mahattanatawee (Eds.), Volatile Sulfur Compd. Food, American Chemical Society, Washington D.C., 2011: pp. 3–31. doi:10.1021/bk-2011-1068.ch001.

[7] Z. Witkiewicz, M. Mazurek, J. Szulc, Chromatographic analysis of chemical warfare

agents, J. Chromatogr. 503 (1990) 293–357. doi:10.1016/S0021-9673(01)81514-4.

[8] K. Ganesan, S.K. Raza, R. Vijayaraghavan, Chemical warfare agents, J. Pharm. Bioallied Sci. 2 (2010) 166–178. doi:10.4103/0975-7406.68498.

[9] D.M. Coulson, L.A. Cavanagh, J. Stuart, Gas Chromatography of Pesticides, J. Agric. Food Chem. 7 (1959) 250–251. doi:10.1021/jf60098a001.

[10] H. Jing, A. Amirav, Pesticide analysis with the pulsed-flame photometer detector and a direct sample introduction device., Anal. Chem. 69 (1997) 1426–35. doi:10.1021/ac961110k.

[11] A.T. James, A.J.P. Martin, Gas-liquid partition chromatography: the separation and micro-estimation of volatile fatty acids from formic acid to dodecanoic acid, Biochem. J. 50 (1952) 679–690.

[12] C. Zwiener, T. Glauner, F.H. Frimmel, Biodegradation of Pharmaceutical Residues Investigated by SPE-GC/ITD-MS and On-Line Derivatization, J. High Resol. Chromatogr. 23 (2000) 474–478.

[13] J.M. Warren, D.R. Parkinson, J. Pawliszyn, Assessment of thiol compounds from garlic by automated headspace derivatized in-needle-NTD-GC-MS and derivatized in-fiber-SPME-GC-MS, J. Agric. Food Chem. 61 (2013) 492–500. doi:10.1021/jf303508m.

[14] S.C. Terry, J.H. Herman, J.B. Angell, A Gas Chromatographic Air Analyzer Fabricated on a Silicon Wafer, IEEE Trans. Electron Devices. 26 (1979) 1880–1886. doi:10.1109/T-ED.1979.19791.

[15] S.J. Lehotay, J. Hajšlová, Application of gas chromatography in food analysis, Trends Anal. Chem. 21 (2002) 686–697. doi:10.1016/S0165-9936(02)00805-1.

[16] F.L. Dorman, J.J. Whiting, S. Joseph, J.W. Cochran, J. Gardea-torresdey, Gas Chromatography, Anal. Chem. 82 (2010) 4775–4785.

[17] V.P. Campos, A.S. Oliveira, L.P.S. Cruz, J. Borges, T.M. Tavares, Optimization of parameters of sampling and determination of reduced sulfur compounds using cryogenic capture and gas chromatography in tropical urban atmosphere, Microchem. J. 96 (2010) 283–289. doi:10.1016/j.microc.2010.04.003.

[18] T. Belal, T. Awad, C.R. Clark, Determination of paracetamol and tramadol hydrochloride in pharmaceutical mixture using HPLC and GC-MS, J. Chromatogr. Sci. 47 (2009) 849–854. doi:10.1093/chromsci/47.10.849.

[19] B.N. Barman, V.L. Cebolla, L. Membrado, Chromatographic Techniques for Petroleum and Related Products, Crit. Rev. Anal. Chem. 30 (2000) 75–120. doi:10.1080/10408340091164199.

[20] Z. Al-Attabi, B.R. D'Arcy, H.C. Deeth, Volatile sulphur compounds in UHT milk, Crit. Rev. Food Sci. Nutr. 49 (2009) 28–47. doi:10.1080/10408390701764187.

[21] F. Ahmadi, Y. Assadi, S.M.R.M. Hosseini, M. Rezaee, Determination of organophosphorus pesticides in water samples by single drop microextraction and gas chromatography-flame photometric detector., J. Chromatogr. A. 1101 (2006) 307–12. doi:10.1016/j.chroma.2005.11.017.

[22] J. de Zeeuw, J. Luong, Developments in stationary phase technology for gas chromatography, TrAC - Trends Anal. Chem. 21 (2002) 594–607. doi:10.1016/S0165-9936(02)00809-9.

[23] Y. Xiao, S.C. Ng, T.T.Y. Tan, Y. Wang, Recent development of cyclodextrin chiral stationary phases and their applications in chromatography, J. Chromatogr. A. 1269

(2012) 52–68. doi:10.1016/j.chroma.2012.08.049.

[24] K.B. Thurbide, C.D. Anderson, Flame photometric detection inside of a capillary gas chromatography column, Analyst. 128 (2003) 616–622. doi:10.1039/b212727j.

[25] K.B. Thurbide, T.C. Hayward, Improved micro-flame detection method for gas chromatography, Anal. Chim. Acta. 519 (2004) 121–128. doi:10.1016/j.aca.2004.05.047.

[26] A.D. Radadia, R.D. Morgan, R.I. Masel, M.A. Shannon, Partially buried microcolumns for micro gas analyzers, Anal. Chem. 81 (2009) 3471–3477. doi:10.1021/ac8027382.

[27] A.D. Radadia, R.I. Masel, M.A. Shannon, J.P. Jerrell, K.R. Cadwallader, Micromachined GC columns for fast separation of organophosphonate and organosulfur compounds, Anal. Chem. 80 (2008) 4087–4094. doi:10.1021/ac800212e.

[28] T.C. Hayward, K.B. Thurbide, Novel on-column and inverted operating modes of a microcounter-current flame ionization detector, J. Chromatogr. A. 1200 (2008) 2–7. doi:10.1016/j.chroma.2008.02.053.

[29] A. Ghosh, C.R. Vilorio, A.R. Hawkins, M.L. Lee, Microchip Gas Chromatography Columns, Interfacing and Performance, Talanta. 10 (2018) 1–11. doi:10.1016/j.jep.2018.04.033.

[30] A. Ghosh, A.R. Foster, J.C. Johnson, C.R. Vilorio, L.T. Tolley, B.D. Iverson, et al., Stainless-Steel Column for Robust, High-Temperature Microchip Gas Chromatography, Anal. Chem. 91 (2019) 792–796. doi:10.1021/acs.analchem.8b04174.

[31] M. Agah, J.A. Potkay, G. Lambertus, R. Sacks, K.D. Wise, High-performance

temperature-programmed microfabricated gas chromatography columns, J. Microelectromechanical Syst. 14 (2005) 1039–1050. doi:10.1109/JMEMS.2005.856648.

[32] E. Darko, K.B. Thurbide, G.C. Gerhardt, J. Michienzi, Characterization of low-temperature cofired ceramic tiles as platforms for gas chromatographic separations, Anal. Chem. 85 (2013) 5376–5381. doi:10.1021/ac400782f.

[33] C.F. Poole, The Essence of Chromatography, Elsevier Science B.V., Amsterdam, 2003.

[34] P. Sandra, G. Redant, E. Schacht, M. Verzele, In situ cross-linking of the stationary phase in capillary columns. Part 1: Introduction and preparation of apolar columns, J. High Resolut. Chromatogr. 4 (1981) 411–412. doi:10.1002/jhrc.1240040810.

[35] Y. Yang, Subcritical water chromatography: A green approach to high-temperature liquid chromatography, J. Sep. Sci. 30 (2007) 1131–1140. doi:10.1002/jssc.200700008.

[36] D.J. Miller, S.B. Hawthorne, Method for Determining the Solubilities of Hydrophobic Organics in Subcritical Water, Anal. Chem. 70 (1998) 1618–1621. doi:10.1021/ac971161x.

[37] M.O. Fogwill, K.B. Thurbide, Chromatography using a water stationary phase and a carbon dioxide mobile phase, Anal. Chem. 82 (2010) 10060–7. doi:10.1021/ac1018793.

[38] J.N. Murakami, K.B. Thurbide, Packed Column Supercritical Fluid Chromatography Using Stainless Steel Particles and Water As a Stationary Phase, Anal. Chem. 87 (2015) 9429–9435. doi:10.1021/acs.analchem.5b02399.

[39] J.A. Gallant, K.B. Thurbide, Properties of water as a novel stationary phase in capillary gas chromatography, J. Chromatogr. A. 1359 (2014) 247–54. doi:10.1016/j.chroma.2014.07.018.

[40] A.F. Scott, K.B. Thurbide, Retention characteristics of a pH tunable water stationary phase in supercritical fluid chromatography, J. Chromatogr. Sci. 55 (2017) 82–89. doi:10.1093/chromsci/bmw153.

[41] M.T. Saowapon, K.B. Thurbide, Dehydration of a Water Stationary Phase as a Novel Separation Gradient in Capillary Supercritical Fluid Chromatography, Chromatographia. 82 (2019) 991–1001. doi:10.1007/s10337-019-03735-8.

[42] M.T. Saowapon, K.B. Thurbide, Adjustable column length using a water stationary phase in supercritical fluid chromatography, Can. J. Chem. 6 (2019) 1–6. doi:10.1139/cjc-2019-0157.

[43] E. Darko, K.B. Thurbide, Capillary gas chromatographic separation of organic bases using a pH-adjusted basic water stationary phase, J. Chromatogr. A. 1465 (2016) 184–189. doi:10.1016/j.chroma.2016.08.059.

[44] E. Darko, K.B. Thurbide, Capillary Gas Chromatographic Separation of Carboxylic Acids Using an Acidic Water Stationary Phase, Chromatographia. 80 (2017) 1225–1232. doi:10.1007/s10337-017-3333-z.

[45] E. Darko, K.B. Thurbide, Dynamic Control of Gas Chromatographic Selectivity during the Analysis of Organic Bases, Anal. Chem. 91 (2019) 6682–6688. doi:10.1021/acs.analchem.9b00703.

[46] D.G. McMinn, H.H. Hill, The Flame Ionization Detector, in: Detect. Capill. Chromatogr., John Wiley & Sons, 1992: pp. 7–21.

[47] M. Dressler, Flame Photometric Detector, in: Sel. Gas Chromatogr. Detect., Elsevier, 1986: pp. 133–160.

[48] I.G. McWilliam, R.A. Dewar, Flame Ionization Detector for Gas Chromatography, Nature. 181 (1958) 760.

[49] J. Harley, W. Nel, V. Pretorius, Flame Ionization Detector for Gas Chromatography, Nature. 181 (1958) 177–178.

[50] A. Aue, H.H. Hill, A hydrogen-rich flame ionization detector sensitive to metals, J. Chromatogr. 74 (1972) 319–324.

[51] M.A. Morrissey, H.H. Hill, Metal selective flame ionization detection after supercritical fluid chromatography, J. High Resolut. Chromatogr. 11 (1988) 375–379. doi:10.1002/jhrc.1240110503.

[52] A.F. Scott, K.B. Thurbide, D. Quickfall, A comparison of hydrocarbon and alkali metal response in the flame ionization detector used in subcritical water chromatography, Can. J. Chem. 93 (2015) 784–789. doi:10.1139/cjc-2015-0095.

[53] S. Zimmermann, S. Wischhusen, J. Müller, Micro flame ionization detector and micro flame spectrometer, Sensors Actuators, B Chem. 63 (2000) 159–166. doi:10.1016/S0925-4005(00)00353-1.

[54] S. Zimmermann, P. Krippner, A. Vogel, J. Müller, Miniaturized flame ionization detector for gas chromatography, Sensors Actuators, B Chem. 83 (2002) 285–289. doi:10.1016/S0925-4005(01)01060-7.

[55] W. Kuipers, J. Müller, Sensitivity of a planar micro-flame ionization detector, Talanta. 82 (2010) 1674–1679. doi:10.1016/j.talanta.2010.07.042.

[56] R.P. Raut, K.B. Thurbide, Characterization of Titanium Tiles as Novel Platforms for

Micro-Flame Ionization Detection in Miniature Gas Chromatography, Chromatographia. 80 (2017) 805–812. doi:10.1007/s10337-017-3281-7.

[57] S.S. Brody, J.E. Chaney, Flame Photometric Detector: The Application of a Specific Detector for Phosphorus and for Sulfur Compounds — Sensitive to Subnanogram Quantities, J. Gas Chromatogr. 4 (1966) 42–46. doi:10.1093/chromsci/4.2.42.

[58] W.A. Aue, H. Singh, Chemiluminescent photon yields measured in the flame photometric detector on chromatographic peaks containing sulfur, phosphorous, manganese, ruthenium, iron or selenium, Spectrochim. Acta Part B. 56 (2001) 517–525. doi:10.1016/S0584-8547(01)00176-8.

[59] W.A. Aue, C.G. Flinn, Chemical linearization of chalcogen response in a flame photometric detector, J. Chromatogr. Sci. 158 (1978) 161–170.

[60] R.S. Hutte, J.D. Ray, Sulfur-Selective Detectors, in: H.H. Hill, D.D. McMinn (Eds.), Detect. Capill. Chromatogr., Wiley, 1992: pp. 193–218.

[61] P. Liu, C. Xu, Q. Shi, N. Pan, Y. Zhang, S. Zhao, et al., Characterization of Sulfide Compounds in Petroleum : Selective Oxidation Followed by Positive-Ion Electrospray Fourier Transform Ion Cyclotron Resonance Mass Spectrometry, Anal. Chem. 82 (2010) 6601–6606.

[62] W. Gries, K. Küpper, G. Leng, Rapid and sensitive LC–MS–MS determination of 2-mercaptobenzothiazole, a rubber additive, in human urine, Anal. Bioanal. Chem. (2015) 3417–3423. doi:10.1007/s00216-015-8533-5.

[63] T. Reemtsma, O. Fiehn, G. Kalnowski, M. Jekel, Microbial Transformations and Biological Effects of Fungicide-Derived Benzothiazoles Determined in Industrial Waste-Water, Environ. Sci. Technol. 29 (1995) 478–485. doi:10.1021/es00002a025.

[64] J.W. Nielsen, K.S. Jensen, R.E. Hansen, C.H. Gotfredsen, J.R. Winther, A fluorescent probe which allows highly specific thiol labeling at low pH, Anal. Biochem. 421 (2012) 115–120. doi:10.1016/j.ab.2011.11.027.

[65] B. Eskenazi, A. Bradman, R. Castorina, Exposures of children to organophosphate pesticides and their potential adverse health effects., Environ. Health Perspect. 107 (1999) 409–419. doi:10.1289/ehp.99107s3409.

[66] S. Kendler, S.M. Reidy, G.R. Lambertus, R.D. Sacks, Ultrafast gas chromatographic separation of organophosphor and organosulfur compounds utilizing a microcountercurrent flame photometric detector, Anal. Chem. 78 (2006) 6765–6773. doi:10.1021/ac060851a.

[67] S.O. Farwell, C.J. Barinaga, Sulfur-selective detection with the FPD: Current enigmas, practical usage, and future directions, J. Chromatogr. Sci. 24 (1986) 483–494. doi:10.1093/chromsci/24.11.483.

[68] G.H. Liu, P.R. Fu, Effects of hydrocarbon quenching in gas chromatography when using the flame photometric detector, Chromatographia. 27 (1989) 159–163. doi:10.1007/BF02265869.

[69] T. Sugiyama, Y. Suzuki, T. Takeuchi, Interferences of S2 molecular emission in a flame photometric detector, J. Chromatogr. 80 (1973) 61–67.

[70] P.L. Patterson, R.L. Howe, A. Abu-Shumays, A dual-flame photometric detector for sulfur and phosphorus compounds in gas chromatograph effluents, Anal. Chem. 50 (1978) 339–344. doi:10.1021/ac50024a042.

[71] P.L. Patterson, Comparison of quenching effects in single- and dual-flame photometric detectors, Anal. Chem. 50 (1978) 345–348. doi:10.1021/ac50024a043.

[72] W.E. Rupprecht, T.R. Phillips, The utilisation of fuel-rich flames as sulphur detectors, Anal. Chim. Acta. 47 (1969) 439–449. doi:10.1016/S0003-2670(01)95644-2.

[73] T.C. Hayward, K.B. Thurbide, Quenching-resistant multiple micro-flame photometric detector for gas chromatography, Anal. Chem. 81 (2009) 8858–8867. doi:10.1021/ac901421s.

[74] A.G. Clark, K.B. Thurbide, An improved multiple flame photometric detector for gas chromatography, J. Chromatogr. A. 1421 (2015) 154–161. doi:10.1016/j.chroma.2015.04.007.

[75] R.L. Benner, D.H. Stedman, Universal sulfur detection by chemiluminescence, Anal. Chem. 61 (1989) 1268–1271. doi:10.1021/ac00186a018.

[76] S. Risticevic, D. Vuckovic, J. Pawliszyn, Solid-Phase Microextraction, in: J. Pawliszyn, H.L. Lord (Eds.), Handb. Sample Prep., John Wiley & Sons, Hoboken, 2010: pp. 81–102.

[77] Q. Wang, J.M. Chong, J. Pawliszyn, Determination of thiol compounds by automated headspace solid-phase microextraction with in-fiber derivatization, Flavour Fragr. J. 21 (2006) 385–394. doi:10.1002/ffj.1724.

[78] D.R. Knapp, Handbook of Analytical Derivatization Reactions, John Wiley & Sons, 1979.

[79] J.S. Thomson, J.B. Green, T.B. McWilliams, Determination of sulfides and thiols in petroleum distillates using solid-phase extraction and derivatization with pentafluorobenzoyl chloride, Energy and Fuels. 11 (1997) 909–914. doi:10.1021/ef960165m.

[80] C. Zwiener, F.H. Frimmel, Oxidative treatment of pharmaceuticals in water, Water

Res. 34 (2000) 1881–1885. doi:10.1016/S0043-1354(99)00338-3.

[81] R. Alzaga, R.W. Ryan, K. Taylor-Worth, A.M. Lipczynski, R. Szucs, P. Sandra, A generic approach for the determination of residues of alkylating agents in active pharmaceutical ingredients by in situ derivatization-headspace-gas chromatography-mass spectrometry, J. Pharm. Biomed. Anal. 45 (2007) 472–479. doi:10.1016/j.jpba.2007.07.017.

[82] J.M. Halket, D. Waterman, A.M. Przyborowska, R.K.P. Patel, P.D. Fraser, P.M. Bramley, Chemical derivatization and mass spectral libraries in metabolic profiling by GC/MS and LC/MS/MS, J. Exp. Bot. 56 (2005) 219–243. doi:10.1093/jxb/eri069.

[83] X. Tao, Y. Liu, Y. Wang, Y. Qiu, J. Lin, A. Zhao, et al., GC-MS with ethyl chloroformate derivatization for comprehensive analysis of metabolites in serum and its application to human uremia, Anal. Bioanal. Chem. 391 (2008) 2881–2889. doi:10.1007/s00216-008-2220-8.

[84] P. Hušek, Chloroformates in gas chromatography as general purpose derivatizing agents, J. Chromatogr. B. 717 (1998) 57–91. doi:10.1016/S0378-4347(98)00136-4.

[85] L.E. Musumeci, I. Ryona, B.S. Pan, N. Loscos, H. Feng, M.T. Cleary, et al., Quantification of polyfunctional thiols in wine by HS-SPME-GC-MS following extractive alkylation, Molecules. 20 (2015) 12280–12299. doi:10.3390/molecules200712280.

[86] F. Lyumugabe, J. Gros, P. Thonart, S. Collin, Occurrence of polyfunctional thiols in sorghum beer “ikigage” made with Vernonia amygdalina “umubirizi,” Flavour Fragr. J. 27 (2012) 372–377. doi:10.1002/ffj.3114.

[87] A. Belancic Majcenovic, R. Schneider, J.P. Lepoutre, V. Lempereur, R. Baumes,

Synthesis and stable isotope dilution assay of ethanethiol and diethyl disulfide in wine using solid phase microextraction. Effect of aging on their levels in wine, J. Agric. Food Chem. 50 (2002) 6653–6658. doi:10.1021/jf020478h.

[88] W.A.E. McBryde, Petroleum deodorized: Early canadian history of the 'doctor sweetening' process, Ann. Sci. 48 (1991) 103–111. doi:10.1080/00033799100200161.

[89] J.P. Nehlsen, J.B. Benziger, I.G. Kevrekidis, Removal of Alkanethiols from a Hydrocarbon Mixture by a Heterogeneous Reaction with Metal Oxides, Ind. Eng. Chem. Res. 42 (2003) 6919–6923. doi:10.1021/ie030665k.

[90] J.P. Nehlsen, J.B. Benziger, I.G. Kevrekidis, A process for the removal of thiols from a hydrocarbon stream by a heterogeneous reaction with lead oxide, Energy and Fuels. 18 (2004) 721–726. doi:10.1021/ef034064h.

[91] J.J. Frantz, K.B. Thurbide, Chiral Separations Using a Modified Water Stationary Phase in Supercritical Fluid Chromatography, Chromatographia. 81 (2018) 969–979. doi:10.1007/s10337-018-3534-0.

[92] P.Y. Chen, M.H. Tsai, W.K. Yeh, M.H. Jing, Y. Chang, Relationship between wafer edge design and its ultimate mechanical strength, Microelectron. Eng. 87 (2010) 2065–2070. doi:10.1016/j.mee.2009.12.083.

[93] A.G. Clark, K.B. Thurbide, Properties of a novel linear sulfur response mode in a multiple flame photometric detector, J. Chromatogr. A. 1326 (2014) 103–109. doi:10.1016/j.chroma.2013.12.050.

[94] D.A. Ferguson, L.A. Luke, Critical Appraisal of the Flame Photometric Detector in Petroleum Analysis, Chromatographia. 12 (1979) 197–203. doi:0009-5893/79/040197-07.

[95] L. Blomberg, Gas chromatographic separation of some sulphur compounds on glass capillary columns using flame photometric detection, J. Chromatogr. 125 (1976) 389–397. doi:10.1016/S0021-9673(00)83370-1.

[96] I. Al-Zahrani, C. Basheer, T. Htun, Application of liquid-phase microextraction for the determination of sulfur compounds in crude oil and diesel, J. Chromatogr. A. 1330 (2014) 97–102. doi:10.1016/j.chroma.2014.01.015.

[97] D.D. Link, P. Zandhuis, The distribution of sulfur compounds in hydrotreated jet fuels: Implications for obtaining low-sulfur petroleum fractions, Fuel. 85 (2006) 451–455. doi:10.1016/j.fuel.2005.08.029.

[98] Á. Stumpf, K. Tolvaj, M. Juhász, Detailed analysis of sulfur compounds in gasoline range petroleum products with high-resolution gas chromatography-atomic emission detection using group-selective chemical treatment, J. Chromatogr. A. 819 (1998) 67–74. doi:10.1016/S0021-9673(98)00444-0.

[99] C. Lopez Garcia, M. Becchi, M.F. Grenier-Loustalot, O. Paisse, R. Szymanski, Analysis of aromatic sulfur compounds in gas oils using GC with sulfur chemiluminescence detection and high-resolution MS, Anal. Chem. 74 (2002) 3849–3857. doi:10.1021/ac011190e.

[100] J. Luong, R. Gras, R.A. Shellie, H.J. Cortes, Tandem sulfur chemiluminescence and flame ionization detection with planar microfluidic devices for the characterization of sulfur compounds in hydrocarbon matrices, J. Chromatogr. A. 1297 (2013) 231–235. doi:10.1016/j.chroma.2013.04.080.

[101] A. Pavlova, P. Ivanova, T. Dimova, Sulfur Compounds in Petroluem Hydrocarbon Streams, Pet. Coal. 54 (2012) 9–13.

[102] M.T. Timko, E. Schmois, P. Patwardhan, Y. Kida, C.A. Class, W.H. Green, et al., Response of Different Types of Sulfur Compounds to Oxidative Desulfurization of Jet Fuel, Energy & Fuels. 28 (2014) 2977–2983. doi:10.1021/ef500216p.

[103] W. Wardencki, Problems with the determination of environmental sulphur compounds by gas chromatography, J. Chromatogr. A. 793 (1998) 1–19. doi:10.1016/S0021-9673(97)00997-7.

[104] W. Wardencki, Sulfur Compounds: Gas Chromatography, Encycl. Sep. Sci. (2000) 4285–4301. doi:10.1016/B0-12-226770-2/06201-3.

[105] J. Sevcik, N.T.P. Thao, The Selectivity of the Flame Photometric Detector, Chromatographia. 8 (1975) 559–562. doi:10.1007/BF02314040.

[106] D.F.S. Natusch, T.M. Thorpe, Element selective detectors in gas chromatography, Anal. Chem. 45 (1973) 1184–1194. doi:10.1021/ac60336a018.

[107] M.H. Abraham, J. Le, The correlation and prediction of the solubility of compounds in water using an amended solvation energy relationship, J. Pharm. Sci. 88 (1999) 868–880. doi:10.1021/js9901007.

[108] D. Mackay, W.Y. Shiu, K. Ma, S.C. Lee, Handbook of Physical-Chemical Properties and Environmental Fate for Organic Chemicals, Second Edi, Taylor & Francis Group, LLC, Boca Raton, FL, 2006. doi:10.1201/9781420044393.

[109] G. Liu, Oxidation of thiols within gas chromatographic columns, J. Chromatogr. 441 (1988) 312–315. doi:10.1016/S0021-9673(01)83881-4.

[110] Y. Fang, M.C. Qian, Sensitive quantification of sulfur compounds in wine by headspace solid-phase microextraction technique, J. Chromatogr. A. 1080 (2005) 177–185. doi:10.1016/j.chroma.2005.05.024.

[111] M. Mestres, C. Sala, M.P. Martí, O. Busto, J. Guasch, Headspace solid-phase microextraction of sulphides and disulphides using Carboxen-polydimethylsiloxane fibers in the analysis of wine aroma, J. Chromatogr. A. 835 (1999) 137–144. doi:10.1016/S0021-9673(98)01050-4.

[112] K.R. Christensen, G.A. Reineccius, Gas Chromatographic Analysis of Volatile Sulfur Compounds from Heated Milk Using Static Headspace Sampling, J. Dairy Sci. 75 (1992) 2098–2104. doi:10.3168/jds.S0022-0302(92)77968-5.

[113] C.L. Silva, M. Passos, J.S. Câmara, Solid phase microextraction, mass spectrometry and metabolomic approaches for detection of potential urinary cancer biomarkers—A powerful strategy for breast cancer diagnosis, Talanta. 89 (2012) 360–368. doi:10.1016/j.talanta.2011.12.041.

[114] J. Kwak, M. Gallagher, M.H. Ozdener, C.J. Wysocki, B.R. Goldsmith, A. Isamah, et al., Volatile biomarkers from human melanoma cells, J. Chromatogr. B Anal. Technol. Biomed. Life Sci. 931 (2013) 90–96. doi:10.1016/j.jchromb.2013.05.007.

[115] S. Bouatra, F. Aziat, R. Mandal, A.C. Guo, M.R. Wilson, C. Knox, et al., The Human Urine Metabolome, PLoS One. 8 (2013) e73076. doi:10.1371/journal.pone.0073076.

[116] R.H. Waring, S.C. Mitchell, G.R. Fenwick, The chemical nature of the urinary odour produced by man after asparagus ingestion, Xenobiotica. 17 (1987) 1363–1371. doi:10.3109/00498258709047166.

[117] E. Bloem, S. Haneklaus, E. Schnug, Milestones in plant sulfur research on sulfur-induced-resistance (SIR) in Europe, Front. Plant Sci. 5 (2015) 1–12. doi:10.3389/fpls.2014.00779.

[118] Y. Zhang, Z. Liu, W. Wang, Z. Cheng, B. Shen, Research on the MgO-supported

solid-base catalysts aimed at the sweetening of hydrogenated gasoline, Fuel Process. Technol. 115 (2013) 63–70. doi:10.1016/j.fuproc.2013.03.046.

[119] A. Roland, R. Schneider, A. Razungles, F. Cavelier, Varietal thiols in wine: Discovery, analysis and applications, Chem. Rev. 111 (2011) 7355–7376. doi:10.1021/cr100205b.

[120] N. Dulsat-Serra, B. Quintanilla-Casas, S. Vichi, Volatile thiols in coffee: A review on their formation, degradation, assessment and influence on coffee sensory quality, Food Res. Int. 89 (2016) 982–988. doi:10.1016/j.foodres.2016.02.008.

[121] E. Ott, E.E. Reid, Reactions of lead mercaptides with sulfur, Ind. Eng. Chem. 22 (1930) 884–887. doi:10.1021/ie50248a022.

[122] W. Faragher, J. Morrell, G. Monroe, Quantitative determination of sulfur and sulfur derivatives of hydrocarbons in naptha solutions and in petroleum distillates, Ind. Eng. Chem. 19 (1927) 1281–1284. doi:10.1021/ie50215a027.

[123] H. Zhao, D. Xia, Separation and analysis of thiols in FCC and RFCC gasoline, Pet. Sci. Technol. 22 (2004) 1641–1653. doi:10.1081/LPET-200027751.

[124] D.-H. Xia, Y.-X. Su, J.-L. Qian, Separation and identification of thiols in FCC gasoline, Pet. Sci. Technol. 15 (1997) 545–557. doi:10.1080/10916469708949674.

[125] S.M. Corrêa, G. Arbilla, Mercaptans emissions in diesel and biodiesel exhaust, Atmos. Environ. 42 (2008) 6721–6725. doi:10.1016/j.atmosenv.2008.05.036.

[126] Z. Wei, P. Mankiewicz, C. Walters, K. Qian, N.T. Phan, M.E. Madincea, et al., Natural occurrence of higher thiadiamondoids and diamondoidthiols in a deep petroleum reservoir in the Mobile Bay gas field, Org. Geochem. 42 (2011) 121–133. doi:10.1016/j.orggeochem.2010.12.002.

[127] S.K. Ganguly, G. Das, S. Kumar, B. Sain, M.O. Garg, Mechanistic kinetics of catalytic oxidation of 1-butanethiol in light oil sweetening, Catal. Today. 198 (2012) 246–251. doi:10.1016/j.cattod.2012.03.073.

[128] A.P. Topolyan, M.A. Belyaeva, M.S. Slyundina, V.V. Ilyushenkova, A.A. Formanovsky, V.A. Korshun, et al., A novel trityl/acridine derivatization agent for analysis of thiols by (matrix-assisted)(nanowire-assisted)laser desorption/ionization and electrospray ionization mass spectrometry, Anal. Methods. 9 (2017) 6335–6340. doi:10.1039/c7ay01965c.

[129] R. Gras, J. Luong, V. Carter, L. Sieben, H. Cortes, Practical method for the measurement of alkyl mercaptans in natural gas by multi-dimensional gas chromatography, capillary flow technology, and flame ionization detection, J. Chromatogr. A. 1216 (2009) 2776–2782. doi:10.1016/j.chroma.2008.09.029.

[130] P.J. de Wild, R.G. Nyqvist, F.A. de Bruijn, E.R. Stobbe, Removal of sulphur-containing odorants from fuel gases for fuel cell-based combined heat and power applications, J. Power Sources. 159 (2006) 995–1004. doi:10.1016/j.jpowsour.2005.11.100.

[131] S.W. Myung, S. Huh, J. Kim, Y. Kim, M. Kim, Y. Kim, et al., Gas chromatographic–mass spectrometric analysis of mercaptan odorants in liquefied petroleum gas and liquefied natural gas, J. Chromatogr. A. 791 (1997) 367–370. doi:10.1016/S0021-9673(97)00843-1.

[132] T. Tamaki, S. Sonoki, Volatile sulfur compounds in human expiration after eating raw or heat-treated garlic, J. Nutr. Sci. Vitaminol. (Tokyo). 45 (1999) 213–222.

[133] M.M. Løkke, M. Edelenbos, E. Larsen, A. Feilberg, Investigation of volatiles emitted

from freshly cut onions (Allium cepa L.) by real time proton-transfer reaction-mass spectrometry (PTR-MS), Sensors. 12 (2012) 16060–16076. doi:10.3390/s121216060.

[134] P.G. Hill, R.M. Smith, Determination of sulphur compounds in beer using headspace solid-phase microextraction and gas chromatographic analysis with pulsed flame photometric detection., J. Chromatogr. 872 (2000) 203–213. doi:10.1016/S0021-9673(99)01307-2.

[135] F. Jabalpurwala, O. Gurbuz, R. Rouseff, Analysis of grapefruit sulphur volatiles using SPME and pulsed flame photometric detection, Food Chem. 120 (2010) 296–303. doi:10.1016/j.foodchem.2009.09.079.

[136] K. Takoi, M. Degueil, S. Shinkaruk, C. Thibon, K. Maeda, K. Ito, et al., Identification and characteristics of new volatile thiols derived from the hop (Humulus luplus L.) cultivar nelson Sauvin, J. Agric. Food Chem. 57 (2009) 2493–2502. doi:10.1021/jf8034622.

[137] M. Simon, A.P. Hansen, C.T. Young, Effect of various dairy packaging materials on the headspace analysis of ultrapasteurized milk, J. Dairy Sci. 84 (2001) 774–83. doi:10.3168/jds.S0022-0302(01)74533-X.

[138] J.C. Morrell, W.F. Faragher, Role of Lead Sulfide in the Sweetening of Petroleum Distillates and chemistry of the Mercaptans, Ind. Eng. Chem. 1114 (1927) 1045–1049. doi:10.1021/ie50213a031.

[139] J.W. Matthews, C.J. Kircher, R.E. Drake, Oxides formed on the (111) surface of lead II. Red PbO or litharge, Thin Solid Films. 47 (1977) 95–108. doi:10.1016/0040-6090(77)90349-2.

[140] E. Ott, E.E. Reid, Reactions of Some Mercaptans with Alkaline Sodium Plumbite

Solutions, Ind. Eng. Chem. 22 (1930) 878–881. doi:10.1021/ie50248a020.

[141] G. Mazza, S. Ciaravolo, G. Chiricosta, S. Celli, Volatile flavor components from ripening and mature garlic bulbs, Flavour Fragr. J. 7 (1992) 111–116. doi:10.1002/ffj.2730070303.

[142] F. Suarez, J. Springfield, J. Furne, M. Levitt, Differentiation of mouth versus gut as site of origin of odoriferous breath gases after garlic ingestion, Am. J. Physiol. Liver Physiol. 276 (1999) G425–G430. doi:10.1152/ajpgi.1999.276.2.G425.

[143] K. Takagi, H. Kataoka, M. Makita, Determination of glutathione and related aminothiols in mouse tissues by gas chromatography with flame photometric detection., Biosci. Biotechnol. Biochem. 60 (1996) 729–31. doi:10.1271/bbb.60.729.

[144] S. Budavari, ed., Lead Formate, The Merck Index. (1996) entry 5243.

[145] R.P. Rodgers, A.M. McKenna, Petroleum analysis., Anal. Chem. 83 (2011) 4665–87. doi:10.1021/ac201080e.

[146] V.R. Reid, A.D. McBrady, R.E. Synovec, Investigation of high-speed gas chromatography using synchronized dual-valve injection and resistively heated temperature programming, J. Chromatogr. A. 1148 (2007) 236–243. doi:10.1016/j.chroma.2007.03.029.

[147] R. Sacks, H. Smith, M. Nowak, High-speed gas chromatography, Anal. Chemi. 70 (1998) 29A-37A. doi:10.1021/ac981715b.

[148] G.M. Whitesides, The origins and the future of microfluidics, Nature. 442 (2006) 368–373. doi:10.1038/nature05058.

[149] M. Stadermann, A.D. McBrady, B. Dick, V.R. Reid, A. Noy, R.E. Synovec, et al., Ultrafast Gas Chromatography on Single-Wall Carbon Nanotube Stationary Phases in

Microfabricated Channels Ultrafast Gas Chromatography on Single-Wall Carbon Nanotube Stationary Phases in Microfabricated Channels, Mech. Eng. 78 (2006) 5639–5644. doi:10.1021/ac060266.

[150] J.A. Contreras, A.J. Murray, S.E. Tolley, J.L. Oliphant, H.D. Tolley, S.A. Lammert, et al., Hand-portable gas chromatograph-toroidal ion trap mass spectrometer (GC-TMS) for detection of hazardous compounds, J. Am. Soc. Mass Spetrometry. 19 (2008) 1425–1434.

[151] F. Haghighi, Z. Talebpour, A. Sanati-Nezhad, Through the years with on-a-chip gas chromatography: A review, Lab Chip. 15 (2015) 2559–2575. doi:10.1039/c5lc00283d.

[152] K.B. Thurbide, B.W. Cooke, W.A. Aue, Novel flame photometric detector for gas chromatography based on counter-current gas flows, J. Chromatogr. A. 1029 (2004) 193–203. doi:10.1016/j.chroma.2003.12.020.

[153] W. Kuipers, J. Müller, Characterization of a microelectromechanical systems-based counter-current flame ionization detector, J. Chromatogr. A. 1218 (2011) 1891–1898. doi:10.1016/j.chroma.2011.01.084.

[154] E. Darko, Characterization of novel materials as platforms for performing microfluidic gas chromatography, MSc Thesis, University of Calgary, 2013.

[155] O. Khandan, D. Stark, A. Chang, M.P. Rao, Wafer-scale titanium anodic bonding for microfluidic applications, Sensors Actuators, B Chem. 205 (2014) 244–248. doi:10.1016/j.snb.2014.08.083.

[156] Y.T. Zhang, F. Bottausci, M.P. Rao, E.R. Parker, I. Mezic, N.C. MacDonald, Titanium-based dielectrophoresis devices for microfluidic applications, Biomed. Microdevices. 10 (2008) 509–517. doi:10.1007/s10544-007-9159-y.

[157] J. Ge, L. Zhao, L.R. Chen, Y.P. Shi, Titanium-coated silica spheres prepared by self-assembly technique for use as HPLC packing, J. Chromatogr. Sci. 48 (2010) 29–34. doi:10.1093/chromsci/48.1.29.

[158] V. Gupta, M. Talebi, J. Deverell, S. Sandron, P.N. Nesterenko, B. Heery, et al., 3D printed titanium micro-bore columns containing polymer monoliths for reversed-phase liquid chromatography, Anal. Chim. Acta. 910 (2016) 84–94. doi:10.1016/j.aca.2016.01.012.

[159] A.G. Clark, K.B. Thurbide, Spectral examination of a multiple-flame photometric detector for use in chromatography, Can. J. Chem. 92 (2014) 629–634. doi:10.1139/cjc-2014-0159.

[160] W.A. Aue, Response of filter-less flame photometric detector to hetero-organics, J. Chromatogr. 87 (1973) 232–235. doi:10.1016/S0021-9673(01)91538-9.

[161] K.H. McKelvie, K.B. Thurbide, Analysis of sulfur compounds using a water stationary phase in gas chromatography with flame photometric detection, Anal. Methods. 9 (2017) 1097–1104. doi:10.1039/C6AY03017C.

[162] B. Boulinguiez, P. Le Cloirec, Adsorption/Desorption of Tetrahydrothiophene from Natural Gas onto Granular and Fiber-Cloth Activated Carbon for Fuel Cell Applications, Energy & Fuels. 23 (2009) 912–919. doi:10.1021/ef800757u.

[163] G.J.M. Der Van Der Kerk, J.G.A. Luijten, Investigations on organo-tin compounds. III. The biocidal properties of organo-tin compounds, J. Appl. Chem. 4 (2007) 314–319. doi:10.1002/jctb.5010040607.

APPENDIX A: COPYRIGHT PERMISSION FOR USE OF PUBLISHED WORK

RE: publication re-use in thesis

CONTRACTS-COPYRIGHT (shared)
Mon 3/30/2020 1:05 AM
To:Kaylan McKelvie

Dear Kaylan

The Royal Society of Chemistry (RSC) hereby grants permission for the use of your paper(s) specified below in the printed and microfilm version of your thesis. You may also make available the PDF version of your paper(s) that the RSC sent to the corresponding author(s) of your paper(s) upon publication of the paper(s) in the following ways: in your thesis via any website that your university may have for the deposition of theses, via your university's Intranet or via your own personal website. We are however unable to grant you permission to include the PDF version of the paper(s) on its own in your institutional repository. The Royal Society of Chemistry is a signatory to the STM Guidelines on Permissions (available on request).

Please note that if the material specified below or any part of it appears with credit or acknowledgement to a third party then you must also secure permission from that third party before reproducing that material.

Please ensure that the thesis includes the correct acknowledgement
(see http://rsc.li/permissions for details) and a link is included to the paper on the Royal Society of Chemistry's website.

Please also ensure that your co-authors are aware that you are including the paper in your thesis.

Regards

Gill Cockhead
Contracts & Copyright Executive

Gill Cockhead
Contracts & Copyright Executive
Royal Society of Chemistry

SPRINGER NATURE LICENSE
TERMS AND CONDITIONS

Apr 06, 2020

This Agreement between University of Calgary -- Kaylan McKelvie ("You") and Springer Nature ("Springer Nature") consists of your license details and the terms and conditions provided by Springer Nature and Copyright Clearance Center.

License Number	4763180737506
License date	Feb 06, 2020
Licensed Content Publisher	Springer Nature
Licensed Content Publication	Chromatographia
Licensed Content Title	A Rapid Analytical Method for the Selective Quenching-Free Determination of Thiols by GC-FPD
Licensed Content Author	Kaylan H. McKelvie et al
Licensed Content Date	Sep 29, 2018
Type of Use	Thesis/Dissertation
Requestor type	academic/university or research institute
Format	print and electronic
Portion	full article/chapter
Will you be translating?	no
Circulation/distribution	1 - 29
Author of this Springer Nature content	yes
Title	Thesis: Novel Strategies for Organosulfur Analysis with GC-FPD
Institution name	University of Calgary
Expected presentation date	Mar 2020
Requestor Location	University of Calgary 2500 University Dr. NW Calgary, AB T2N 1N4 Canada Attn: University of Calgary
Total	**0.00 USD**

SPRINGER NATURE LICENSE
TERMS AND CONDITIONS

Apr 06, 2020

This Agreement between University of Calgary -- Kaylan McKelvie ("You") and Springer Nature ("Springer Nature") consists of your license details and the terms and conditions provided by Springer Nature and Copyright Clearance Center.

License Number	4763180603226
License date	Feb 06, 2020
Licensed Content Publisher	Springer Nature
Licensed Content Publication	Chromatographia
Licensed Content Title	Micro-Flame Photometric Detection in Miniature Gas Chromatography on a Titanium Tile
Licensed Content Author	Kaylan H. McKelvie et al
Licensed Content Date	Apr 19, 2019
Type of Use	Thesis/Dissertation
Requestor type	academic/university or research institute
Format	print and electronic
Portion	full article/chapter
Will you be translating?	no
Circulation/distribution	1 - 29
Author of this Springer Nature content	yes
Title	Thesis: Novel Strategies for Organosulfur Analysis with GC-FPD
Institution name	University of Calgary
Expected presentation date	Mar 2020
Requestor Location	University of Calgary 2500 University Dr. NW Calgary, AB T2N 1N4 Canada Attn: University of Calgary
Total	**0.00 CAD**